Application of Series Compensation to Improve the Voltage Stability and Power Quality of Wind Farms

Tahsin Fahima Orchi

A thesis submitted in partial fulfilment
of the requirements of the degree of
Masters By Research

School of Engineering and Information Technology
The University of New South Wales
Canberra, Australia

October 2013

Copyright Statement

Tahsin Fahima Orchi
UNSW, Canberra

Authenticity Statement

I certify that the Library deposit digital copy is a direct equivalent of the final officially approved version of my thesis. No emendation of content has occurred and if there are any minor variations in formatting, they are the result of the conversion to digital format.

Tahsin Fahima Orchi
UNSW, Canberra

Originality Statement

I hereby declare that this submission is my own work and to the best of my knowledge it contains no materials previously published or written by another person, or substantial proportions of material which have been accepted for the award of any other degree or diploma at UNSW or any other educational institution, except where due acknowledgement is made in the thesis. Any contribution made to the research by others, with whom I have worked at UNSW or elsewhere, is explicitly acknowledged in the thesis. I also declare that the intellectual content of this thesis is the product of my own work, except to the extent that assistance from others in the project's design and conception or in style, presentation and linguistic expression is acknowledged.

Tahsin Fahima Orchi
UNSW, Canberra

Abstract

This thesis deals with the dynamic responses of fixed-speed and variable-speed wind turbines (WTs) in terms of voltage stability and power quality issues using series compensation in both a transmission and distribution network. The main power quality aspects, such as voltage sag, flicker and harmonics, due to uneven power production by intermittent wind sources are presented, with static and dynamic voltage stability analyses under normal and contingency periods conducted. The latest regulations enforced by different utilities on wind power plants are studied and the impacts of power system modelling on stability analysed. Compensating devices, wind farms and loads are considered harmonics generating sources and are modeled according to the international standards. Both short-term and long-term flicker emissions of fixed-speed wind turbine (FSWT) and doubly-fed induction generator (DFIG) based wind farms are presented using series compensation while voltage sag analysis is carried out using failure data. To enhance transmission efficiency series compensation is implemented to utilise full transmission assets by reducing voltage drops in a long transmission line and feeder as most WTs are remotely located to obtain suitable wind conditions, and loss in a transmission line degrades the voltage profile of the network. Like the shunt compensation, series compensation can increase transient voltage stability and, to some extent, contribute to local voltage regulation. The case studies presented in this thesis illustrate the contributions of wind power plants and voltage source converter (VSC) based series compensation on the fault levels of symmetrical and asymmetrical faults. From stability and power quality analyses, the cases studied show that large-scale wind power penetration substantially degrades the voltage stability but that series compensation can enhance the collapse margin and reduce flicker and the sensitivity of bus voltage to reactive power, as well as improve both dynamic and transient voltage stability, including providing effective fault ride-through (FRT) support.

Acknowledgements

I would like to express my deepest gratitude and appreciation to my supervisor, Associate Professor Hemanshu Roy Pota, for his invaluable guidance, advice and continuous encouragement throughout this research. I am also thankful to my co-supervisor, Md. Jahangir Hossain at Griffith University, for his support, patience and skilled guidance during the completion of this work. It was an immense privilege for me to follow my higher education under their supervision and continuous technical and editorial assistance.

Further, many thanks go to the Power System and Control Group members for providing valuable suggestions and making the working environment enjoyable. Furthermore, I would like to thank all the members of the institute for their generosity and support in my research journey. Sincere thanks to Ms Denise Russell and N. K. Roy for their contributions regarding the proof reading of this thesis. Also, the financial support for this research provided by the University of New South Wales is gratefully acknowledged.

Finally, I would like to thank my family, especially my husband, Md. Shihanur Rahman, for their support and love throughout my research journey.

Dedicated to my parents and my husband, Md. Shihanur Rahman

List of Publications

Refereed Conference Papers

1. T. F. Orchi, H. R. Pota, and M. J. Hossain, "Stability Improvement of Wind Farms using Shunt and Series Compensation," *22nd Australasian Universities Power Engineering Conference (AUPEC)*, 26–29 September 2012, Bali, Indonesia.
2. T. F. Orchi, M. J. Hossain, H. R. Pota and M. S. Rahman, "Impact of Distributed Generation and Series Compensation on Distribution Network," *8th IEEE Conference on Industrial Electronics and Applications (ICIEA)*, 19–21 June 2013, Melbourne, Australia.
3. T. F. Orchi, M. J. Hossain, H. R. Pota and M. S. Rahman, "Voltage Stability and Power Quality Issues of Wind Farm with Series Compensation," *IEEE Electrical Power and Energy Conference (EPEC)*, 21–23 August 2013, Halifax, Canada.

Contents

List of Tables

List of Figures

List of Symbols

Symbols

δ	rotor angle
ω_s	synchronous speed of the generator
ω	rotor speed of the synchronous generator
H	inertia constant of the synchronous generator
P_m	mechanical power
E'_q	quadrature-axis transient voltage of the generator
I_{dq}	direct-axis and quadrature-axis currents of the generator
X'_{dq}	direct-axis and quadrature-axis transient reactance
D	damping constant
E_{fd}	excitation voltage of the generator
T'_{do}	transient open-circuit time constant
G_{PSS}	transfer function of the PSS
K_{stab}	gain of the PSS
T_w	time constant of washout filter
T_1	time constant of phase lead
T_2	time constant of phase lead
T_3	time constant of phase lead
T_4	time constant of phase lead
P	active power of the load
Q	reactive power of the load
P_0	initial value of the active load power
Q_0	initial value of the reactive load power
V	bus voltage magnitude
P_w	kinetic energy of the wind
ρ	air density
v_w	wind speed
A	swept area of the rotor
N_g	gear ratio

T_{ae}	aerodynamic torque of the wind turbine
P_{ae}	aerodynamic power of the wind turbine
R	rotor radius of the wind turbine
C_p	coefficient of performance
λ	tip speed ratio
λ_i	torque coefficient
θ	pitch angle
ω_m	rotor shaft speed of the wind turbine
ω_g	rotor speed of the wind generator
H_g	inertia constant of the wind generator
H_m	inertia constant of the wind turbine
θ_m	torsion angle
K_s	torsion stiffness
D_m	torsion damping of the wind turbine
D_g	torsion damping of the wind generator
T_e	electrical torque
f	grid frequency
f_T	homogeneous solution of the movement equation
H_l	lumped inertia constant
ω_l	rotor speed for lumped inertia constant
D_l	lumped damping constant
λ_{dqr}	direct-axis and quadrature-axis rotor flux linkages of the generator
λ_{dqs}	direct-axis and quadrature-axis stator flux linkages of the generator
v_{dqr}	direct-axis and quadrature-axis rotor voltage
v_{dqs}	direct-axis and quadrature-axis stator voltage
i_{dqr}	direct-axis and quadrature-axis rotor current
i_{dqs}	direct-axis and quadrature-axis stator current
s	slip
R_s	stator resistance of the wind generator
X_s	stator reactance of the wind generator
R_r	rotor resistance of the wind generator
X_r	rotor reactance of the wind generator

L_{ls}	armature leakage inductance
L_m	magnetising inductance of the wind generator
L_{lr}	rotor leakage inductance
P_s	stator active power of the wind generator
Q_s	stator reactive power of the wind generator
P_r	rotor active power of the wind generator
Q_r	rotor reactive power of the wind generator
w_{SL}	slip speed
i_{gdq}	direct-axis and quadrature-axis grid side converter current of the wind generator
v_{gdq}	direct-axis and quadrature-axis grid side converter voltage of the wind generator
L_g	inductance of the grid side filter of the DFIG
R_g	resistance of the grid side filter of the DFIG
v_{dc}	DC voltage of the DC-link capacitor of the DFIG
P_g	grid side active power
I_{SC}	current in the series compensated line
P_{SC}	active power in the series compensated line
R_L	internal resistance of the DC link capacitor
X_L	line reactance
k	degree of series compensation
Q_c	reactive power in the series compensated line
C_{dc}	DC link capacitor of the converter
X_c	capacitive reactance
I	line current
n_c	turns ratio of the transformer
k_c	converter constant
α	delay angle of the thyristor
I_s	reactive current drawn by the synchronous voltage source
X_{eff}	effective reactance
R	line resistance
V_{sag}	voltage during fault
Z_f	impedance between source and fault location

Z_s	source impedance
V_s	pre-fault voltage
I_n	harmonic current
n	harmonic order
P_{st}	flicker emission from the wind turbine
S_k	short-circuit apparent power of the grid
S_n	rated apparent power of the wind turbine
T_p	duration of the voltage variation due to the switching operation
$K_f\psi_k$	flicker step factor
$K_u\psi_k$	voltage change factor
$C(\psi_k)$	flicker coefficient
v_n	nominal voltage
v_{max}, v_{min}	minimum and maximum voltage due to the switching
R_k	resistance of the fictitious grid
X_k	reactance of the fictitious grid
ψ_k	phase angle of the fictitious grid
P_{st-sw}	short-term flicker due to switching of the wind farm
P_{lt-sw}	long-term flicker due to switching of the wind farm
$P_{st-cont}$	short-term flicker due to continuous operation of the wind farm
$P_{lt-cont}$	long-term flicker due to continuous operation of the wind farm
N_{10}	maximum number of switching operation in a 10 min period
N_{120}	maximum number of switching operation in a 120 min period
U_s	output signal of the PI controller
E_s	input error signal of the PI controller
k_p	proportional gain of the PI controller
k_i	integral gain of the PI controller

Abbreviations and Acronyms

AC	Alternating Current
AVR	Automatic Voltage Regulator
CCT	Critical Clearing Time
DC	Direct Current
DFIG	Doubly-Fed Induction Generator
DG	Distributed Generator
DSC	Distributed Series Capacitor
DSSC	Distributed Static Series Compensator
DSTATCOM	Distributed Static Synchronous Compensator
DTCSC	Distributed Thyristor Controlled Series Compensator
EMT	Electro Magnetic Transient
FACTS	Flexible AC Transmission System
FSWT	Fixed-Speed Wind Turbine
FRT	Fault Ride-Through
GSC	Grid Side Converter
HV	High Voltage
IPFC	Interline Power Flow Controller
LV	Low Voltage
LVRT	Low-Voltage Ride-Through
MV	Medium Voltage
PCC	Point of Common Coupling
PSS	Power System Stabiliser
PWM	Pulse-Width Modulation
SC	Series Capacitor
SCC	Short Circuit Capacity
SMIB	Single-Machine Infinite Bus
SSR	Sub Synchronous Resonance
SSSC	Static Synchronous Series Compensator
STATCOM	Static Synchronous Compensator
SVC	Static VAR (volt-ampere reactive) Compensator
SVS	Synchronous Voltage Source

TCSC	Thyristor Controlled Series Compensator
TCSC	Total harmonic Distortion
RSC	Rotor Side Converter
WT	Wind Turbine
UPFC	Unified Power Flow Controller
VSC	Voltage Source Converter
VSWT	Variable Speed Wind Turbine
XRR	Line Reactance to Resistance Ratio
ZIP	Constant Impedance, Current, and Power load model

Chapter 1

Introduction

Due to environmental concerns, governmental policies have provided an impetus for the use of sustainable energy [1]. Renewable power plants such as wind farms introduce additional uncertainty into the operation of power systems due to the random nature of the wind and some anomalous arrangements which are contradictory to the structure of a conventional power system. All factors related to wind power generation that may influence the quality of the power system operation must be considered in order to provide a certain level of reliability and stability of supply. Voltage stability and quality issues are one of the key problems because of the increasingly large proportion of wind farms entering the electricity market, as noted in the wind power integration reports [2].

The diversification of generation to cater for long transmission distances from load centres necessitates the efficient transmission of bulk amounts of power from large wind farms. Series compensation in the capacitive mode can generate reactive compensating power with changes in the in-line current flow and increase the power transmission capability and stability of the the system [3]. Series compensation also has the capability to minimise system disturbances which helps to ensure the traditional stability margin as well as enhance transient stability and oscillations [4]. These benefits of series compensation can be implemented to focus on the integration of wind power, this thesis concentrates mainly on the impact of series compensation for dealing with the stability and power quality issues provoked by wind energy.

1.1 Background

With increasing penetration levels of wind power being developed in power systems, the overall performance of a power grid will be affected by the operating characteristics of a wind power plant, the worlds fastest growing energy source [5], [6]. During faulty conditions, the terminal voltage of a wind turbine (WT), as well as its electromagnetic torque and output power, drops rapidly. The mechanical input torque is considered constant and the acceleration torque acting on the machine becomes positive and causes an increase in the speed of the rotor. As the speed of the induction generator increases, so does the slip which results in more reactive power being consumed from the power grid. Consequently, the post-fault voltage of the network is not likely to return to its pre-fault value. If the reactive power demand of the generator is not fulfilled after a fault, the machine will be unstable and should be disconnected from the power system. Therefore, the quick recovery of voltage and reestablishment of the electromagnetic torque are crucial [7].

There are different types of generator systems for generating power from wind energy and an overview of different types of wind generation technologies are discussed in [8], [9]. The fixed-speed wind turbine (FSWT) is well known for its ruggedness, reliability and simplicity but it has great difficulty in maintaining good power quality as it converts wind speed fluctuation into mechanical fluctuations. Under undesirable voltage fluctuations, requires reactive power compensation from the grid which leads to increased line loss [10], [11]. As, to compensate this reactive power consumption, it is necessary to connect a capacitor bank or flexible AC transmission system (FACTS) devices to the system, a suitable FACTS device controller can help to attain stable operation of a FSWT. In contrast to the FSWT, the doubly-fed induction generator (DFIG) has a number of advantages, such as improved power quality, high energy efficiency, low investment cost, flexible and independent control of active and reactive powers, variable speed operation, low environmental impact, low mechanical stress and reduced audible noise [12–15]. Also, a DFIG is equipped with a bidirectional back-to-back converter which partially reduces the need to use an additional capacitor or FACTS device. A proper controller for rotor side converter (RSC) not only controls the reactive power but also the active power by controlling the components of the rotor current [11].

The following section surveys the literature available on the background to emerging wind power, and the impacts and integration limitations of wind farms due to different constraints. For wind farm applications, shunt compensation has already drawn a great deal of attention from researchers and details of it can be found in several publications. Incorporating series compensation due to its attractive features could be a possible way of addressing large-scale wind penetration issues, this needs to be explored as this has some limitations, such as subsynchronous resonance (SSR) and harmonics. A literature review of some practical experiences of implementing series compensation shows that these limitations can be overcome by adopting empirically implementable mitigation technique.

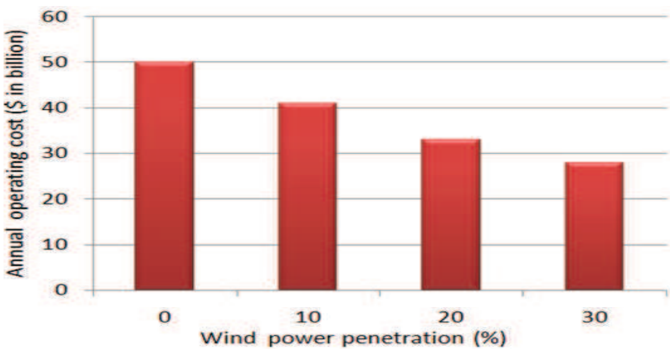

Figure 1.1. Reduced operational costs with increasing penetration levels of wind energy [16]

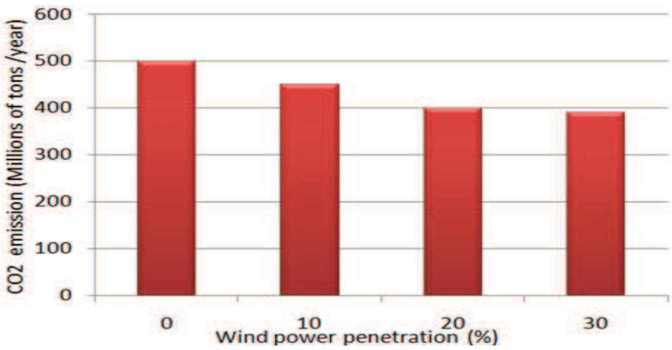

Figure 1.2. Reduced CO_2 emissions with increasing penetration levels of wind energy [16]

1.1.1 Promotion and integration of wind power

Numerous energy-conscious regional, operational, technical and planning reports, and studies related to wind energy conducted by renowned organisations, such as AEMO, EirGrid, Transpower, Western Power, Energinet.dk, ERCOT, are evidence of the increasing concern regarding the feasibility of wind power evolving to fulfil its potential. According to the report by the Western Wind and Solar Integration Study (WWSIS), based on a 35 percent renewable energy penetration, including wind, in the WestConnect group utilities which support five regions in the U.S.A., wind energy has reduced fuel costs for a 30 percent penetration by 40 percent and CO_2 emission rates by 25 to 45 percent [16], as shown in Fig. 1.1 and Fig. 1.2, respectively. In the last 12 years, the total installed wind capacity has increased almost exponentially, as shown in Fig. 1.3. In European countries, especially Denmark, wind energy generation has become an important means of decentralised electricity generation following a great deal of dedicated research and effort which resulted in

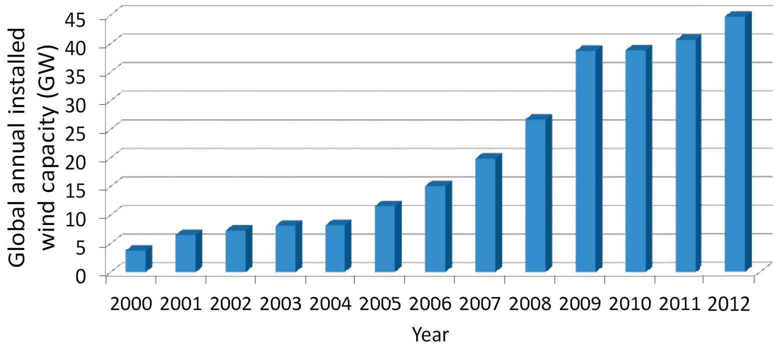

Figure 1.3. Increase in global annually installed wind capacity [17]

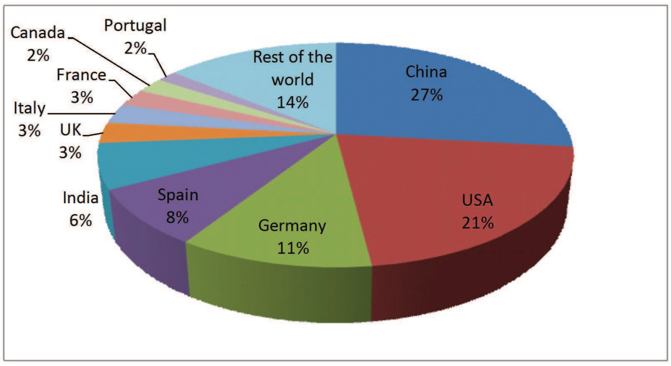

Figure 1.4. Cumulative capacity of wind energy installed in 2012 [17]

the implementation of aerodynamic formula of lift and drag in 1918. The 10 countries in the world with the highest numbers of wind installations according to the report of Global Wind Energy Council, of which seven are European with the USA second with approximately 60 GW, are shown in Fig. 1.4 [17] while, in Asia, China and India have the highest installation. Australia has a flourishing potential for the development of wind energy.

In Australia, wind energy is the fastest growing energy source due to the influence of government policies, especially carbon emissions reduction and renewable energy target, with an average annual growth of 69.5 percent between 1999 and 2000 [18]. To meet energy production targets and environmental goals, the future grid of Australia will generate more wind power, approximately 4 times more after two decades than at present [19], which will require adequate transmission facilities and the reliable and stable operation of wind farms in terms of their interconnection in the grid.

Several issues, such as the coordination of supply and demand, voltage and power regulation, capacity credit and grid extension, have been identified as having major impacts on the integration of increasing amounts of wind power in grid which will require reinforced grid codes, such as those for low-voltage ride-through (LVRT), reactive power support, terminal voltage control, fault-level contribution and power quality handling, to meet system operators' expectations and necessitates changes to the business-as-usual operation of an electric power system. From the extensive review of wind integration studies around the world, integration issues can be categorised as system adequacy, system security and system operation [20]. The generation adequacy of a wind farm generally emphasises the challenge of meeting existing and future load demands as the generation mix and replacement of conventional sources introduces more uncertainty into fulfilling the demand. Large wind power integration can change the predominant oscillatory mode of a network [20] and hamper system security which deals mainly with stability, fault current contribution and frequency regulation scenarios. The adequate operation of a wind farm ensures that its system has suitable primary, secondary and tertiary reserves and that its voltage, frequency and reactive power are properly controlled so that it is capable of withstanding contingencies, its execution within normal regulating margins is guaranteed and that it can deal with mismatches of load forecasting errors and scheduled equipment outages [20], [21].

Wind energy integration is a complex issue which requires proper planning for its successful operation [22]. A diagram of the main issues relating to the integration of a wind farm into a grid according to the literature is provided in Fig. 1.5 in which, for simplicity, other relevant issues are not included; for example, congestion management [23] can be further classified into on-shore and off-shore WT transmission arrangements. Also, some issues are interrelated, such as voltage control [24] for maintaining the proper operation of a WT can be viewed as part of stability maintenance and, frequency control [25] can be associated with generation adequacy and stability matters.

Modelling a wind farm along with a power system is important for planning as proper modelling will help assists in practical implementation with less trouble [26]. Stability and power quality assessments are also dependent on modelling. Operational efforts generally ensure the stability and power quality issues of a wind farm under normal and faulty conditions, any abnormal deflection requires proper

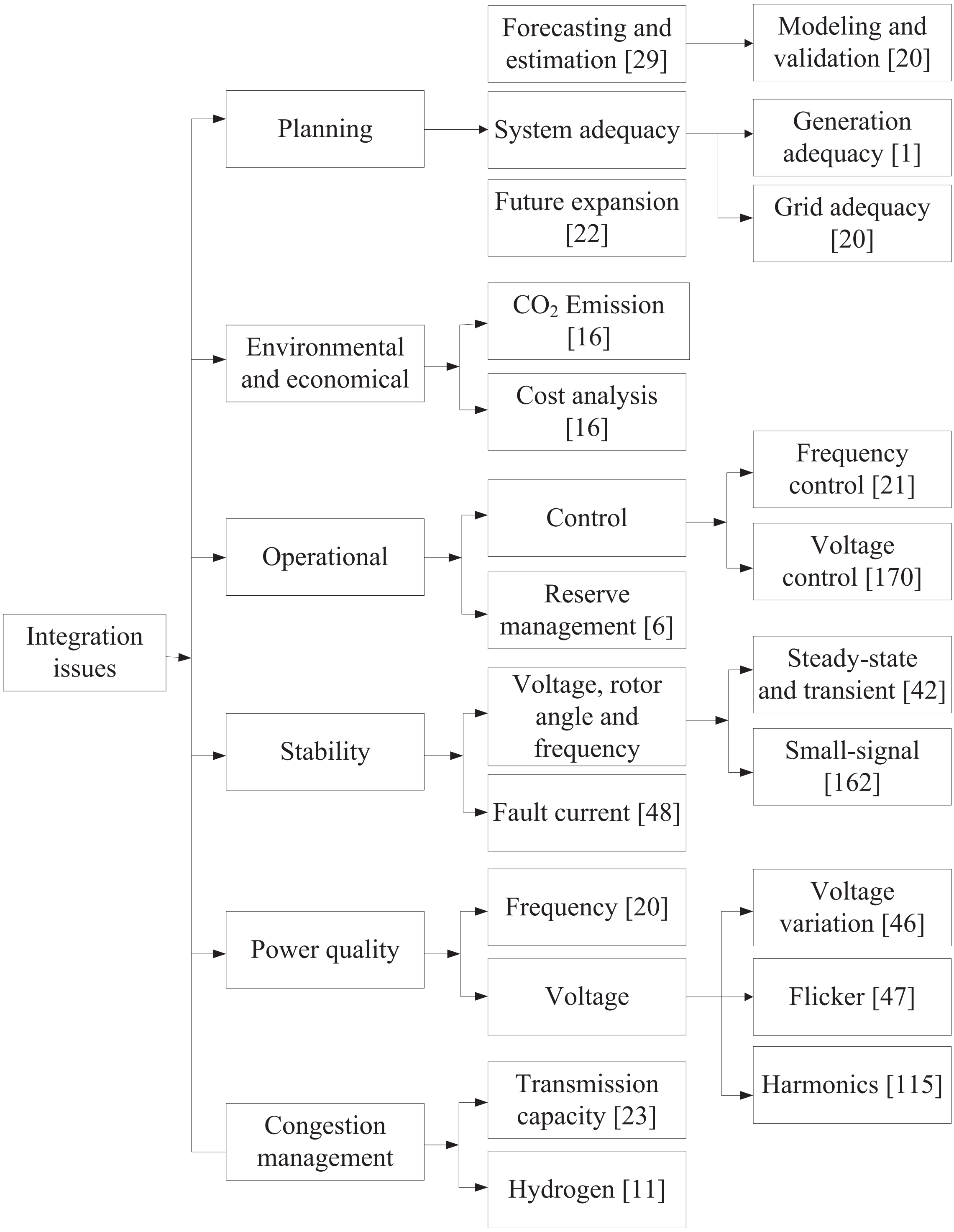

Figure 1.5. Wind energy integration issues

control to force the malfeasance into its operational limit which requires proper modelling. The modelling issues related to wind farms in a power system are described in Chapter 3. This thesis concentrates mainly on voltage stability issues of which power quality is often considered a sub-division. Again, a high short-circuit current introduces high reactive power demand in a line, which initiates severe voltage dip problems that lead to voltage instability [27]. The following paragraphs describe the voltage stability, power quality and fault-level issues which hamper the integration of wind farms in a grid.

A conventional power plant is designed to operate in a such way that it has the capacity to deliver power according to load to fulfil customer demands at any time. The integration of a new power plant changes the active and reactive power flows in the network which can contrarily influence the thermal and voltage limits and affect the voltage profile due to the changing quantity of reactive power available [28]. As it is difficult to firmly predict power generation from wind forecasting data, this may result in over-supply or under-supply [29]. The standard practice of voltage regulation is based on radial power flows from the substation to loads [30] whereas, as distributed generator (DG) introduces meshed power flows [28], the system is affected.

The electrical counter torque produced in a wind power generator is proportional to the operating slip and the square of the voltage magnitude [31]. A reduction in system voltage increases the slip which, in turn, increases the stator current which increases the reactive power intake from the grid and may cause WTs to accelerate and may result in voltage collapse. The AEMO wind integration study, WP4(A), pointed out that, in Australia, as the load centre is far away from generation, the worst-case scenario is a high power transfer during peak demand [20]. A remotely located wind farm often requires a long transmission line and the weak connection of wind farms in remote areas, along with line loss, means that a great deal of attention needs to be paid to voltage restoration.

A distribution network is considered more susceptible to voltage regulation than a transmission network. Most wind DGs sink reactive power from the grid and static stability analyses of wind farms [32] shows a decrease in the stability limit with an increasing penetration of wind power. A small-signal stability analysis has shown that the integration of a DG unit and closely placed dynamic load interaction generates a new ‘voltage mode’ on the top of the electromechanical and sub-synchronous oscillation modes, which are excited by the voltage states of the machines [33]. Again, T. Aziz et al. shows in [34] that grid loss increases after certain levels of renewable DG penetration. The penetration level of wind DG is limited due to voltage stability problems but can be increased by increasing the maximum short-circuit current capacity, curtailing generation and increasing the grid adequacy, i.e., decreasing generation for exceeding the upper voltage limit and adding reactive power compensating devices [32], [35], [36].

The transient response of a wind farm, i.e., the contribution it makes to fault ride-through (FRT) and post-fault recovery, has a considerable impact on the system [37]. Due to lack of online synchronous generator to provide sufficient reactive power both during and after a contingency, the situation becomes more challenging. Depending on their turbine types and reactive power supporting schemes for FRT, many existing wind farms, especially those equipped with FSWTs, are allowed to trip or curtail reactive power demand during severe contingency periods [20]. Modern wind farms require FRT support with additional reactive power or reactive current injection, and to some extent, voltage control [38], [39].

For a sudden generation loss, switching, transmission line tripping and maximum wind power generation with a minimum load and vice versa can change the voltage to an acceptable level [39], [40]. Maintaining its voltage profile under all operating conditions is a challenge for a wind power plant as its output power is inevitably variable in nature which changes the steady-state and dynamic stability characteristics of the network. Wind farms do not naturally contribute to regulating the voltage of a grid [31] as, although they increase the local voltage level of a network, they also decrease its transient stability [41] if they are not provided with additional reactive power support and inferior voltage control can lead to system voltage instability and collapse. In the case of DG, in spite of standard control, proper size and placement it can not be operated to provide system support as both high and low voltage can occur due to its incompatibility with the system [28]. Common means of controlling voltage are using a capacitor bank, transformer tap changers and compensating devices.

Introducing compensating devices, either externally or internally, to WTs for VAR control and voltage support often present power quality issues at the point of interconnection which is an important concern, especially at the local level. An external device can be a static synchronous series compensator (STATCOM) or series or shunt capacitor, and an internal device can be a WT's converter. These types of equipment can distort the current or voltage when there is any disturbance in the network and initiate complications, such as harmonics, flicker and slow-voltage variations [4], [11]. A common assessment of the contribution of WT's to power quality is that it is determined by the grid strength. If a wind power plant exceeds 2 percent of the grid's fault-level, as power quality adequacy may be hampered, this needs to be considered [31], and this criterion is also applicable to voltage stability [42].

Although, ideally, stiff grid connections of wind farms can anticipate detrimental affect of power quality, this is not practical. The production of harmonic currents, which depends on the type of inverter used [43], affects the power transformer and interferes with the protection operations can result in derating of the connected equipment due to the additional heat generated by the harmonic [44]. DG units are considerable sources of harmonics and flicker [28]. The flicker issue is related to humans' sensitivity to the luminescence of incandescent lamps which is greatly influenced by the fluctuating frequencies and voltages generated by wind farms [45], [46] which can be caused their start-up or step changes in their power. In addition, vertical wind gradients and the tower shadow effect also cause voltage variations [47]. T. Larsson and C. Poumarede showed that not only the reactive current but also the active current impact on flicker due to the resistive voltage drop in the line [45].

The reduction in its fault-level makes it more difficult to maintain voltage during a short-circuit fault. It is difficult to draw conclusions about the impact of wind farms on short-circuit levels because fault-levels depend on a WT's topology and location and the network conditions, i.e., the presence of a conventional power plant, its load demand and distance from WTs, the WT's power converter control algorithm, the substation transformer configuration, etc. [48], [49]. The contribution of one small DG unit to a fault may be ignored, the aggregation of many can considerably affect the fault level and be responsible for the mis-coordination of a fuse. The behaviour of short-circuit currents for Type A, C and D wind farms with substation transformers winding and grounding configurations is well described in [50].

The short-circuit capacity of a wind farm is lower than that of a synchronous generator [20]. The fault current in a short-circuited bus with an asynchronous generator starts at 500 to 1000 percent of the rated current and decays more rapidly than that in a synchronous machine, generally within 10 cycles [28]. A wind power plant decreases the short-circuit level if it has replaced conventional generators or is located in a region with significant conventional generation [39]. However, where there is local generation, wind farms increase the local fault level [51]. Steady-state analysis is a common form of investigation method for this type of fault. As decreasing the fault-level may produce voltage instability, flicker and harmonic resonance, correct operational fault-level analysis is recommended by many grid-codes, such as NEM, DENA, All island, REE and REN.

The capabilities of series compensation to address voltage stability and power quality issues are described in the following section.

1.1.2 Series compensation

Series compensation has the capability to increase power transfer, improve transient and steady-state stabilities, optimise the power flow between parallel lines and reduce system loss. Field tests and experience have proven the effectiveness and reliability of a series capacitor (SC) as an economical way of mitigating voltage drop and flicker at the feeder in a distribution network. Split-compensation can also be implemented at different sections of a line if required. A SC is a cost effective way of uprating the voltage to improve power quality compared with traditional solutions, such as reconductor the feeder or reconstructing the substation which are expensive operations [52]. Distributed static series compensation (DSSC) to improve the voltage profile and control the power flow, which reduces the voltage drop by approximately 42.85 percent, is proposed in [36], [53].

In a distribution network, to solve the voltage drop in a medium-voltage (MV), 23 kV, feeder a SC was implemented in AES SUL, Brazil [54]. The feeder was equipped with three shunt capacitors for voltage regulation but faced serious voltage drop problems at some critical nodes due to the vicinity of large dynamic loads. Two cases were presented: in the first, the interaction between the SC and induction motor loads used for cultivation provoked voltage oscillations due to ferroresonance and SSR and overcompensation of capacitors which made the system unstable and difficult to work with. However, in the second case, the SC was successfully implemented in another feeder and the desired voltage regulation achieved.

The Duke Power Company in the USA also implemented a SC on a distribution feeder as a solution to the voltage flicker caused by the induction machine load, generally known as the hunting phenomena of the motor [52]. As the start-up process of the induction motor drew a large current with a poor power factor, the high reactive power demand caused voltage dips and customers sharing the same feeder had to face voltage flicker. For economic reasons, a SC, rather than a synchronous condenser or static VAR compensator, was recognised as a potential solution to this problem. The self-voltage regulating nature of a SC creates a voltage rise in the feeder line and instantaneously reduces the flicker level on the load side [52]. This experience demonstrated that implementing a SC did not produce any SSR issue although some limitations were detected, such as excessive maintenance required for the protective gap of the SC and ferroresonance. A high-energy varistor arrangement and inrush bypass device were implemented as a remedy for these problems [52].

A thyristor controlled series compensator (TCSC) was first implemented in the Kayenta substation, Arizona, in 1992 and increased the system's transmission capacity by 30 percent [55]. In spite of that, to damp inter-area low-frequency power oscillations, and SSR and to enhance the stability margin, using dynamic voltage support and control of the power flow in a TCSC has been effectively implemented around the world, especially in transmission networks [55], [56]. A fault-current limiter and unbalanced voltage compensation of a TCSC in a wind farm application is explored in [57] where the TCSC is operated in the inductive mode, i.e., at its maximum inductive impedance, although this can be done by injecting series voltage, i.e., operating TCSC in the capacitive mode. The controlled impedance characteristic of a TCSC can also be utilised to reduce the overheating and mechanical stress caused by an unbalanced voltage and torque pulsation, respectively. It has been clearly demonstrated that a TCSC can enhance dynamic stability both during and after a network disturbance [58] and as it has the advantage of voltage regulation, it can provide a higher DG penetration rate within an allowable voltage range [56] which could be useful for wind DG integration. In [58], the author shows that the harmonics produced by a TCSC circulate within the LC loop, and, as a small percentage interfere with the system to which they are connected, their penetration level depends on the critical firing angle. Although setting the operating firing angle away from the critical zone can reduce harmonics, those harmonic in the LC loop can cause overheating of the capacitor that requires mitigation.

A SSSC is capable of providing controllable compensating voltage irrespective of the magnitude of the line current. In addition to series reactive compensation, either inductive or capacitive, it is capable of controlling real power with the support of an external DC source or storage [59], [60]. However, the real part of the variable series impedance contributes less than the reactive part in post-fault voltage recovery [60]. These features make a SSSC capable of improving voltage and angle stability, and to mitigating harmonics, SSR and power system oscillations [61], [62]. The power system oscillations damping capability of SSSC is better than that of a STATCOM and the device capacity it requires is small [60], [63]. A SSSC can be used in a wind farm to improve the power quality by smoothing steady-state voltage fluctuations and limiting inrush currents [60]. The power system oscillation damping of SSSC has been well proven for a synchronous generator [64], permanent magnet synchronous generator-based offshore wind farm [65] and other network configuration. An embedded SSSC for power flow and voltage control, which shows the compensation is effective for a certain distribution level, is also proposed in [66].

A static synchronous series compensator (SSSC) with a small energy storage has often been used to inject a series voltage into the line which is another approach for LVRT [61] and is known as a dynamic voltage restorer (DVR) which can be connected at the distribution level [67]. It is capable of injecting a dynamic voltage in a series which is the inverse of the fault voltage and can protect a wind farm from voltage sag and swell. This characteristic of DVR is implemented in [68] to increase the high voltage ride through capability of a wind farms in which, under normal conditions, the injected voltage is controlled to zero and, during a voltage swell with no phase-angle jump criteria, it draws a fraction of the rated real power from the WT [68].

A series power quality compensator can isolate its receiving end, up to its bandwidth capacity, from the harmonics generated from the grid side and restore the voltage at the customer end during voltage sag and swell and protect the load [69]. To protect the RSC of the DFIG from the high transient current generated from a voltage sag, series voltage compensation has been implemented to increase the stator voltage level to create the required flux at the RSC [70]. From a small-signal stability analysis, it has been shown that a proportional feedback control loop is adequate for removing SSR and supersynchronous modes in a series compensated network and driving the system into a stable region [71]. The elimination of harmonic and transient depends on the converter's switching frequency, with a higher switching frequency eliminating higher order harmonics and quickly damping transients [69].

Series capacitive compensation can cancel out a portion of inductive reactance in a transmission line and represent the supply side as a 'stiff voltage' source for loads. This characteristic is used with the intermittent wind energy source to handle dynamic disturbances and increase support for post-fault voltage restoration. Although the equipment cost of a SC is higher than that of a shunt capacitor, its total installation cost per MVAR is less [72] and to increase transmission capability, the cost is only approximately 10 percent of that of a new transmission line [3]. Another cost-benefit analysis shows that implementing a TCSC to improve the voltages and power flows of selected buses can reduce generation costs by 3.67 percent which means a saving of $31.51 per hour [73]. The SSSC is expensive due to its additional requirements for DC voltage support but the cost of the SSSC can be reduced by implementing the 'chain–cell' approach [74]. With respect to its performance SSSC is more economical series compensation when it acts as capacitive compensation and a SSR suppressor [74].

1.2 Motivation and Objectives of Current Research

With the introduction of emerging wind energy technology in modern power systems, voltage stability and power quality have become important considerations. Series compensation has been well proven to increase the power flow in a transmission line and be reliable which makes it feasible for incorporation in a distribution network. Different issues related to wind energy, such as voltage fluctuation, sensitivity and instability, can be diminished or partially minimised by using the attractive features of series compensated devices. Like any other compensating technology, series compensation has some drawbacks that might limit its widespread use, the major drawbacks can be addressed by some simple modifications. SSR and harmonics are two major challenges that are focused on in this thesis. NGH scheme (proposed by N. G. Hingorani) with TCSC is implemented to remove SSR. The motivation and objectives of the research are as follows.

- Series compensation ensures the utilisation of full transmission assets and its capability to partly cancel out the reactance of a line makes it possible to minimise receiving-end voltage variations and prevent voltage collapse. These favourable technical characteristics have encouraged the use of series compensation in wind farms which are remotely located in areas where transmission efficiency needs to be improved. To gain a deeper insight and understanding, it is important to assess their dynamic behaviours, steady state performances, and consequences on wind energy-assisted power system networks with regard to their reactive power profiles and voltage control.

- A decentralised wind energy source, which has an irregular and random nature, is opposite to the historically centralized structure of a conventional power system. As wind turbulence and variations cause the output power from a WT terminal, which does not participate in the supply-demand balance, to fluctuate, this raises serious concerns about system security and stability and worsening load variations, especially in the distribution network. The lack of reactive power support during both normal and contingency periods is primarily liable for voltage stability deterioration as most WTs are not provided with a full reactive power regulation capability. The exigent demands regarding voltage stability should be fulfilled by the sharp increasing wind energy. To assess the impacts of different types series compensation for the support of wind farms require extensive dynamic voltage stability analysis.
- The power quality of a wind farms varies extensively as it depends on the wind speed, sizes, numbers, turbine topologies, and the control algorithm. A minimum power quality level needs to be guaranteed as this type of intermittent source magnifies the risk factors for power quality issues, especially at the interconnection point of a grid. Different standards identify voltage fluctuations or flicker, voltage dips and harmonics as the major power quality problems related to wind farms. The influence of series compensation on power quality issues, especially at the point of common coupling (PCC), requires a thorough investigation given the capriciousness of wind energy.
- One major disadvantage of series compensation is that it generates SSR with the interaction of WT technology and may cause electromechanical oscillations at the sub-synchronous frequencies and leading to turbine-generator shaft failure. The excitation of torsional oscillations results in a high magnitude shaft torque which endangers mechanical operations and reduces the lifetime of a WT while the impact of series compensation with a multi-inertia shaft of a WT needs to be thoroughly analysed and to maintain stability, SSR is minimised using the NGH damper circuit.

1.3 Contributions of This Research

In a power system, dynamic voltage instability is a common phenomenon which can lead the system to a critical condition. Series compensation with wind power to improve voltage stability is analysed. The major contributions of this thesis, which address its motivation and objectives discussed in the previous section, are:

- interpreting the impact of renewable wind energy sources on voltage and power quality issues using different types of series compensation, such as a SC, TCSC and SSSC, connected at the PCC;
- analysing the comprehensive voltage stability of wind farms connected to a transmission network by utilising static and dynamic study tools for shunt and series compensation considering contingencies, such as large disturbances and load variations, and also taking into account the sizes and positions of compensating devices;
- conducting thorough research into wind DG integration on the distribution side, from which series compensation is advised as a means of improving static and dynamic voltage stabilities and justified by a comprehensive dynamic simulation as well as static stability analysis of such as the critical voltage stability margin and bus sensitivity, and addressing various practical issues, such as an, asymmetrical fault, motor star-up, torque variations in a synchronous machine and degree of series compensation;
- illustrating the transient, sub-transient and peak currents and other essential parameters related to fault level estimation, resulting from the effects of symmetrical and asymmetrical faults in the line and the switching operation of the WT, where a variable speed wind farm is connected to a multi-machine power system with the aid of a series compensated long transmission line;
- investigating the voltage sag characteristics defined by standards with probabilistic data for both FSWT and VSWT types of wind farms using static and variable series compensation which reveals the dependency of the sag intensity on the degree of compensation and its consequences, which are mostly apparent at the buses in the vicinity of the compensating device;
- calculating both short-term and long-term flicker with the help of a standard flickermeter, as well as unbalanced harmonic current emissions, and assessing their effects at the PCC using series capacitive compensation devices for Type

A and C WTs which demonstrates that the flicker emission rate is low for compensation while the harmonic contribution depends on system impedance.

1.4 Thesis Outline

According to the motivation and objectives presented in the previous sections, this thesis is organised in the following six chapters, including this review of relevant literature.

Chapter 1 provides a background on wind energy integration issues and their impacts on the grid and the series compensation techniques used in different applications in a power system. Also, the motivation for, and objectives and contributions of, this research work are summarised.

Chapter 2 presents a brief review of the literature on the voltage stability and power quality issues of wind farms. It also provides a brief review of the grid codes of different countries for dealing these types of issues.

Chapter 3 presents an introduction to the dynamic modelling of various parts of a power system, such as the synchronous machine, static and dynamic loads and FACTS devices, and impacts of their modelling on system stability and power quality. The model of the FSWT and DFIG-type WTs used in this thesis for assessing the voltage stability and power quality issues are briefly discussed.

Chapter 4 concentrates on the behaviour and interaction of a WT with the utility under both transient and steady state conditions with regard to voltage stability. Extensive simulations are carried out to analyse different case studies for VSC-based shunt and series, STATCOM and SSSC compensation in a transmission network and the results compared. Also, series compensation using a SC and TCSC is implemented in an industrial and commercial distribution network and static and dynamic stability analyses are presented. Fault-level calculations are performed using SSSC in the transmission line and, for a WT start-up, its capability to reduce the peak current and reactive power demand is shown.

Chapter 5 deals with different power quality issues that arise as a result of connecting a stochastic wind energy generating source. Large-scale wind power penetration on the transmission side using a STATCOM and SC is presented to improve the voltage profile and increase the CCT and LVRT capability and incur less flicker emission at the PCC. Positive and negative sequence harmonic current at the PCC are analysed using series compensation. The impacts of DFIG-based wind

DG and series compensation using a SC and TCSC on the voltage sag characteristics, stability margins, flicker emissions and harmonic distortions of a distribution network are also investigated in detail. Case studies of widely used 15-bus and 43-bus distribution networks are presented and their simulation results and voltage sag characteristics demonstrate the impact of series compensation on the collapse margin and bus voltage sensitivity to reactive power and flicker.

Chapter 6 presents the general conclusions drawn from this thesis and provides recommendations for future research.

Chapter 2

Literature Review

2.1 Introduction

Voltage stability and reactive power compensation are crucial requirements for a power system and are issues of major concern for power system planning, development and operation. As the power output of a wind turbine (WT) generator normally fluctuates significantly with incoming wind speed variations, dynamic stability improvements and voltage control are increasingly important for maintaining stable operation of a wind farm. The objective of this chapter is to investigate different cases of voltage instability of wind farms and use different types of series compensating techniques to improve the dynamic stability of a system with integrated wind energy.

Voltage instabilities have caused a number of black-outs throughout the world, for example, in France in 1987, in northern Belgium in 1982, in Sweden in 1983 and in Moscow in 2005 [75], [76]. Most of these instabilities were initiated by a voltage drop due to different phenomena which, in the long run, rapidly affected other parts of the network due to the cascade tripping of protection devices. The US-Canada black-out in 2003 caused an interruption of a 63 GW load due to insufficient reactive power which led to voltage instability [77]. A poor voltage profile also reduces the reactive power reserve margin for supporting any contingencies as generating units operate close to their limits [77]. A major cascading breakdown in 2006 in a part of Europe, due to the disconnection of a unit caused an imbalance between generation and demand affecting 15 million households [78].

Voltage collapse is a dynamic consequence which can be manifested by the sensitivity of reactive power generation with respect to load [79]. There are different measures for calculating stability. The stability index, which is the distance between the operating point and steady state voltage stability limit, is a measure of static voltage stability. In [75], an algorithm for obtaining the stability index by calculating the minimum singular value of the Jacobian matrix extracted from the power flow, is proposed. A sensitivity analysis of buses is an another index of voltage stability which provides useful information on critical nodes in a network which are sensitive to reactive power and suitable compensation and protection are required for those vulnerable parts of the network. A stability algorithm is proposed in [80–82] for a radial ill-conditioned distribution network to identify critical nodes by indicating the severity of its loading situation or identifying the bus that is operating at close to the stability limit. To enhance the system stability of a network, a reconfiguration is proposed in [83] which may not be practical as, in many cases, all the nodes in a distribution system do not have the facility to branch exchange.

To achieve a high-efficiency by minimising the losses is another consideration for a utility. From the well known L theorem, proposed by Jasmon and Lee [84], it can be concluded that minimum loss will generate a minimum value of L and that maximum voltage instability in a distribution network is achieved when the system is operated under minimum loss conditions. Series compensation in distribution network can increase the power flow capacity of the line and reduce losses.

The generation side of a power system consists of conventional generating units, such as synchronous generators and renewable energy sources. The integration of a large wind power plant will introduce more uncertainties into the reliable operation of a power grid than a small wind park. This is due to the non-self-excitation of an induction machine in the case of a fixed-speed wind turbine (FSWT) and limited reactive power compensation in the case of a doubly-fed induction generator (DFIG) [85] which are WTs widely used to generate electricity from intermittent wind sources. As wind energy technology has to fulfil the expected voltage and power stability requirements of the relevant grid code, flexible AC transmission system (FACTS) devices, such as reactive power compensation, dynamic voltage support, flexible power-flow control and, consequently, better transmission capacity with improved damping capability, are used [61], [86].

The participation of high wind energy in the grid has an impact not only on the voltage at the point of common coupling (PCC) but also on the other bus voltages in the network. Again, the expected number of voltage dips in a power system network can vary from a few dozen to a thousand per year [11] and cause undesirable disturbances to generation and load points. One major aim of reliable network operation is to secure an uninterrupted power supply. For this reason, voltage sag, which can affect the operation of a wind farm, needs to be assessed. The critical clearing time (CCT) is an important parameter for stability measurement.

Different parameters of a wind farms such as the shaft stiffness, rotor inertia, WT operating power factor, and power injection level have important contributions to change the CCT [87]. It is observed that the frequency of voltage sag occurrence is reduced at low remaining fault voltages, and low-voltage ride-through (LVRT) recovery is quicker with a longer CCT with the aid of a series capacitor (SC).

Large-scale wind power plants are often located in areas distant from the main power grid which require efficient transmission planning for transporting power. Losses in a regional network also imposes limitations on the integration of wind power. Voltage or load stability can be hampered under heavily loaded conditions or in a faulted situation in which the generating unit and other types of reserve are not able to meet the demand for reactive power and resulting in voltage instability problems and collapse. Short-circuit capacity (SCC) ratio dictates a grid's strength, with a weak grid characterised by a low SCC. In [42], the weak connection of a wind farm is analysed and it is shown that the maximum penetration of a wind farm is about 20 percent of the SCC at the PCC, beyond which it will be unstable. A wind farm can be connected to a sub-transmission network up to a certain limit without any compensation and without significantly increasing the loading of the lines [88]. However, greater penetration increases the risk of a reactive power shortage in the network, resulting in additional loss which increases the burden on the existing system. The integration of wind power makes the total system more vulnerable to voltage instability as a wind farm lowers the system's reactive reserve margin. Series compensation can effectively reduce net line loss and enhance the reactive power reserve margin and a wind farm connected to the power grid through a regional network can be operated beyond traditional voltage stability limits and up to its thermal limits with the aid of FACTS devices [89].

There are several technical constraints, steady-state or dynamic, for the integration of a wind farm into a weak network. The reactive power demand of a wind farm can be partially compensated with a DFIG type of WT which can provide reactive power regulation by absorbing or producing reactive power during normal operation and also has a better voltage recovery than the same rated FSWT-based WT [2]. Because of the limited capacity of its pulse width modulation (PWM) converter, the DFIG can not support reactive power according to the demand as effectively as the synchronous generator [2]. Thus, system security and stability is a serious concern with wind energy integration even with the DFIG as voltage instability occurs when the reactive power requirement is beyond its capability.

A distribution network is different from a transmission network in both its operation and characteristics. Voltage regulation is a well-recognised phenomenon in distribution systems which are faced with ever-increasing load demands [90]. Generally, the structure of a transmission system is a loop type of network that exchanges large blocks of power from the generation side while a distribution network has a radial structure that transmits power to loads [81]. A voltage stability analysis of a distribution network is presented in [91]. As a modern power distribution network, especially in an industrial area, experiences distinct and frequent changes from low to high load levels, it is very challenging to meet demands and fulfil voltage requirements using renewable sources as their input driving forces are highly unpredictable. It has been observed and reported in [91], [92] that, under certain critical loading conditions, periodic voltage collapse in a distribution system, which requires additional reactive-compensating devices, is common.

Distributed generator (DG) has increasingly been integrated in low-voltage distribution networks in recent years due to environmental and economic issues. Although DG can enhance the network efficiency and dramatically reduce system loss, it can create a number of problems, for example, in terms of voltage regulation and power quality [93]. In most cases, DG units are operated at the unity power factor and they do not participate in voltage control while series compensation can be used to minimise the negative impacts caused by their integration. The basic operating principle of a series compensator is to reduce the transfer reactance between the supply point and load by inserting a voltage in a series so that the load side voltage is within the desired level in spite of any disturbance in the source voltage and, thereby, voltage drops in a line are compensated [4].

Fan et al. discuss the modal analysis of a series-compensated network with variable speed wind turbine (VSWT) in [71] but the impact of series compensation on its LVRT capability is not analysed. Shunt compensation using a static synchronous compensator (STATCOM) and static VAR compensator (SVC) is analysed in many papers [37], [94], [95] for LVRT and various load excursions, while series-shunt compensation, such as with a unified power flow controller (UPFC) [96] and series compensation with a dynamic braking resistor and thyristor controlled series compensator (TCSC) are analyzed in [57], [97], [98] for LVRT and fault current limiter capabilities. To meet the grid code, a study [61] of FACTS devices focused on the use of a STATCOM which has better performance than static synchronous series compensator (SSSC) in terms of voltage stability, flicker mitigation and generator speed stability. For a single machine infinite bus (SMIB) system, a comparison of the STATCOM and SSSC in [99] demonstrates that the STATCOM perform better for first-swing stability but the SSSC's damping capability is better. The SSSC's capability to improved oscillation damping is also described in [94] in which only load variations are highlighted. For power system oscillation damping, the STATCOM and SSSC are compared in many papers [62], [63], and for a SMIB with a conventional source, the latter has better response than the former.

Type A and Type B WTs contain induction generators directly connected to the grid and, as they do not contain a power electronic converter, are not expected to play any role in generating harmonics that cause significant voltage distortions [11]. Again, there is no agreed convention for measuring harmonics emissions from induction machines and, according to IEC $61400-21$, it is not necessary to assess those from a FSWT [11] which is often equipped with a capacitor bank and STATCOM for power factor correction, dynamic voltage support and reactive power compensation. The harmonic impedance of a network can change by connecting a capacitor bank which can cause significant harmonic voltage distortions which add to existing harmonic sources. As a converter can generate harmonics, capacitor banks and STATCOM converters connected to wind farms should be taken into account in harmonic analysis. Harmonic current emissions from the power electronic devices of Type C and Type D WTs must also be considered as they generate harmonics in the kilo Hertz range [11].

The switching and continuous operations of wind farms cause power fluctuations which result in flickers or voltage variations in the grid and may annoy consumers by creating changes in the luminescence from lamps. Power quality conditions in wind farms pertain to flicker and can impose restrictions on integrating WTs in both weak and strong grids depending on their penetration levels and numbers of turbines [100]. There are different mitigation techniques, such as using a switched capacitor, SVC, STATCOM [101], grid impedance power factor control [100], active voltage control [102] and active power control [103], although the last two are discouraged for use in different grids and a STATCOM is not a cost-effective solution to all situations.

A SC is an effective means of efficiently enhancing the stability and reliability of a power system, whereas SSR, the limiting factor, can be mitigated by different approaches, such as, a blocking filter, NGH damper [4] and metal-oxide varistor (MOV) [52]. Again, the cost of a SC bank is approximately five times lower than that of a SVC and one-tenth that of a new transmission line. In [52] and, [54] a SC is implemented on the grid side to improve voltage stability and reduce flicker using conventional generation. Again, in [70], a series converter is introduced at the DFIG stator to improve its LVRT capability and prevent disconnection. In this thesis, to verify the impact of inserting a series compensator on LVRT, the harmonic currents and flicker emissions for both Type A and C WTs are analysed.

The grid codes of different countries related to voltage stability and reactive power consumption is briefly discussed in the next section as they are important for voltage control, which is related to the reactive power drawn by a WT, in order to maintain the stability of a system.

2.2 Integration Aspect of Wind Power to Grid

Dynamic reactive compensation, which is necessary for the operation of a wind farm, depends on the type of wind power generating technology and parameters of the utility while voltage stability can be maintained by a dynamic reactive compensation unit [104], the robustness of which influences the efficiency of the system. Modern grid codes are more stringent than in the past and disconnections of wind generators during disturbances are no longer allowed beyond a certain range known as the LVRT or FRT, the characteristics of which are numerically distinctive from one grid code to another. A detailed review of different international grid codes can be found in [105–107]. The Australian grid code requires wind farms to withstand all types of symmetrical and asymmetrical faults with a voltage drop to zero for 0.4 s followed by a voltage recovery to 0.7 pu for the next 2 s. Like Australia, Canada, Denmark, Germany and New Zealand also require a WT to be connected to the grid even if the voltage at the PCC drops to zero though their post fault-voltage and critical times are different. In the UK, Ireland and USA (FERC), WTs need to be connected to the grid if their fault voltage levels are higher than or equal to 0.15 pu. In the UK, the fault duration time is 0.15 s whereas minimum time for post-fault voltage recovery is set by Sweden, 0.25 s. Voltage restoration to 0.90 pu is common and

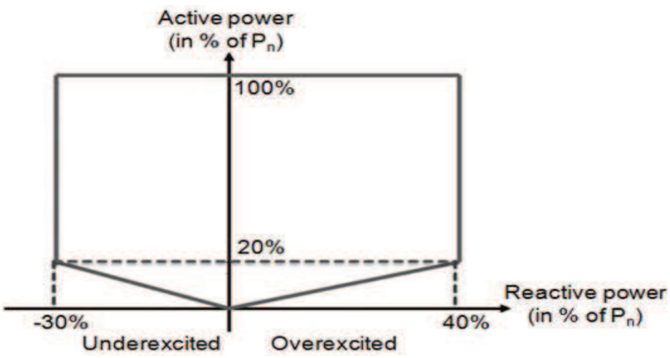

Figure 2.1. P/Q operating range in terms of nominal power P_n [107]

required in the USA, Germany, Ireland and many other countries. Sweden and Denmark, have two LVRT requirements depending on the capacity of the WT and the voltage rating, respectively [107].

Recent grid codes include specific reactive power specifications for wind and, generally, the reactive power regulation capability is expressed by either a specific power factor or specific reactive power range correlated with the active power output of the WT and terminal voltage. Grid codes often require reactive power control in response to network voltage variations. According to the UK grid code, a wind power plant needs to provide full reactive power for ±5 percent variations in the nominal voltage. The German grid code is shown in Fig. 2.1, in which reactive power generation is expressed as within a ±5 percent range of the active power around the rated voltage [107]. In Denmark, Ireland and Ontario, the grid code reactive power ranges are ±0.33 percent of full output although the points at which this requirement is specified are different. In Australia, the range is 0.395 at the point of interconnection throughout the operating range of the voltage and power, with the minimum access standard being 'no capability to supply or absorb' which means a zero reactive power exchange with the system [19]. A 0.95 leading or lagging full load power factor requirement is common in many countries, such as Denmark, the UK and Ireland [19], [107]. According to the Hydro-Quebec, an automatic voltage regulation system is required to contribute to voltage regulations under abnormal and dynamic operating conditions as well as normal conditions.

The German grid code demands a 2 percent injection of reactive current at the low-voltage side of the transformer for each percent of voltage dip [107]. According to the Spanish grid code, reactive power injection is recommended within 150 ms

Table 2.1. Installed wind energy capacities in different Australian states

Wind capacity (MW) / Year	SA	TAS	VIC	NSW	QLD
2011	1019	223	531	186	12
2020	2177	1298	1390	536	79

of fault recovery whereas, in the UK and Ireland, the maximum reactive current during a voltage dip must be produced by WTs.

Wind power generation has become a significant proportion of total power generation. According to a recent report by AEMO, approximately 8000 MW of new wind generation will be added to the existing 2000 MW in the next 20 years [19]. By 2020, approximately 5480 MW of wind generation is expected from the southern region of Australia (Tasmania, Victoria and South Australia) [20]. The present and expected (in 2020) wind power capacities of different states in Australia are shown in Table 2.1. The system adequacy and security will depend on the efficiency of its power flow through weak interconnections of the network via high-voltage (HV) long-distance transmission lines. Most grid integration issues focus on balancing demand, frequency management and voltage stability. The ability to generate reactive power during a fault is another requirement for quickly restoring voltage after a fault. Also fault-current analyses are considered in the Australian, German, Irish, New Zealand and Spanish grid codes because a short-circuit fault draws a large amount of current and then addition of a new wind power-generating unit or the replacement of a conventional unit with a WT can change the fault-current level of a power system [20]. For protection purposes, it is necessary to know the expected fault current level for appropriate protection settings. An asynchronous type of wind generator has a less efficient short-circuit capability than a conventional generating unit though this depends on the technology used to generate power [39]. An increasing wind penetration level can also change the local fault current level of a network.

2.3 Power Quality Issues due to Integration of Wind Power

Any aberration in a system's electrical parameters, i.e. voltage, current or frequency, which may lead to an equipment failure or malfunction is potentially a power quality problem [108]. Major issues hampering voltage stability are voltage fluctuations due to variations in loads and sources, harmonics, flicker and transients. The role of a WT as a power production unit also creates voltage variations not only because of wind fluctuations but also the start-up, emergency shutdown and harmonic current emissions from additional power electronics devices which can cause both the power and voltage to fluctuate. A brief review of voltage sag analysis, harmonics and flicker injection is presented in the following section.

2.3.1 Voltage sag

A voltage sag is defined as a decrease in the root mean square (rms) of the voltage between 0.1 and 0.9 pu for a duration from 1 ms to 1 min [11]. Both the voltage sag or the ride through capacity are serious problems for wind farms and sensitive loads, such as an automated system operated with programmable logic control and adjustable speed drive, are usually initiated by power system faults or the switching of heavy loads and can cause economic damage to both a utility and consumers. Load variations, which are common in a distribution network, can concurrently affect a substation bus and connected feeder during a contingency period, and may cause the tripping of protection devices and the disconnection of loads which can be worsen by increasing DG penetration.

As, according to grid codes, wind farms need not to be disconnected during a fault if its voltage level is higher than a threshold value and not after a fault if its post-fault voltage meets the minimum specified voltage after a certain period of time, a voltage stability analysis is required both during and after a fault. A voltage sag analysis is an assessment that shows the remaining voltage during a fault, the frequency of occurrence of voltage sag in a year and the LVRT capability for dealing with post-fault voltage recovery. A major concern in grid codes for wind energy integration, besides the severity of a voltage dip, is the capability of withstanding successive faults. According to Energinet, wind farms should be capable of coping with the following events [109]:

- at least 2 single-phase faults within 2 min and at least 6 single-phase faults within 5 min;
- at least 2 two-phase short-circuit faults within 2 min and at least 6 two-phase short-circuit faults with 5 min; and
- at least 2 three-phase short circuit faults within 2 min and at least 6 three-phase short-circuit faults within 5 min.

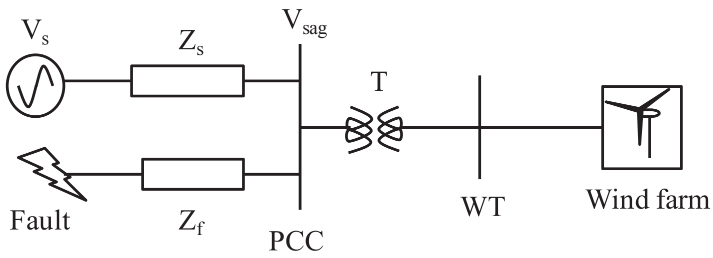

Figure 2.2. Voltage divider model

Broadly, voltage dips are categorised as either balanced, which are generated by three-phase fault, or unbalanced, which are generated by single-phase and two-phase faults. A voltage sag can also be characterised by sag magnitude, duration and frequency. The ABC classification of dips depending on their phasor characteristics is well described in [108], where class A is characterised as a symmetrical fault and B to G asymmetrical faults. A voltage sag characteristic generated at a fault location can be shifted during propagation through a network due to changes in its phasor components while passing a transformer [109]. If a sag's frequency is high and the remaining voltage during the sag is low, the sag is said to be severe.

In this chapter, using a voltage sag tool, short-circuits at selected load points within the system are calculated by the failure data of the system components to extract the voltage sag probability until the protection system disconnects the defective component. A voltage sag analysis is initiated at a specific load point and proceeds to the neighbouring busbars until the exposed area limit, which is the critical remaining voltages of all busbars, is reached. If the result is a volt age higher than this limit, short-circuit calculation does not proceed. If the short-circuit impedances and voltages of all load points are known, the remaining voltage at the busbar is estimated. Network topology is another consideration in voltage sag analysis. Most low-voltage (LV) networks are radial types and mainly responsible for both deep and shallow sag, whereas a HV network is a meshed type which seems to cause moderate sag [110].

Voltage sag characteristics are well illustrated by the voltage-divider model shown in Fig. 2.2, and the remaining fault voltage, V_{sag}, can be expressed by the following equation, where V_{s} is the pre-fault voltage from which the sag is calculated, Z_{s} is the source impedance and Z_f is the impedance between the source and fault location.

$$V_\mathrm{sag} = V_\mathrm{s} \frac{Z_\mathrm{f}}{Z_\mathrm{f} + Z_\mathrm{s}} \tag{2.1}$$

The difference between the source and fault impedances not only causes a substantial voltage drop but also gives rise to the phase-angle jump phenomenon [111].

2.3.2 Harmonics distortion

When a sinusoidal voltage is applied to a non-linear load, the current becomes non-sinusoidal and is responsible for voltage distortion due to a non-sinusoidal voltage drop in the line. The distorted waveform is the sum of the harmonics and inter-harmonics, i.e., sinusoids with frequencies equal to integer and non-integer multiples of the fundamental frequency, respectively [112]. The appearances of harmonics and inter-harmonics cause malfunctions of the protective and measuring devices, over-heating of neutral conductors, shortening of equipment life, light fluctuations, asymmetry and core saturation of the transformer and thermal ageing of the induction motor load [113], [114].

The PWM converter of the STATCOM and DFIG is modelled as an unbalanced harmonic source and the load is modelled as type C equipment. Grid codes limit on the harmonic current injection of a WT at the PCC. According to IEC $61000-4-7$, the harmonic current of order n, I_n, can be represented by the following equation [11] by considering the aggregation of N harmonic sources if the $n < 5$, $5 \leq n \leq 10$, $n > 10$ exponent α is 1, 1.4 and 2, respectively.

$$I_\mathrm{n} = [\sum_{k=0}^{N} I_\mathrm{n,k}^{\alpha}]^{\frac{1}{\alpha}} \tag{2.2}$$

Equation (2.2) describes a 'second summation law' which is applicable for both the harmonic voltage and current.

EN 50160 specifies a total harmonic distortion (THD) of $\leq$ 8 percent in the defined range of the relative magnitude, where the 5th order has the highest magnitude of 6 percent [11] for the current harmonics, those up to the 50th order have to be specified. Generally, most industrial standards follow IEEE standard 519 for the harmonic governing of a wind power plant, as shown in Table 2.2 [115]. According to IEC standard $61800-3$, the harmonic current emissions of types C and D wind farms are assigned odd and even-order harmonics for frequencies up to 50 times the fundamental grid frequency, as shown in Table 2.3 [116]. According to Swedish standard SS $421-18-11$, the odd harmonics should not exceed 4 percent and even 1 percent with a THD of 6 percent [117]. According to IEEE standard, $519-1992$, depending on the maximum SCC ratio and demand current, the harmonic emissions given for a distribution network (120 V to 6.9 kV) can be found in [118].

Table 2.2. Current distortion limits for transmission system > 161kV

Harmonic order	< 11	$11 \leq n < 17$	$17 \leq n < 23$	$23 \leq n < 35$	$35 \leq n$	TDD
Limit (%)	2.0	1.0	0.75	0.3	0.15	2.5
Limit (A)	3.4	1.7	1.3	0.5	0.3	4.3

Table 2.3. Current emission limits with THD ≤ 5 percent

Harmonic order	< 11	$11 \leq n < 17$	$17 \leq n < 23$	$23 \leq n < 35$	$23 \leq n < 50$
Odd (%)	4.0	2.0	1.5	0.6	0.3
Even (%)	1.0	0.5	0.4	0.2	0.1

2.3.3 Flicker

As specified in IEEE standard 1453-2011, any noticeable change in illumination levels due to a voltage fluctuation in an electrical power system is termed flicker [103] which is a problem perceived mainly in lighting equipment. A flickermeter calculates flicker severity according to fluctuations in a voltage signal measured based on the responses of an incandescent lamp to voltage variations by considering the human eye and brain responses to variations in illumination [47]. The human eye is most sensitive to incandescent lamps but least sensitive to fluorescent lamps as its reactions differ with changes in dynamic voltage and frequency [103], [119].

A variation in wind speed of 1 m/s produces a 20 percent change in the magnitude of a power fluctuation [47]. The amplitudes of voltage fluctuations in a wind farm depend on many factors, such as wind variations, tower shadow effect, grid strength, i.e., SCC ratio, WT topology, grid impedance angle, number of operating turbines, spacing between turbines, turbulence intensity and switching period. Variable-speed wind farms potentially generate less flicker than fixed-speed wind farms due to their capability to control speed that helps to smooth a machine's torque and 3p oscillations. If the number of WTs is increased to produce the same amount of power as that produced by a fewer number, N, with higher capacities, the flicker emission level is found to be lower from a wind farm with more turbines of smaller sizes [103] and the attenuation rate is $\sqrt{N}$. Again, a weak grid with a low XRR actuates higher levels of flicker than a strong grid with a high one.

The flicker coefficient, $C(\psi_{\mathrm{k}})$, flicker step factor, $k_{\mathrm{f}}(\psi_{\mathrm{k}})$ and voltage change factor, $k_{\mathrm{u}}(\psi_{\mathrm{k}})$ are some normalised measures of flicker and voltage variations during continuous and switching operations and their expressions are given in equations (2.3), (2.4) and (2.5) [11], [47], the parameters of which are sensitive to the network phase angle, ψ_{k}. The short-circuit apparent power of the grid, S_{k}, also depends ψ_{k}. As the conventional flicker curve is based on a single frequency distribution, it is limited for measuring the flicker emissions of wind farms which are characterised as commutative frequencies (0 to 10 Hz) in the output power spectrum. According to the IEC standard, the flicker severity, P_{st}, needs to be calculated for a 10 min period and the flickermeter standard for calculating P_{st} is also specified while good descriptions of the different parts of a flickermeter are provided in [47]. In the following equations, S_{n} is the rated apparent power of a WT, T_{p} is the duration of voltage variation, N_{wt} is the total number of WTs and v_{max} and v_{min} is the voltage deviations during the switching period.

$$C(\psi_{\mathrm{k}}) = P_{\mathrm{st}} \frac{S_{\mathrm{k}}}{S_{\mathrm{n}}} \tag{2.3}$$

$$k_{\mathrm{f}}(\psi_{\mathrm{k}}) = \frac{1}{130} \frac{S_{\mathrm{k}}}{S_{\mathrm{n}}} P_{\mathrm{st}} T_{\mathrm{p}}^{0.31} \tag{2.4}$$

$$k_{\mathrm{u}}(\psi_{\mathrm{k}}) = \sqrt{(}3) \frac{S_{\mathrm{k}}}{S_{\mathrm{n}}} \frac{v_{\mathrm{max}} - v_{\mathrm{min}}}{v_{\mathrm{n}}} \tag{2.5}$$

The short-circuit apparent power can be calculated from a fictitious reference grid for which the fictitious flicker level index is calculated using a flickermeter and defined as,

$$S_{\mathrm{k}} = \frac{v_{\mathrm{n}}^2}{\sqrt{R_{\mathrm{k}}^2 + X_{\mathrm{k}}^2}} \tag{2.6}$$

where V_n is the nominal voltage of the grid. The phase angle of the fictitious grid is

$$\tan(\psi_\mathrm{k}) = \frac{X_\mathrm{k}}{R_\mathrm{k}} \tag{2.7}$$

Short-term flicker and long term flicker are calculated by [11],

$$P_\text{st-sw} = \frac{18}{S_\mathrm{k}} N_{10} [\sum_{i=1}^{N_\mathrm{wt}} [k_\mathrm{f,i}(\psi_\mathrm{k}) S_\mathrm{n,i}]^{3.2}]^{0.31} \tag{2.8}$$

$$P_\text{lt-sw} = \frac{8}{S_\mathrm{k}} N_{120} [\sum_{i=1}^{N_\mathrm{wt}} [k_\mathrm{f,i}(\psi_\mathrm{k}) S_\mathrm{n,i}]^{3.2}]^{0.31} \tag{2.9}$$

$$P_\text{lt-cont} = P_\text{st-cont} = \frac{1}{S_\mathrm{k}} [\sum_{i=1}^{N_\mathrm{wt}} [C_\mathrm{i}(\psi_\mathrm{k}) S_\mathrm{n,i}]^{2}]^{0.5} \tag{2.10}$$

where suffix sw denotes switching operation and cont denotes continuous operation.

The relative voltage change due to switching operation of wind farms is expressed as

$$d_\text{u-sw} = 100 k_\mathrm{u}(\psi_\mathrm{k}) \frac{S_\mathrm{n}}{S_\mathrm{k}} \tag{2.11}$$

The compatibility levels of flicker emissions vary in different grid codes. Generally, P_st remains between 0.35 and 1 and P_lt between 0.1 and 0.8 and their limits depend on the interconnection voltage level, number of operating turbines and their sizes. According to the IEC standard, the compatibility limits of a feeder are $P_\mathrm{st} \leq 1$ and $P_\mathrm{lt} \leq 0.8$, which are the cumulative emissions of flicker from the generators and loads connected at that feeder. For an individual wind farm's flicker emissions, $P_\mathrm{st} \leq 0.35$ and $P_\mathrm{lt} \leq 0.25$. The Swedish grid code also specifies a flicker emission rate depending on the number of wind generators. For a single wind farm, the maximum allowable long-term emission rate is 0.1 and, for several wind farms with the same feeder connection, the rate is ≤ 0.25 [120]. Like the subdivided flicker rate of the planning level specified by the IEC [121], Denmark's regulation for the emission rate depends on the voltage level. If a wind farm is connected to a network with a voltage level higher than 35 kV, the long-term flicker rate should not exceed 0.35, otherwise it is limited to 0.5 [103]. In France, the flicker compatibility level depends on the size of the wind farm with 5 MW or lower allowed to emit a maximum P_st of

0.35 and a linear increase in emissions up to a maximum 0.44 is permitted for larger sizes [121].

2.4 Conclusion

In this chapter, literatures are reviewed based on the voltage instability and power quality issues of wind farms. Relevant grid codes are also analysed in Section 2.2 and Section 2.3. Voltage regulation is an important factor which is presented by correlating reactive power, active power, power-factor or reactive current depending on grid codes. Section 2.3 also provides a brief description of flicker, voltage dip and harmonic related power quality issues. The next chapter will describe the modelling of different parts of a power system including wind energy conversion system and FACTS devices used in this thesis.

Chapter 3

Power System Dynamic Modelling

3.1 Introduction

The modelling of a power system is an area of evolving interest in application involving transmission and distribution management and control systems [122]. Most analyses in power system research begin mainly with the formulation of appropriate models for simulations to provide the accuracy necessary for the planning and operation of modern power systems. Depending on the purpose of an analysis, the same physical system can be represented by different models with assorted degrees of complexity [123]. Models implemented for analysing the continual operation of a power system are typically more extensive and complex than those used for planning and, generally, 100 to 1000 sets of different classes of information are involved in manipulating those operational models [122].

According to G. Andersson [124], in power system analysis, a model must appropriately describe the interactions among different quantities in a time frame by accurately representing their behaviour in the form of mathematical linear or nonlinear equations or relationships and considering the network's laws and operational limits. In a strict mathematical sense, most variables related to system modelling vary with time as, in a power system, small load changes and switching actions are spontaneous and generate small transients with very fast damping, a situation regarded as the steady-state. As a power system predominantly operates in a steady-state mode in which variations in its variables are too small to affect the dynamic time-varying model, can be analysed using a set of algebraic equations; an example of which is a set of algebraic equations which perform a load-flow to extract the initial conditions of different buses.

A dynamic phenomenon in a power system is initiated by a disturbance in it which results in large oscillations. Different types of events, such as an insulation failure, a flashover of line initiated by a lightning stroke or accidental faulty operation, can launch a variety of different dynamic phenomena in a system which can cause deflection in its variables from its steady-state equilibrium point. In such a case, as algebraic equations will no longer be more an appropriate representation, the employment of a dynamic model, i.e., a set of differential time-varying equations, is useful. Although, these types of dynamic events are common in a power system, representing all its equipment in a great deal of detail can increase the complexity of a large power system analysis as enormous amounts of parameter data are required. To provide a deeper insight into, and easier interpretation of, such a complex network, deriving a relevant simplified approximation of it which correctly captures its dynamic phenomena of interest is beneficial for analysis. For instance, to overcome the undesired situation of representing a large wind farm using individual turbines, shafts and generator models, which increases complexity and leads to time-consuming simulations, aggregating all or a part of it is a common practice for stability studies involving large power systems.

A power system's components, such as conventional generators and their exciters, wind generators and other renewable sources, dynamic loads, flexible AC transmission system (FACTS) and switching devices, exhibit dynamic characteristics during an event which can affect its stability [125]. As, currently, a power system comprises a number of intermittent sources, including wind energy, its nature is far more divergent than in the past due to the integration of distributed generator (DG)-units at load levels and the increased use of non-linear loads. Distribution networks are characterised as active rather than passive with a bi-directional power flow. To understand the more challenging dynamic processes of a complex interconnected network and details of its performance, its proper modelling is the primary step. An incorrectly structured model or improper selection of parameters can produce erroneous conclusions which may lead to an over-estimated stability margin with misleading system operation and control or an impractical application approach involving increasing computational time and costs [125].

As the dynamic nature of a wind turbine (WT) due to its different parts, i.e., turbine shaft, generator, gear box and, sometimes, a converter unit, has both adverse and constructive effects on an interconnected power system [126], it is very important to use an appropriate model of a wind power generation system. The model of a doubly-fed induction generator (DFIG)-based wind generator includes its aerodynamics, its turbine shaft, DFIG machine, DC-link capacitor dynamics, and its rotor-side converter (RSC) and grid-side converter (GSC) control systems [127]. Whereas, fixed-speed wind turbine (FSWT) is much simpler than a DFIG as it does not include any converter or DC-link capacitor dynamics due to its short-circuited squirrel cage rotor and has the advantages of being simple, robust and reliable, less costly and well-proven although its disadvantages are an uncontrollable reactive power consumption, mechanical stress and limited power quality control [11]. Different types of WT systems are described and compared in [8] in which emphasis is placed on brush-less generator and direct drive generators as alternative to the DFIG to meet the grid code requirements and avoid the problem of maintaining the brush and reducing loss in the gear box [8]. However, for a full converter, its loss is increased and the system becomes expensive [10].

The dynamic states in a power system can be divided into three groups: electromagnetic transients (EMTs); electro-mechanical swings; and non-electrical dynamics [124]. Electromagnetic transients lie in the frequency range from 100 Hz to several MHz whereas the other two have ranges from 0.1 to 3Hz and tens of Hz, respectively. Depending on the level of detail in its model, an induction generator can be represented in different ways, such as EMT [12], [127], [128] (considering stator transients), electromechanical transient [13], [129], [130] (neglecting stator transients) and steady-state models. In the steady-state model, as all the dynamics related to the electrical components are assumed to be zero, it is not very suitable for analysing a power system. Instead of a full-order model, a reduced-order model of a WTs is analysed in [126], [131].

According to Wasyncuk [132], a WT's drive train can be seen as a multi-mass system consisting of three inertias, the generator rotor, turbine hub and blades, which exhibit multi-torsion modes [26]. Although [13], [133], [134] do not consider the shaft model, one-mass model [12], two-mass model [71], [129] and three-mass shaft models [135] are considered in many studies in the literature. Neglecting a shaft model can give a misleading idea about stability but a two-mass model is sufficient for a stability analysis.

DC-link dynamics and grid-side filter are important parts of a DFIG that needed to be accounted [13], [71] while its converter block dynamics related to its power electronics are often neglected due to their low impact on a power system network.

3.2 Modelling of Power System Devices

This section provides an overview of the modelling processes for the power system devices used in this thesis, with their interfaces to the network. Source and load are the important parts of power system that will be discussed in this section.

The next two section will discuss the modelling of different parts of FSWT and DFIG as the parts of wind power generation system and modelling of FACTS devices.

3.2.1 Modelling of synchronous generator

The synchronous generator is the most widely used generator in the power industry as it can control a system's active and reactive powers independently according to the grid requirements. Due to its parameter variations, for a load change or network disturbance, the power demand of a the network changes frequently. Its real and reactive powers are independently controlled by a load frequency control loop and an automatic voltage regulator (AVR). As its reactive power is less sensitive to the changes in frequency and depended mainly on voltage magnitude, to control the reactive power flow, its generator is equipped with an excitation system that maintains the voltage. The field excitation is generally controlled using the AVR which maintains its terminal voltage at a specified level. An increase in reactive power demand, which is mainly of an inductive type is accompanied by a drop in terminal voltage and vice versa and these changes are sensed by a sensor or transducer which can be simply represented by a first-order transfer function [136]. To increase damping, a power system stabiliser (PSS), which measures changes in speed and applies a control signal to the AVR so that it changes the input electrical torque in proportion to the change in the angular velocity.

The synchronous generator can be modelled by the following set of non-linear differential equations [33], [71], [137]:

$$\dot{\delta} = \omega_{\mathrm{s}}(\omega - 1) \tag{3.1}$$

$$\dot{\omega} = \frac{1}{2H}[P_{\mathrm{m}} - E'_{\mathrm{q}}I_{\mathrm{q}} - (X'_{\mathrm{d}} - X'_{\mathrm{q}})I_{\mathrm{d}}I_{\mathrm{q}} - D\omega] \tag{3.2}$$

$$\dot{E}'_{\mathrm{q}} = \frac{1}{T'_{\mathrm{do}}}[E_{\mathrm{fd}} - E'_{\mathrm{q}} - (X_{\mathrm{d}} - X'_{\mathrm{d}})I_{\mathrm{d}}] \tag{3.3}$$

$$\dot{V}'_{\mathrm{tr}} = \frac{1}{T'_{\mathrm{r}}}(V_{\mathrm{t}} - V_{\mathrm{tr}}) \tag{3.4}$$

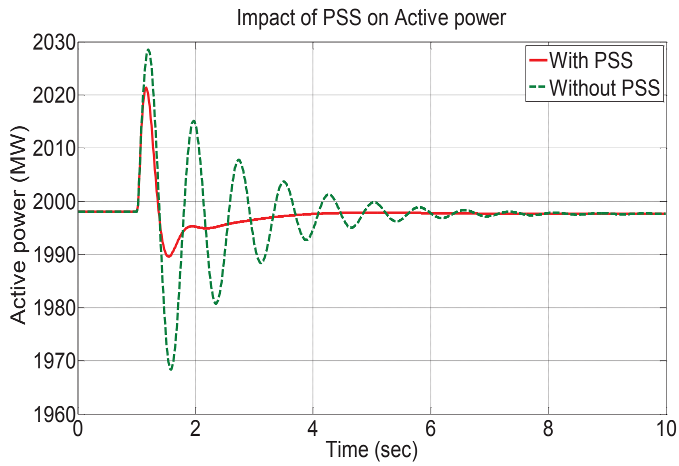

Figure 3.1. Impact of PSS on active power using IEEE STAB1 [138]

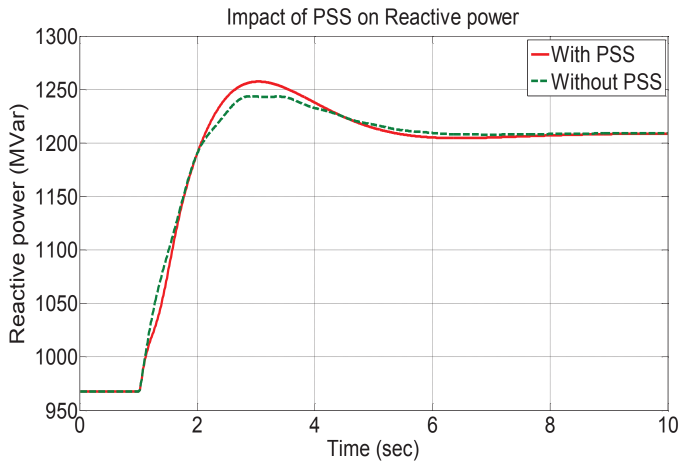

Figure 3.2. Impact of PSS on reactive power using IEEE STAB1 [138]

The transfer function of a classical PSS can be represented by the following equation as it comprises a washout filter followed by a lead compensator and limiter.

$$G_{\mathrm{PSS}} = K_{\mathrm{stab}} \left(\frac{sT_{\mathrm{w}}}{1 + sT_{\mathrm{w}}} \right) \left(\frac{1 + sT_1}{1 + sT_3} \right) \left(\frac{1 + sT_2}{1 + sT_4} \right) \tag{3.5}$$

The influence of a PSS is shown in Fig. 3.1, Fig. 3.2 and Fig. 3.3 in which its improved damping capability as a result of step response test of the AVR for a single-machine infinite-bus (SMIB) system is evident. The network parameters are given in Appendix I.

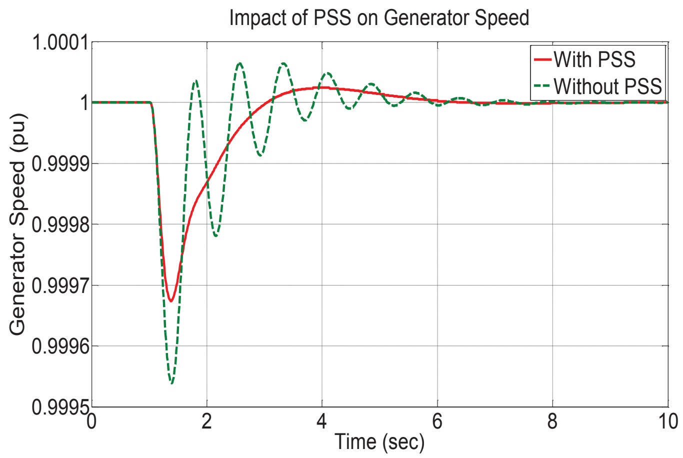

Figure 3.3. Impact of PSS on generator speed damping using IEEE STAB1 [138]

3.2.2 Modelling of load

For a power system, load modelling is important as high or low load conditions might lead to too low or too high voltage, respectively, and cause voltage instability. Generally, power system load models are classified into two categories: static and dynamic.

The static model of a load is time-invariant and can be represented as an algebraic function of the voltage magnitude and frequency [139]. The voltage dependency of load is generally described by the following exponential representation [139], [140].

$$P = P_o \left(\frac{V}{V_o}\right)^a \tag{3.6}$$

$$Q = Q_o \left(\frac{V}{V_o}\right)^b \tag{3.7}$$

The model represents constant power, constant current or constant impedance characteristics depending on whether the exponents a and b are 0, 1 or 2, respectively. Representing an individual load by an identical model is impractical and also difficult to estimate. In a stability analysis, for a typical load bus composed of a large number of devices, load composition is used while, for a composite load, the exponent values in equations (3.6) and (3.7) depend on its aggregated characteristics are used; the usual ranges of these exponents can be found in [139].

The polynomial model is an alternative load model widely used to represent the voltage dependency of load. It is also known as the ZIP model as it represents a proportion of each element of the constant impedance, constant current and constant power components. In DIgSILENT, the polynomial model of load is used with a scaling factor [141], [142].

A different component-based approach to modelling load is described in [143], [144]. The delivery points of a bulk power system are categorised into load classes, such as industrial, commercial, residential, agricultural, etc., which are sub-divided into load components and, according to their characteristics, an aggregated composite model is derived. The drawback of this model is its inability to capture the transient voltage, active and reactive powers, and steady-state Q-V responses [139], [144].

The static model is justified for such cases in which responses of the composite load to voltage and frequency changes are sufficiently fast to reach steady state quickly. As 60 to 70 percent of the total energy supplied by a utility is consumed by the motor load [139], its load dynamics can be significantly affected with the integration of embedded generation [33]. The dynamic non-linear load model greatly influence inter-area oscillation, voltage stability, long-term stability and small-signal stability analyses and detail of it can be found in [145]. In this study, induction motor loads are considered as dynamic loads as they, in particular, are the workhorses of the electrical power industry. The modelling of an induction machine is described in Section 3.3.3, with the only difference between its generation and motoring modes the change in current direction in their characteristic equations. The same scenario also applies to a synchronous motor.

A low-power consumption lamp, induction motors with irregular magnetising current associated with their saturated iron-cores, and all equipment with built-in switching devices, i.e., internal loads with non-linear voltage or current characteristics, are potential sources of harmonic currents which cause harmonic voltage drops across the impedance of a line while a voltage magnification is caused by the reactive load in conjunction with the cable capacitance. Therefore, for harmonic analysis, load modelling is significant and for harmonic current limitations, electric equipment are classified as belonging to Class A, B, C or D. Portable tools are Class B, lighting loads are Class C and equipment with a specified power of $\leq$ 600 W, such as computers and television receivers, are Class D while balanced three-phase equipment and other equipment not considered in the other three classes are included in

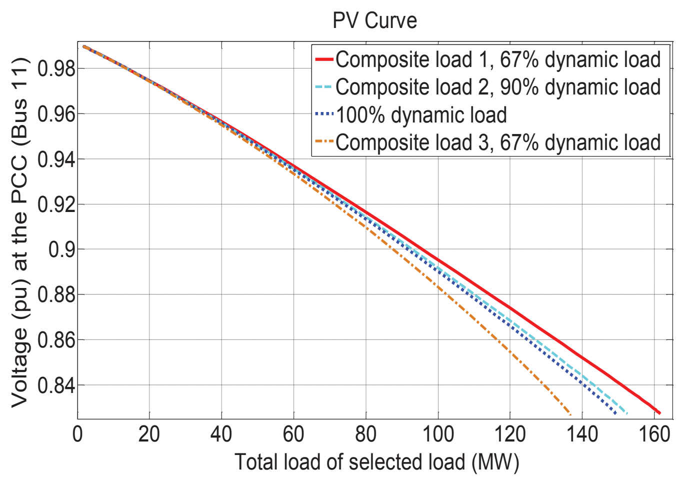

Figure 3.4. Impact of load modelling on PV curve

Class A. The limits of the harmonic currents for the odd and even orders of these four classes are given in [146]. For harmonic analysis, harmonic current emission of loads are modelled by considering these limits. More details of the harmonic domain modelling of loads are well described in [113].

The impacts of different load modelling on the stability criteria are shown in Fig. 3.4 in the form of PV curves. PV curve is an effective tool for analysing voltage stability limit which represent the maximum possible load of each bus or selected bus in terms of critical voltage and collapse margin [147]. Composite loads 1 and 2 have the same type of dynamic load characteristics, i.e., the same critical and normal operating slips. With an increase in dynamic load from 67 percent to 90 percent the critical stability margin reduces and using a 100 percent dynamic load further decrease the stability limit. Composite load 3, with a 67 percent dynamic load, is modelled with a different type of dynamic load but the same proportion of static load. This combination is seen to reduce the stability margin by more than that using a 100 percent dynamic load. Load modelling significantly affects stability and power quality due to their dependance on voltage and frequency. The responses shown in Fig. 3.4 are the results from simulations in a test system where a DFIG is connected to an infinite bus.

3.3 Modelling of Wind Generation System

The nonlinear model of a horizontal-axis three-blade WT considered in this thesis is based on a static model of its aerodynamics, a two-mass model of its drive train, and

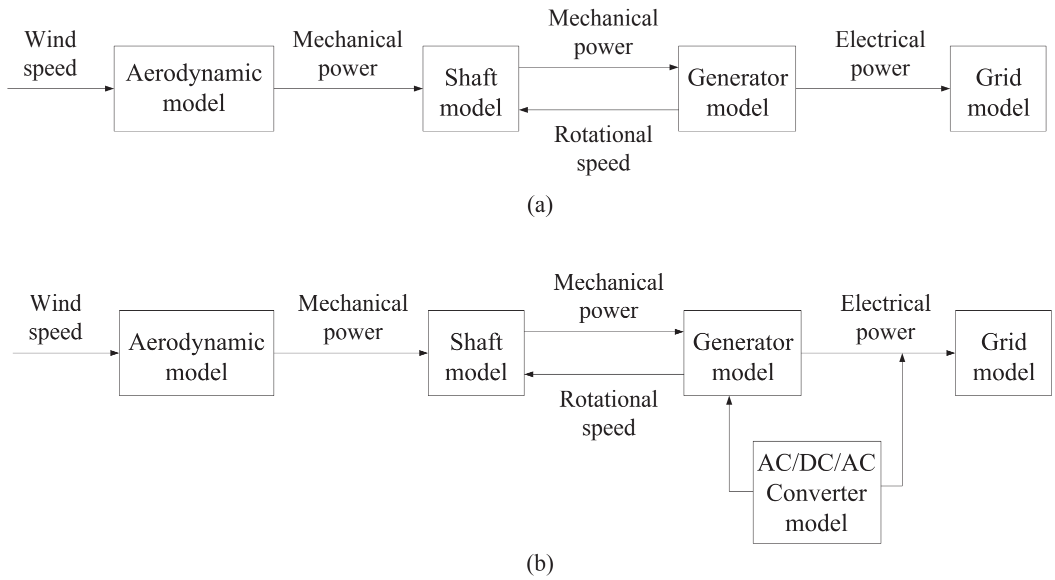

Figure 3.5. General structures of a wind generator (a) FSWT and (b) DFIG

a Park's model of its induction generator. From a structural stability viewpoint, the number of its blades of horizontal axis WT should be odd and greater or equal to 3. Most commercially available modern WTs are three-bladed as more than three blade result in low efficiency due to the interference among them. In the case of a DFIG, its system modelling is extended to include its converter and DC-link capacitor. The basic structures of the FSWT and DFIG WTs are given in Fig. 3.5.

3.3.1 Aerodynamic model

The wind's kinetic energy depends on its velocity and mass and the area through which it passes. If the mass per unit volume of air or air density is ρ and the velocity of the wind is v_w, the kinetic energy, P_w, passing through the area A is [148]

$$P_\mathrm{w} = \frac{\rho}{2} A v_\mathrm{w}^3 \tag{3.8}$$

The total power available in the wind is P_w, only a fraction of which can be extracted by a wind-driven machine. In 1972, A. Betz showed that the maximum fraction of power in the wind which can be obtained by an ideal aero motor is $\frac{16}{27}$ or 59.3% [149] which is known as the Betz limit. Because of aerodynamic imperfections and mechanical and electrical losses within the gearbox, bearings, generator, power converter and other components the acquired power is less than that [148]. Most practical WT rotors with three blades can reach an overall efficiency of approximately 50%. The turbine co-efficient of performance, C_p, which is a function of the tip speed ratio, λ, and blade pitch angle, θ, is a measure of that fraction of the wind energy actually extracted by the WT due to the flow of wind through the swept area which the aerodynamic effects of the WT's blades convert into aerodynamic torque. For a horizontal axis WT, the cross section area, A, is the circular section covered by the rotating blade of the WT and is given by πR^2, where R is the rotor radius. The aerodynamic torque, T_ae, produced by a WT can be represented as in [11], [150] as

$$T_\mathrm{ae} = \frac{\rho}{2\omega_\mathrm{m}} \pi R^2 v_\mathrm{w}^3 C_\mathrm{p}(\lambda, \theta) \tag{3.9}$$

$$P_\mathrm{ae} = T_\mathrm{ae}\omega_\mathrm{m} \tag{3.10}$$

According to [151], C_p is expressed as

$$C_\mathrm{p} = c_1 \left(\frac{c_2}{\lambda_\mathrm{i}} - c_3\theta - c_4\theta_5^c - c_6 \right) exp \left(-\frac{c_7}{\lambda_\mathrm{i}} \right) \tag{3.11}$$

A parametric approximation of the torque coefficient, λ_i, in terms of λ and θ is given by

$$\lambda_\mathrm{i} = \frac{1}{\lambda + c_8\theta} - \frac{c_9}{\theta^3 + 1} \tag{3.12}$$

In equations (3.11) and (3.12), c_1 to c_9 are constants which depends on the manufacturer's data. In [11], these constants are given for different types of WTs which shows that, as variations in approximations from one WT to another are not great, any set of data can be selected. A detail review on different factors affecting wind energy conversion system can be found in [152].

A graphical representation of the parameters involved in equation (3.11) is shown in Fig. 3.6 and the mechanical power as a function of the rotor speed with changing wind speeds in Fig. 3.7. The maximum value of C_p that can be obtained for a 0 ° pitch angle and a tip speed ratio of 6.0 is 0.48 which is known as the optimal value of λ. The tip speed ratio, λ, is an important parameter in a dynamic model of a WT as it is the only means of torque control. To capture maximum efficiency, it is necessary to vary the rotational speed of the WT to maintain λ close to its optimal value as the wind speed is uncontrollable and the radii of the blades are fixed. This is one of the advantages of a VSWT over a FSWT, since its rotor speed can be

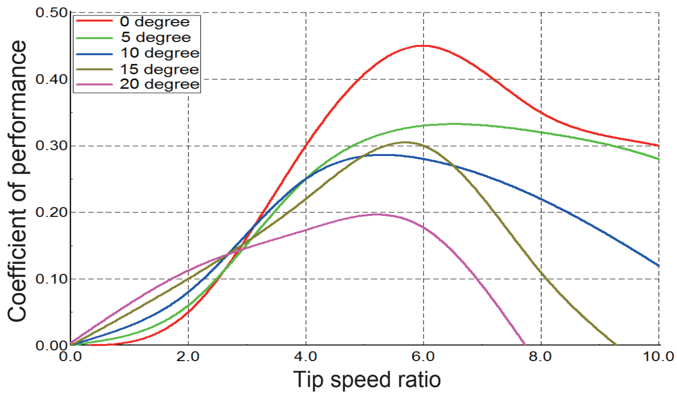

Figure 3.6. Typical C_p versus tip speed ratio λ curves for different pitch angles, θ

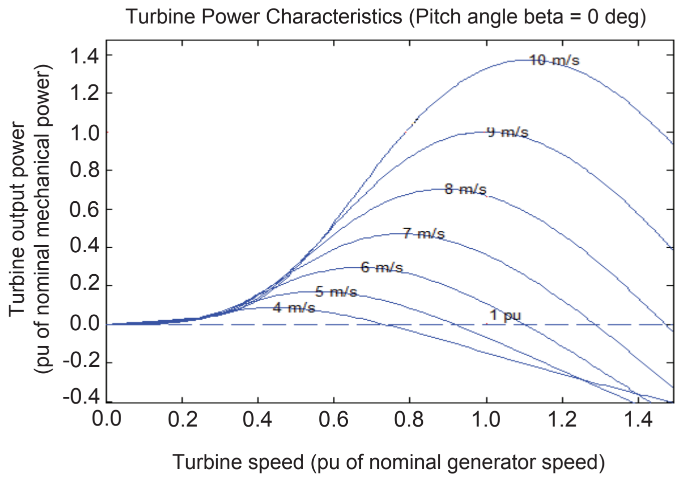

Figure 3.7. Typical P versus rotor speed, ω_r, curves for different wind speeds, v_w

varied according to changes in the wind speed to keep λ close to the optimal value. For a typical wind speed profile, a the VSWT captures 2.3% more energy per year than a FSWT [11].

In a stall regulated WT, its blades are designed so that C_p falls dramatically with a high wind speed to prevent the turbine from over-speeding and limit the maximum shaft power to the rated value. Most modern WTs are pitch-regulated, i.e., C_p is controlled by a blade pitch adjustment which allows the energy capture to be optimised over a wide range of wind speeds. Even if the rotational speed of the shaft is constant, over-speed protection is still provided through large adjustments in the pitch angle. For power levels below the rated one, the turbine speed is controlled primarily by the electrical power in order to specify the speed reference.

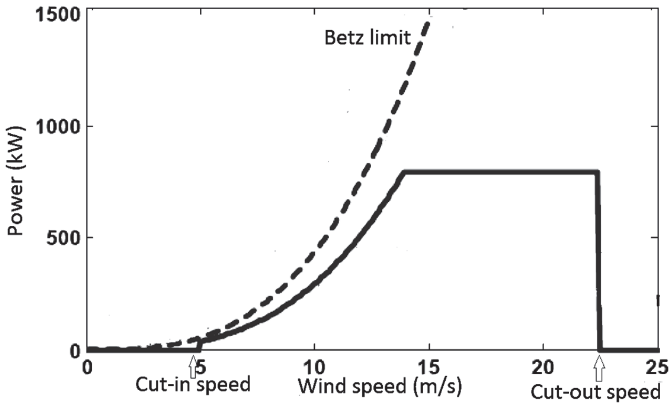

Figure 3.8. Generated power, P, versus wind speed v_{w} [153]

The relationship between the energy of the wind flowing through the WT and the mechanical power available at the rotor is shown in Fig. 3.7. For power levels above the rated one, the rotor speed is controlled mainly by the pitch control, with the speed being allowed to transiently rise above the reference to a threshold point. Typically, a high wind speed threshold is 25 m/s.

There are different methods for calculating the WT characteristic C_{p}; for instance, the blade element momentum method, look-up table and analytical approximation. In this research, the last method is used. A typical wind speed power curve, from the cut-in to cut-out speeds, is shown in Fig. 3.8. With an increase in wind speed, the generated power starts to increase up to its rated capacity and becomes constant until cut-out speed is reached which is normally achieved by pitch control or the stall control method. As a FSWT's rotor speed is approximately constant, it can not be used to extract maximum power whereas the variable rotor speed of a DFIG makes that possible.

3.3.2 Shaft model

The shaft system provides a coupling between the turbine rotor's low-speed shaft (9–21 r.p.m) and generator rotor's high speed shaft (900–2000 r.p.m). Validation of a two-mass model against a practical WT was first presented in [154] in which a Danish wind farm was operated in the islanding mode. To match the generator speed to the blade speed, a gear box is necessary and the shaft of the WT can be sectionalised as a multi-mass model. Hinrichsen [155] showed the influence of the drive train model on power system stability for a grid disturbance. For the analysis

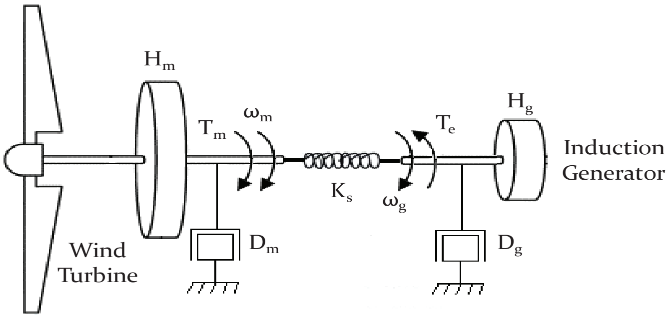

Figure 3.9. Two-mass model of shaft [157]

of power system dynamics, the model of a drive train should have at least two degrees of freedom [155] to represent the first torsional and electrical modes. Due to high damping of the blade mode in a horizontal axis WT, considering the hub and blade inertia separately does not greatly influence the results [155]. There is a strong consensus that a two-mass model is sufficient for a power system stability analysis and that it also reduces the system's complexity. In two-mass model, the drive-train of a WT is modelled as two inertias, those of the WT's shaft and generator rotor, connected to each other through a spring which represents the low stiffness of the drive-train shaft [26]. In [156], a different type of two-mass model, which represents the bending effect of blades by considering the blade tip as a low-speed shaft and the blade root as a high-speed shaft. A structural representation of this two-mass model is shown in Fig. 3.9. Two different damping constants results in a mechanical system with low-speed and high-speed sections connected by a gear-box between them which allows the matching of the generator speed to that of the turbine. The turbine's self damping is due to the aerodynamic resistance of the different parts of the blades and the generator's self damping is due to the mechanical friction and windage. This mutual damping is due to the balancing dynamics between the high-speed and low-speed shafts.

In the literature, the importance of correctly representing the incorporation of a shaft in a model of a WT is given, particularly because of its impact during and after voltage collapses and short-circuits, with those of one-mass and two-mass models given in Fig. 3.10 and Fig. 3.11. Simulations are conducted for a wind farm connected to an infinite bus and the network parameters of which are given in Appendix-II. Mechanical inertia plays an important role in the nature of WT dynamics. A large inertia implies a slow change in mechanical speed which results in significant impact

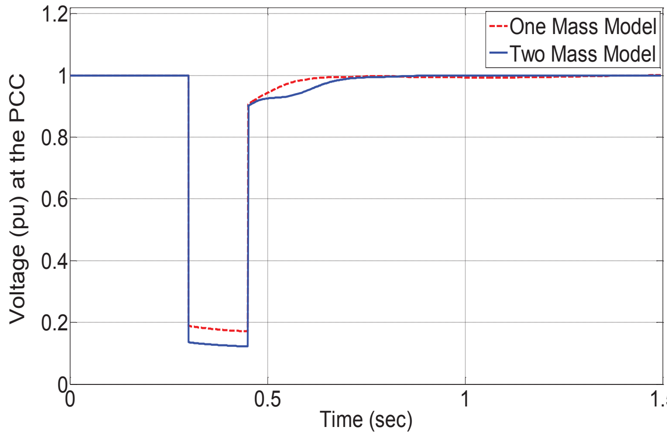

Figure 3.10. Impact of modelling of shaft on voltage at the PCC

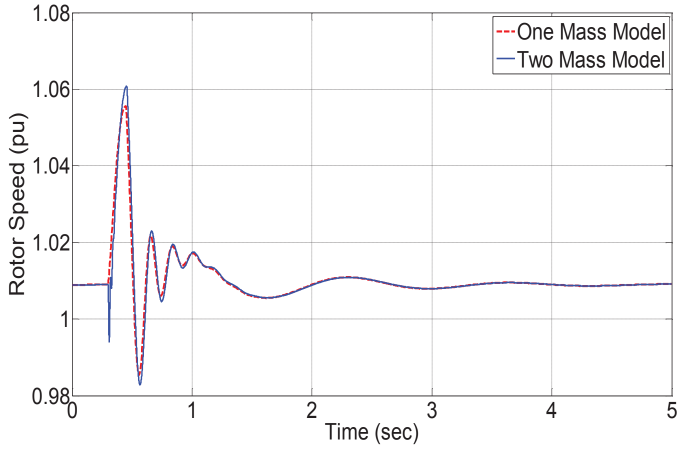

Figure 3.11. Impact of modelling shaft on generator speed

on the controller's response time if the turbine speed is utilised as an input or an error signal in a controller which is a common consideration for controller design.

The shaft dynamics of a WT is represented by a third-order model [129], where ω_{m} and ω_{g} are the rotor speeds of the shaft and generator, respectively, H_{m} and H_{g}, and D_{m} and D_{g} are their inertia constants and torsion dampings, respectively, and T_{e} is the electrical torque. The angular displacement between the two ends of the shaft is denoted by θ_{m} while K_{s} is the shaft stiffness, ω_{s} is the synchronous speed and N_{g} the gearbox ratio. The choice of gearbox ratio depends on the optimum operational speed of the generator and while choosing it, gearbox weight can be a limiting factor as it increases with an increasing ratio [158]. A typical 2–3 MW WTs has a gearbox ratio of approximately 80-100 [26], [159].

$$\dot{\omega}_{\mathrm{m}} = \left(\frac{1}{2H_{\mathrm{m}}}\right)(T_{\mathrm{ae}} - K_{\mathrm{s}}\theta_{\mathrm{m}} - D_{\mathrm{m}}\omega_{\mathrm{m}}) \tag{3.13}$$

$$\dot{\omega}_{\mathrm{g}} = \left(\frac{1}{2H_{\mathrm{g}}}\right)(K_{\mathrm{s}}\theta_{\mathrm{m}} - T_{\mathrm{e}} - D_{\mathrm{g}}\omega_{\mathrm{g}}) \tag{3.14}$$

$$\dot{\theta}_{\mathrm{m}} = 2\pi f\left(\omega_{\mathrm{m}} - \frac{\omega_{\mathrm{g}}}{N_{\mathrm{g}}}\right) \tag{3.15}$$

The shaft stiffness can be defined as

$$K_{\mathrm{s}} = \left(\frac{8\pi^2 f_{\mathrm{T}}^2}{\omega_{\mathrm{s}}^2}\right)\left(\frac{H_{\mathrm{m}}H_{\mathrm{g}}}{H_{\mathrm{m}} + H_{\mathrm{g}}}\right) \tag{3.16}$$

Detail of the derivation of equation (3.16) can be found in [160], where f_{T} is the homogeneous solution of the movement equation. The natural frequency of this primary mode of oscillation is in the range of 1 to 5 Hz. For a WT in the MW range, its mechanical inertia is relatively large with a typical inertia constant, H, of 3 s while, for the generator, it is relatively small, typically about 0.5 s.

Again, the mechanical construction of a WT can be simply represented by a lumped mass model with the lumped inertia constants of the turbine and generator rotor. If a shaft system is relatively low, a two-mass model is used for stability analysis and, if it is greater than or equal to 3 rad, a one-mass model can be used without loss of accuracy [160].

$$H_{\mathrm{l}} = H_{\mathrm{m}} + H_{\mathrm{g}} \tag{3.17}$$

$$\dot{\omega}_{\mathrm{l}} = \left(\frac{1}{2H_{\mathrm{s}}}\right)(T_{\mathrm{m}} - T_{\mathrm{e}} - D_{\mathrm{l}}\omega_{\mathrm{l}}) \tag{3.18}$$

3.3.3 Generator model for FSWT and DFIG

Most WTs use induction generators, especially FSWT, which uses a squirrel cage, and the DFIG, which uses a wound rotor connected to a stator via the RSC and GSC. The third and fifth order models are used in this study and described in this section. If the lumped inertia constant of the generator is larger than 1 s, a third-order generator model is sufficient to represent its behaviour but, for an inertia constant higher than 1 s, a fifth-order generator model is required [125], [160]. Again, where higher frequency modes are significant, it is better to use a fifth-order model, since high-frequency variables related to stator transient quantities may give rise to a pulsating torque [161] and a third-order model does not acknowledge fundamental frequency transients [160].

The generator model is represented in the dq frame [134], [162] by the following equations, where λ_r, λ_s and v_r, v_s and i_r, and i_s are the rotor and stator flux linkages, voltages and currents, respectively, d and q denote the direct and quadrature axis components, respectively, and s, R_r and R_s the slip and machine resistances, respectively.

$$\dot{\lambda}_\mathrm{dr} = \omega_\mathrm{s}(v_\mathrm{dr} - R_\mathrm{r} i_\mathrm{dr} + s\lambda_\mathrm{qr}) \tag{3.19}$$

$$\dot{\lambda}_\mathrm{qr} = \omega_\mathrm{s}(v_\mathrm{qr} - R_\mathrm{r} i_\mathrm{qr} - s\lambda_\mathrm{dr}) \tag{3.20}$$

$$\dot{\lambda}_\mathrm{ds} = \omega_\mathrm{s}(v_\mathrm{ds} - R_\mathrm{s} i_\mathrm{ds} + \lambda_\mathrm{qs}) \tag{3.21}$$

$$\dot{\lambda}_\mathrm{qs} = \omega_\mathrm{s}(v_\mathrm{qs} - R_\mathrm{s} i_\mathrm{qs} - \lambda_\mathrm{ds}) \tag{3.22}$$

$$\dot{\omega}_\mathrm{g} = \left(\frac{P}{2J_\mathrm{g}}\right)(T_\mathrm{m} - T_\mathrm{e}) \tag{3.23}$$

where

$$v_\mathrm{ds} = R_\mathrm{s}(i_\mathrm{ds} - \omega\lambda_\mathrm{qs}) \tag{3.24}$$

$$v_\mathrm{qs} = R_\mathrm{s}(i_\mathrm{qs} + \omega\lambda_\mathrm{ds}) \tag{3.25}$$

$$\lambda_\mathrm{qs} = L_\mathrm{ls} i_\mathrm{qs} + L_\mathrm{m}(i_\mathrm{qs} + i_\mathrm{qr}) \tag{3.26}$$

$$\lambda_\mathrm{ds} = L_\mathrm{ls} i_\mathrm{ds} + L_\mathrm{m}(i_\mathrm{ds} + i_\mathrm{dr}) \tag{3.27}$$

$$\lambda_\mathrm{qr} = L_\mathrm{lr} i_\mathrm{qr} + L_\mathrm{m}(i_\mathrm{qs} + i_\mathrm{qr}) \tag{3.28}$$

$$\lambda_\mathrm{dr} = L_\mathrm{lr} i_\mathrm{dr} + L_\mathrm{m}(i_\mathrm{ds} + i_\mathrm{dr}) \tag{3.29}$$

Equations (3.21) and (3.22), represent the stator transients and, for the third-order model these transients are assumed to be zero which may result in a difference in responses due to the removal of the quickly decaying stator current offset [163]. The representation of an induction generator depends on different phenomena, such as the rotor and stator flux dynamics, eddy current and hysteresis, magnetic saturation, etc. [26], [125]. Including all the dynamics related to these phenomena is not beneficial for stability analysis as not all have a significant impact on stability and they increase the computational complexity of the system. In a normal operating region, the skin effect has a small influence on the low-frequency dynamic behaviour of an induction machine but including it does not increase the order of the system [164] while iron-loss is generally disregarded when the dynamic stability of an IM is the point of interest [165].

In the expression of flux linkages in equations (3.13) and (3.14), v_{dr} and v_{qr} are zero for the FSWT due to the short-circuited rotor of squirrel cage, but not for the DFIG as it uses a wound rotor connected to the grid through converters. For the FSWT, the generated active power, P, and reactive power, Q, can be expressed by the following equations in which the rotor terminals are neglected, as they are short-circuited, while the generator terminal is taken into account because the exchange of P, and Q takes place between the generator and grid only through only the stator terminals [11].

$$P = P_{\mathrm{s}} = v_{\mathrm{ds}} i_{\mathrm{ds}} + v_{\mathrm{qs}} i_{\mathrm{qs}} \tag{3.30}$$

$$Q = Q_{\mathrm{s}} = v_{\mathrm{qs}} i_{\mathrm{ds}} - v_{\mathrm{ds}} i_{\mathrm{qs}} \tag{3.31}$$

In the case of a DFIG, its rotor quantities need to be assessed and the P and Q can be given by [11]

$$P = P_{\mathrm{s}} + P_{\mathrm{r}} = v_{\mathrm{ds}} i_{\mathrm{ds}} + v_{\mathrm{qs}} i_{\mathrm{qs}} + v_{\mathrm{dr}} i_{\mathrm{dr}} + v_{\mathrm{qr}} i_{\mathrm{qr}} \tag{3.32}$$

$$Q = Q_{\mathrm{s}} + Q_{\mathrm{r}} = v_{\mathrm{qs}} i_{\mathrm{ds}} - v_{\mathrm{ds}} i_{\mathrm{qs}} + v_{\mathrm{qr}} i_{\mathrm{dr}} - v_{\mathrm{dr}} i_{\mathrm{qr}} \tag{3.33}$$

The operating region of an induction generator is shown in Fig. 3.12. In the case of a FSWT, its speed is slightly higher than the synchronous speed, ω_{s}, where slip $s < 0$. The advantage of a DFIG is that it can operate in both sub-synchronous ($s > 0$) and super-synchronous ($s < 0$) modes. The induction machine may be considered a rotating transformer as the energy transfer between its stator and rotor of the induction machine takes place in the form of induction [168]. Due to inductive nature, the induction generator absorbs reactive power from its terminals. Due to its non self-excitation, the induction generator takes reactive power from the grid or from

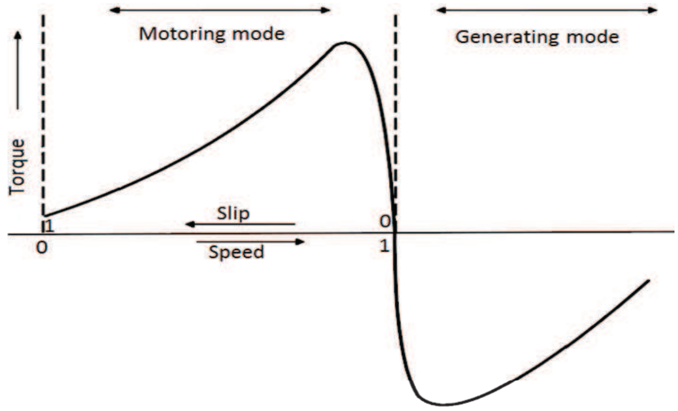

Figure 3.12. Torque-slip characteristic of typical induction machine [166], [167]

some form of capacitive reactor, such as a capacitor or FACTS device, to sustain the rotating magnetic field in the air-gap between its cage rotor and stator [166], [167]. The accuracy of the reduced-order model depends on the machine's parameters and load inertia [169]. With changing winds the rotor resistance of the WT is considered slightly higher than that of normal which also reduces its efficiency. To allow a low cut-in speed, the magnetisation current and no-load stator current are minimised by reducing the magnetic core saturation which also leads to a lower iron loss [151]. The distinctive nature of an induction generator used to produce energy from the wind is further briefly analysed in [161]. The impacts of the third and fifth order models of an induction generator on the rotor current of a DFIG and voltage where the WT is connected are shown in Fig. 3.13 and Fig. 3.14, respectively. This simulation is performed using a test system in which a DFIG is connected to an infinite bus system and with a fifth-order model, the transients are properly captured after a symmetrical fault. The network parameters are given in Appendix-II.

3.3.4 DFIG converter model

For a DFIG, its back-to-back converter connecting its rotor circuit and grid, generally termed the Scherbius scheme [26], is assumed as an ideal converter with a constant DC-link voltage between them. Depending on the voltage-fed current-regulated converter control, a bi-directional power flow is established. Normally, a GSC is equipped with a filter to minimise harmonics due to switching and a RSC is responsible for rotor speed control.

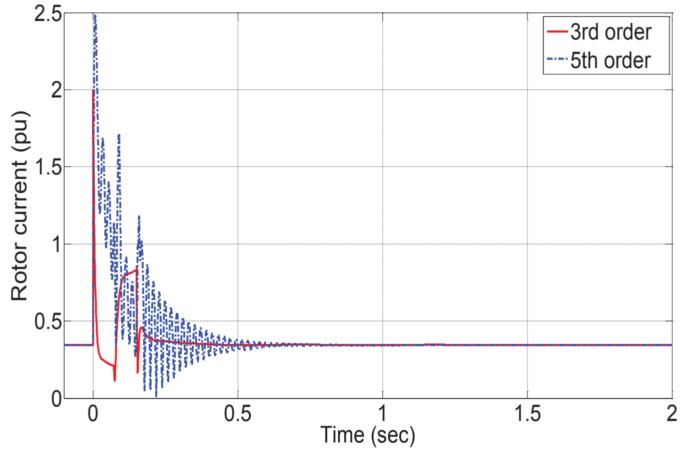

Figure 3.13. Impact of modelling generator on rotor current

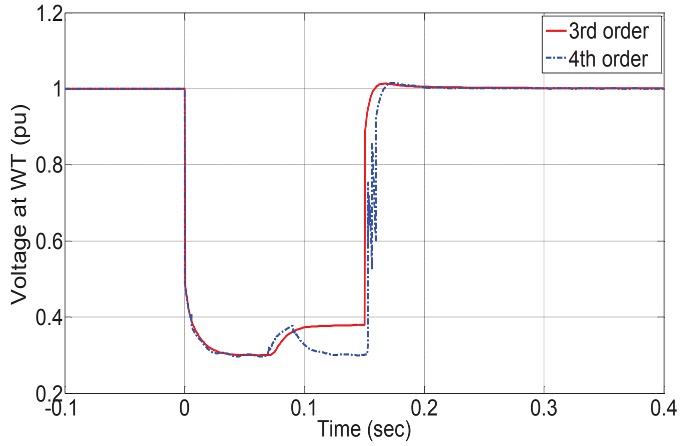

Figure 3.14. Impact of modelling generator on voltage at the WT

The rotor-side current dynamics is described by the following equation, where ω_{SL} is the slip speed with the rotor back e.m.f. E_{dq}, [13].

$$\frac{L_{\mathrm{r}}'}{\omega_{\mathrm{s}}}\dot{i}_{\mathrm{rdq}} = -R_{\mathrm{r}}' i_{\mathrm{rdq}} - j\omega_{\mathrm{SL}} L_{\mathrm{r}}' i_{\mathrm{rdq}} - E_{\mathrm{dq}} + v_{\mathrm{rdq}} \tag{3.34}$$

The terms L_{r}' and R_{r}' are [13]

$$L_{\mathrm{r}}' = L_{\mathrm{r}} - \frac{L_{\mathrm{m}}^2}{L_{\mathrm{s}}} \tag{3.35}$$

$$R'_{\mathrm{r}} = R_{\mathrm{r}} + R_{\mathrm{s}} \left(\frac{L_{\mathrm{m}}}{L_{\mathrm{s}}}\right)^2 \tag{3.36}$$

If L_{g} and R_{g} are the grid-side filter component and i_{gdq} and v_{gdq} the dq component of filter's current and voltage, respectively, the current dynamics related to the grid-side filter can be given as [13]

$$\frac{L_{\mathrm{g}}}{\omega_{\mathrm{s}}}\dot{i}_{\mathrm{gd}} = -R_{\mathrm{g}} i_{\mathrm{gd}} + \omega_{\mathrm{s}} L_{\mathrm{g}} i_{\mathrm{gq}} + v_{\mathrm{gd}} - v_{\mathrm{sd}} \tag{3.37}$$

$$\frac{L_{\mathrm{g}}}{\omega_{\mathrm{s}}}\dot{i}_{\mathrm{gq}} = -R_{\mathrm{g}} i_{\mathrm{gq}} - \omega_{\mathrm{s}} L_{\mathrm{g}} i_{\mathrm{gd}} + v_{\mathrm{gq}} - v_{\mathrm{sq}} \tag{3.38}$$

and the DC-link dynamics is given as [13], [170]

$$C\dot{v_{\mathrm{dc}}} = -V_{\mathrm{dc}}^2 R_{\mathrm{L}} - P_{\mathrm{r}}(t) - P_{\mathrm{g}}(t) \tag{3.39}$$

where, R_{L} is the total loss in the converter, and $P_{\mathrm{r}}(t)$ and $P_{\mathrm{g}}(t)$ the instantaneous output powers of the RSC and GSC converter, respectively.

3.4 Modelling of FACTS Devices

FACTS devices are very popular in power systems because of the rapid developments in power electronics technology and their efficiency. The STATCOM and static synchronous series compensator (SSSC) are the voltage source converter (VSC)-based FACTS devices and the thyristor-controlled series capacitor (TCSC) is the thyristor-based device considered in this study.

The objective of shunt compensation is to make its transmission lines more compatible with the prevailing load condition of a network. Of the different shunt compensation techniques available, those using converter-based technology perform more efficiently as the compensation current is independent of the system voltage. In many works in the literature, a STATCOM is proposed for minimising WT terminal voltage fluctuations, improving the ride-through capability by reactive power compensation and increasing transient voltage stability for both transmission and distribution networks [37], [97], [129], [171], [172]. A STATCOM for controlling VAR in a low-voltage distribution network is studied in [32] using a static voltage analysing tool but this study disregards the dynamic aspect of voltage instability. A STATCOM is also proposed as an efficient means of flicker mitigation in [45], [101] due to the availability of the forced-commutated components which can reduce voltage fluctuations. Voltage dip mitigation is another attractive feature of a STATCOM [173].

Traditionally, series compensation has been used in a long transmission line to increase the power transfer capability of the line by reducing its effective line reactance which is inductive in nature. It also improves steady-state voltage regulation and has been well proven to be highly effective in enhancing the stability of a system and achieving the full utilisation of transmission assets by controlling the power flows in lines [4]. Controllable series line compensation is treated as a cornerstone of FACTS technology as it can prevent loop flows, minimise the effect of a system disturbance and reduce the traditional system's stability margin requirements [4].

To obtain favourable wind conditions and little gearbox noise, most WTs are installed in remote areas and connected to the grid by weak and long transmission lines [159]. Due to the many attractive features of series compensation, it is quite logical to use series compensating devices in transmission lines to increase a network's power flow capacity. The power system oscillation damping capability of STATCOM and SSSC to dampen a power system's oscillations are analysed in [62], [63], where the addition of a SSSC to dampen the rotor angle and load angle oscillations with relatively faster decreases in transient energy during a fault than a STATCOM is detected.

In the literature [97], [98], [171], [174], series compensation is used to enhance the stability and reliability of a system. The current and power flow in the line compensated using a series capacitor (SC) can be represented by the following equations [4]. The degree of compensation is $k = \frac{X_\mathrm{c}}{X_\mathrm{L}}$, where X_c is the reactance of the SC and X_L is the total reactance of the line. If the sending and receiving end voltages are V, then the current in the compensated line can be expressed as

$$I_\mathrm{SC} = \frac{2V}{(1-k)X_\mathrm{L}} \sin\frac{\delta}{2} \tag{3.40}$$

$$P_\mathrm{SC} = V_\mathrm{m} I = \frac{V^2}{(1-k)X_\mathrm{L}} \sin\delta \tag{3.41}$$

The reactive power, Q_c, supplied by the SC is given as [4]

$$Q_\mathrm{c} = I^2 X_\mathrm{c} = \frac{2V^2}{X}\frac{k}{(1-k)^2}(1-\cos\delta) \tag{3.42}$$

Without compensation, the power flow in the line is

$$P = \frac{V^2}{X_\mathrm{L}}\sin\delta \tag{3.43}$$

Therefore, equation (3.44) can be rewritten as

$$P_\mathrm{SC} = \frac{P}{(1-k)}\sin\delta \tag{3.44}$$

With an increase in the degree of series compensation, the power flow in the line will increase and practically, this ratio lies between 25 and 75 percent.

The cost of a SC bank is approximately 10 percent of the cost of a new transmission line and it can be operated reliably in ambient conditions [3]. In the Guichon project, to increase the export of power from Canada to the USA, SC banks increased lines' current carrying capabilities from 1.6 kA to 2.4 kA with 51 percent compensation [3]. Also, series compensation can reduce system loss while achieving improved stability and voltage profiles. Again, the installation of a TCSC in the Kayenta substation, Arizona, increased its transmission line capacity by 30 percent [55] as the capacitor and reactor of the TCSC changed the system's operating voltage due to their dynamic interaction [4].

On the distribution side, as exemplified by the distributed STATCOM [54], distributed SC (D-SC) [56], distributed TCSC (D-TCSC) [56] and distributed static series compensator (D-SSC) [53], [175] are becoming more popular. As WTs have different grid codes that limit their operation [105], [106], it could be factual to analyse the impact of SC on steady-state and dynamic stability, as well as harmonics, flicker and voltage dip characteristics, under the influence of FSWTs and VSWTs in transmission and distribution networks to support grid integration.

For the harmonic domain analysis of a wind farm, a possible harmonic generating source, which includes a high-frequency harmonic filter, turbine auxiliary linear load and converters (for Type 3 and 4 WTs), has been identified by Wind Plant Collector

System Design Working Group [115]. The resonance point of a network depends greatly on the network's impedance which can be changed by the integration of a large wind farm due to the installation of capacitor banks for VAR support, power factor correction and different system configurations. A wind farm may be viewed as a complex chain in which each group is geared with distinctive apparatus for different operational purposes and the accumulation of their effects can shift the natural resonance point whereas the effect of each individual group on the system is negligible.

The industrial practice for harmonic analysis is to consider a harmonic-generating source as an ideal current source. For simplification, the converter and rectifier of a wind farm are often viewed as an ideal current source. The drawback of this type of consideration is that a VSC has a comparatively lower impedance than an ideal current source which is invariant with driving source impedance and other harmonic distortion generating sources [115].

A VSC employed in Types 3 and 4 WTs or reactive compensating equipment, such as a STATCOM, SSSC or unified power flow controller (UPFC), is better characterised as a Norton equivalent source as it accounts for the frequency and phase sequence dependency of impedance related to converter control [4], [115]. A unified harmonic domain modelling of a STATCOM is described in [176] while details of different types of FACTS modelling in the harmonics domains a STATCOM, SSSC and UPFC can be found in [177]. Static VAR compensator (SVC), shunt capacitors and other reactor type filters used in wind farms can be represented as lumped equivalent current injection sources [115].

In this study, the impact of series compensation, with and without a shunt device, is analysed for the voltage stability and power quality issues of FSWT and DFIG wind farms. The modelling of the FACTS device used in this thesis is described in the following, beginning with the converter, which plays an important role in FACTS technology.

3.4.1 Converter model

The VSC is an essential part of a FACTS device and VSC is known as the building block of STATCOM, SSSC, UPFC, interline power flow controller (IPFC) and others, and this concept has some economical and performance advantages over current-source converters [4]. According to the voltage difference between its AC side and its point of connection with the utility grid, a VSC generates a proper current which is injected into the system to control power [173]. With advanced control methodologies, VSC offers rapid and continuous response for dynamic control and reduced requirements for harmonic filtering which allows simultaneous active and reactive power exchanges with additional energy storage devices [159], [178].

A converter is commonly used in a wind generation system to increase the narrow operating speed range of WTs. The total energy losses of the system do not increase with its integration and, for a DFIG, the required rating of the converter is considerably less as it is not directly connected to the grid. Again, the energy loss in an efficient converter is almost negligible and furthermore, using it reduces generator and gear losses [117], [179].

The AC side of a converter model is given by the following differential equation in the rotating dq frame in which it is assumed that the inductors are not saturated and the skin effect is neglected [180], and where L_g and R_g are the filter parameters and v_1 and v_2 are the AC side and grid side voltages, respectively.

$$\dot{i}_\mathrm{dq} = v_\mathrm{1dq} - v_\mathrm{2dq} - R_\mathrm{g} + (j\omega_\mathrm{g}L_\mathrm{g})i_\mathrm{dq} \tag{3.45}$$

The DC side of the converter voltage is unipolar in nature and conventionally supported by a capacitor large enough to withstand the sustained charging or discharging current. The switching sequence of the converter valves and the shifting in phase angle of the switching valves do not change significantly in the DC voltage [4] because of the DC-link capacitor which can be represented as [180]

$$C_\mathrm{dc}\dot{v}_\mathrm{dc} = i_\mathrm{load} - \frac{P_\mathrm{dc}}{v_\mathrm{dc}} \tag{3.46}$$

$$P_\mathrm{dc} = v_\mathrm{dc}i_\mathrm{dc} \tag{3.47}$$

3.4.2 STATCOM model

According to the IEEE, a STATCOM is a static VAR compensator connected in a shunt where the output current, which can be inductive or capacitive in nature, can be controlled independently of the AC system voltage [4], [159]. A STATCOM is capable of enhancing transient stability and damping turbine shaft oscillations of

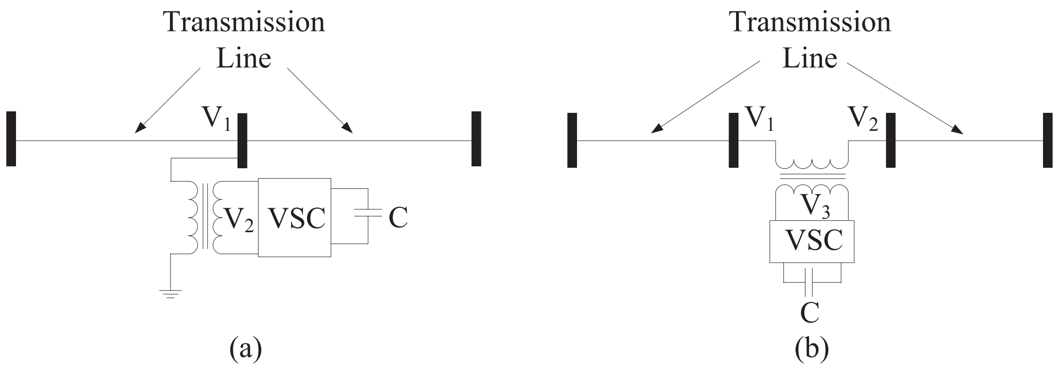

Figure 3.15. Structure of (a) STATCOM and (b) SSSC

a WT [181] and is known as an electronic generator of reactive power. The pulse-width modulation (PWM) technique offers fast and reliable control which enables the STATCOM to mitigate voltage dips, flicker and swells during transient disturbances, and provide voltage regulation [101] [159], [173]. A STATCOM normally exhibits a faster response than the thyristor firing-based concept as it has no time delay [182]. Again, the reactive power capability of a DFIG is not sufficient to maintain the required power factor and reactive power at the point of common coupling (PCC) when the DFIG is operating at high rotor speeds (more than 1.1 pu) [85], [159]. In some of the literature, STATCOM with DFIG-type wind farms for reactive power supports is proposed.

A STATCOM comprises a VSC, which is shunt-connected controlled reactive admittance, a shunt transformer, which couples the VSC to the power network and a DC link capacitor. With proper control, a shunt FACTS device is capable of injecting controllable reactive power into a system by varying the amplitude of the converter output voltage with respect to the line voltage of bus. The structure of a STATCOM is shown in Fig. 3.15(a), where V_1 is the bus voltage and V_2 is the voltage across the VSC which is its core component [173]. If $V_1 > V_2$, the STATCOM acts as an inductor and a lagging current absorbs reactive power from the bus whereas, if $V_1 < V_2$, it acts as a capacitor and a leading current is produced that injects reactive power into the bus. STATCOM can be viewed as a shunt reactive current source [99].

The dynamic model of a STATCOM can be represented as follows, where P_{g} is the supply power and R_{L} is the internal resistance of the capacitor [183].

$$\dot{v}_{\mathrm{dc}} = -\frac{P_{\mathrm{g}}}{C_{\mathrm{dc}}v_{\mathrm{dc}}} - \frac{v_{\mathrm{dc}}}{C_{\mathrm{dc}}R_{\mathrm{L}}} \tag{3.48}$$

3.4.3 SSSC model

In 1989, Gyugyi proposed the VSC-based series compensator known as the SSSC [4]. For normal capacitive compensation, the output voltage lags the line current by 90 degree while, for a synchronous voltage source (SVS), this can be controlled to lead or lag the line current by 90 degree. To compensate series reactance, the VSC acts as a SVS to produce a controllable voltage in quadrature with the line current while the injected voltage is in series with the line irrespective of the line current [4].

A SSSC is capable of maintaining bus voltage, power flow and line reactance [66] and consists of a VSC, DC-link capacitor and coupling transformer. Under proper control, a voltage is injected into a transmission line in quadrature with the line current. If injected voltage is greater than zero, SSSC behaves like a capacitor and if it is less than zero, SSSC behaves like an inductor [99]. The equivalent circuit of the SSSC is shown in Fig. 3.15(b) and the SSSC can be represented by a series voltage source [99].

A generalised expression for the injected voltage, V_{c}, can simply be written in terms of line current, I, and reactive current drawn by the SVS, I_{s}, as [4]

$$V_{\mathrm{q}} = V_{\mathrm{c}} = -jX_{\mathrm{c}}I = -jkX_{\mathrm{L}}I \tag{3.49}$$

$$V_{\mathrm{q}} = \pm jV_{\mathrm{c}}(\alpha)\frac{I}{I_{\mathrm{s}}} \tag{3.50}$$

where, V_{q} is the magnitude of the injected compensating voltage which is tuned by adjusting the control parameter, α, and can vary from 0 to the maximum injected limit.

The injected voltage can be expressed in terms of the DC voltage source, V_{dc}, as [65]

$$v_{\mathrm{cd}} = n_{\mathrm{c}}k_{\mathrm{c}}V_{\mathrm{dc}}\cos\alpha \tag{3.51}$$

$$v_{\mathrm{cq}} = n_{\mathrm{c}}k_{\mathrm{c}}V_{\mathrm{dc}}\sin\alpha \tag{3.52}$$

where, n_c and k_c are the transformer turns ratio and converter constant, respectively.

The transmittable active and reactive power supplied by the receiving end bus can be expressed as [4]

$$P = \frac{V^2}{X_{\text{eff}}^2 + R^2}[X_{\text{eff}} \sin\delta - R(1 - \cos\delta)] \tag{3.53}$$

$$Q = \frac{V^2}{X_{\text{eff}}^2 + R^2}[R \sin\delta + X_{\text{eff}}(1 - \cos\delta)] \tag{3.54}$$

If a SSSC can produce ideal output voltages irrespective of the composition of the line current it will remain neutral to the sub-synchronous resonance (SSR) [4]. SSSC is able to participate in a power system's inter-area oscillation damping by changing the compensated reactance. In terms of damping oscillations under different disturbances, the SSSC has been analysed [64], [65] using WT-based power systems.

The dynamic equation of the DC-link capacitor can be represented in the dq frame as [65]

$$C_{\text{dc}} = n_c k_c (i_d \cos\alpha + i_q \sin\alpha) - \frac{V_{\text{dc}}}{R_L} \tag{3.55}$$

For a 48-pulse inverter [64],

$$K_c = \frac{8\sqrt{6}}{\pi} \tag{3.56}$$

3.4.4 TCSC model

In 1986, Vithayathil proposed the TCSC scheme which is known as a method of "rapid adjustment of network impedance" [4]. To provide a continuously variable capacitor, a thyristor-controlled reactor is used in shunt with a SC. The variable reactance of the fixed SC is achieved by controlling the current in the parallel inductor using two reversed thyristors. As the effective value of the inductor varies depending on the conduction time or delay angle of the thyristor, the level of series compensation changes [184]. It is used to increase line power transfer as well as enhance a system's stability [174]. The TCSC structure is shown in Fig. 3.16 (a) where C is the capacitor bank, L is the bypass inductor and SW the bidirectional thyristors.

The TCSC is a complex dynamic system which comprises a parallel LC circuit consisting of a fixed capacitive reactance, X_C, and a variable inductive reactance,

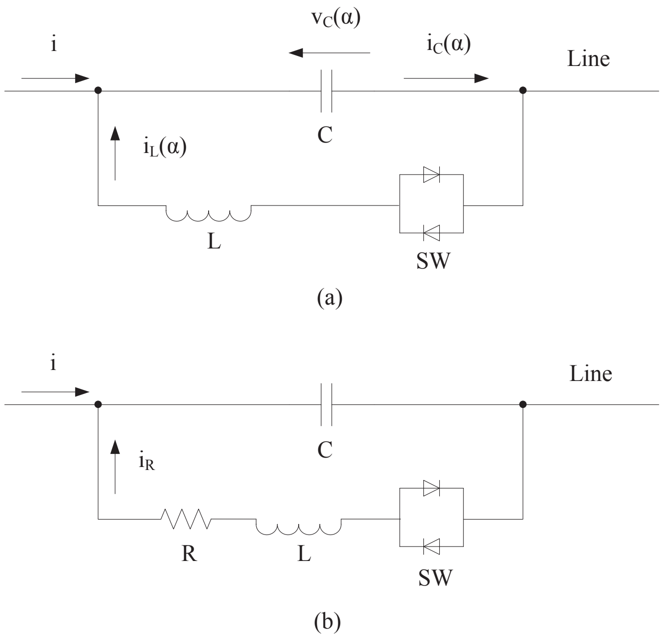

Figure 3.16. General structure of (a) TCSC and (b) TCSC with SSR damper

$X_{\mathrm{L}}(\alpha)$, that is [4],

$$X_{\mathrm{eff}}(\alpha) = -\frac{X_{\mathrm{c}} X_{\mathrm{L}}(\alpha)}{X_{\mathrm{L}}(\alpha) - X_{\mathrm{c}}} \tag{3.57}$$

where, α is the delay angle of the thyristor. The accuracy of the modelling of a TCSC can effectively influence accurate evaluations of its control strategy. It can be operated in two operating modes, where $X_{\mathrm{eff}}(\alpha)$ is inductive or capacitive depending on its internal circuit resonance as a TCSC may present a tunable parallel LC circuit to the line current.

In 1937, SSR, i.e., sustained oscillations below the fundamental system frequency [4] caused by series capacitive compensating devices, was observed. In it, a series compensated line conforms a series resonant circuit with the total circuit inductance of the transmission line with a natural frequency of $f_{\mathrm{n}} = f\sqrt{k}$ [4]. The electrical resonant frequency is less than the power frequency as the degree of series compensation, $k = \frac{X_{\mathrm{c}}}{X_{\mathrm{L}}}$, usually lies between 25 and 75 percent. Due to different types of contingencies the sub-harmonic component of the line current results in an alternating torque on the rotor at the difference frequency of f - f_{n} which may interact with any of the torsional resonances of the turbine and generator that consecutively generate SSR.

N. G. Hingorani proposed the thyristor-controlled damping scheme (NGH damper) for series capacitors [4] shown in Fig. 3.16 (b) and its performance has been well proven to provide effective SSR mitigation. The NGH scheme can be implemented in a TCSC structure to alleviate SSR, and details of this scheme can be found in [4], [185].

3.5 Summary and Conclusion

This chapter discusses the dynamic modelling of different power system components and wind generation systems and those of the FSWT and DFIG implemented in the remaining chapters. The modelling of a power system has significant importance for extracting accurate stability conditions of a network, some of which are represented by simple simulations. For harmonic domain analysis, it is necessary to represent the FACTS devices, loads and other converter systems which are potential harmonic-generating source by a proper model, otherwise erroneous results may be obtained. The next chapter will represents the voltage stability issues relating to FSWT and DFIG WTs with different series and shunt compensating devices.

Chapter 4

Dynamic Voltage Stability Analysis with Wind Power

4.1 Introduction

The integration of wind generation into a grid posses a challenge for the power industry due to the intermittent nature of wind. In the past, a wind farm was treated as a negative load but now-a-days wind farms generate higher than 100 MW in some cases. For the reliable operation of a power system, with a large amount of wind power, it is necessary to maintain its dynamic stability. Voltage stability both during and after fault events, in the external power system, should be maintained without its large wind farms being subsequently disconnected [104]. According to grid codes [20], if a wind farm cannot meet the required stability limit, only then it is permitted to be disconnected from the grid. For a large wind farm, disconnection can cause a mismatch between the load and supply which can lead to voltage collapse.

The voltage collapse phenomenon can be initiated by the tap-changing action of a transformer, the current limiters of generators, inadequate reactive power resources or low-voltage loads [75]. To prevent the disconnection of a wind turbine (WT) and match the load demand are two major challenges of the integration of wind energy in a grid. Tripping a portion of a network may cause an angle difference between two regions which, if large, results in a lower voltage level that will increase reactive power demand to maintain the voltage [186]. A short-circuit fault in an external network can cause over-speeding of the rotor shaft of a WT. As most of WTs are induction generator types which do not have a reactive power control capability, using flexible AC transmission system (FACTS) devices allows full control of both reactive power and voltage. As using a distributed generator (DG) with a reactive power compensating technique will prevent critical overloading during an emergency and help restoration process, local reactive power support will reduce line loss and enhance voltage stability.

The decentralised nature of a wind power plant is aberrant to that of the conventional centralised structure of a power system network and, due to the inherent characteristics of a WT, complexity is increased as they do not participate in either the supply-demand balance or frequency maintenance [187]. This necessitates additional control to provide acceptable voltage (0.95-1.05 pu for both distribution and transmission systems) conditions. A low power factor is another cause of voltage instability as it draws excessive reactive power from the system and is unable to supply adequate reactive power which leads the system to voltage collapse [80].

Although a distribution system is built as a passive network with a unidirectional power flow, the integration of DG units permit a bi-directional flow and, thus, the system behaves as an active network [188]. DG technologies have entered a new era of rapid expansion and commercialisation. DG affects the voltage profile of a distribution network by injecting power and, as this, active power generation tends to increase the voltage locally, further voltage rises or drops depend on the reactive power produced or consumed by the DG units. Again, overheating of the induction generator, due to its low negative sequence impedances, can cause voltage imbalance [188].

FACTS devices can be used in power systems to achieve continuous voltage control and reactive power compensation. The primary goal of a shunt device is to provide reactive power compensation and dynamic voltage support whereas series devices are used to control power flow and damp power oscillations [61]. In [181], the stability of a wind farm is investigated for variable-speed wind turbines (VSWTs) and fixed-speed wind turbines (FSWTs) during network disturbances. A comparison is made between the power converter of a doubly-fed induction generator (DFIG) and the static synchronous compensator (STATCOM) for stability improvement of wind farms under both normal and fault conditions. Due to the fixed speed of a squirrel cage induction generator, a power grid can be severely affected if no compensation is used.

The connection of a wind farm to a network, which can be- a transmission, distribution, sub-transmission or regional network, significantly affects voltage stability. The nature of its connection point, i.e., the grid strength, and the transmission line length can change the stability limit. In this chapter, the following cases are considered and series compensation for different scenarios are the prime focus.

- Voltage instability caused by contingency and load variations of a FSWT-based wind farm is investigated and the performance of STATCOM and static synchronous series compensator (SSSC) are compared.
- A DFIG-based wind farm is connected to a distribution network and the performances of a thyristor controlled series compensator (TCSC) and series capacitor (SC) is investigated for different scenarios in which weak connection of a network is also addressed.
- A short-circuit current analysis, in which a DFIG-driven wind farm is connected to a high voltage (HV) network through a long-distance transmission line which is compensated with a SSSC, is performed. Symmetrical and asymmetrical faults, and WT switching are considered for this fault-level analysis.

Considering these issues, to support the voltage of a network with wind energy, series compensation at the point of common coupling (PCC) is proposed. In the following sections, different series compensating devices are used to increase the dynamic voltage stability. A SSSC is connected at the PCC to investigate the impact of series compensation with wind energy under different scenarios. Then, a SC and TCSC are integrated into an industrial and commercial distribution network, and the conventional generation is replaced by wind generation. Load variations and types, wind energy penetration levels and motor start-up in a weak grid are analysed. Finally, a short-circuit fault current level where a WT is connected to a network via a long-distance transmission line is analysed with the impact of series compensation on limiting the fault current is the prime focus. In addition, a WT start-up is investigated.

4.2 Wind Farm Connected to Infinite Bus using SSSC

WTs have to fulfil the specified active power and reactive power profiles under different grid conditions [61], [189] as the power quality, safety and stability of the grid depends heavily on their characteristics [181]. Although the effects of FACTS devices have been analysed in the literature, those of shunt and series compensation in terms of improving the stability of wind farms have not been investigated in detail. In this study, the impacts of a STATCOM and SSSC on a power system with wind energy penetration under normal operating conditions, changing load conditions and in post-fault voltage recovery are presented. Also, their ratings for post-fault voltage recovery are compared and the effects of load variations and durations on the performances of wind farms are analysed under different operating conditions. The SSSC is placed at two different positions in the system and it is found that the position affects the voltage at the PCC. In this study, the investigation results show that series compensation can provide as good a voltage profile as shunt compensation with a lower MVA rating. Again, a change in the MVA rating of the SSSC shows less voltage regulation than the STATCOM which implies that a lower rating SSSC can be used to enhance the power quality of a wind farm.

The test system comprises a 6 MW wind farm connected to an infinite bus through some step-up transformers. The test case is shown in Fig. 4.1 in which one FSWT is connected to bus 3 and bus 4, where each WT is rated at 3 MW, the total wind power generation is 6 MW. The STATCOM is connected at the PCC (bus 2), as shown in Fig. 4.1(a), followed by a double-circuit transmission line. In Fig. 4.1(b), instead of the STATCOM, a SSSC is connected at the PCC in a series and denoted by SSSC1. To investigate the effect of the SSSC's position in the network, SSSC2, which has the same rating as SSSC1, is connected between bus 1 and bus 2, as shown in Fig. 4.1(c). The load is connected to bus 1 and bus 2 and the total load on the system is 13 MW and 10 MVAR. The parameters of the FSWT, STATCOM, SSSC1, SSSC2 and rest of the network are given in Appendix III.

The simulation is performed using MATLAB Simulink. The wind speed variations with time are shown in Fig. 4.2. For the WT1, the wind speed is 10 m/s for 2 s, after which it starts increasing and, at 4 s, is 12 m/s. At 5 m/s, it begins to increase again and, at 8 s, is 15 m/s while WT2 experiences same wind speed characteristics with a 2 s time delay.

The control schemes of the STATCOM and SSSC are shown in Fig. 4.3, where a PI controller is used to control the modulation index and angle in order to inject the proper current at the point of interconnection to regulate voltage. In Fig. 4.3(a), the dq components of the converter voltage V_2, $V_{2\mathrm{d}}$ and $V_{2\mathrm{q}}$, are measured knowing of I_{dref}, I_{qref}, and the transformer leakage reactance. A PI controller can be represented as

$$U(s) = \left(k_{\mathrm{p}} + \frac{k_{\mathrm{i}}}{s}\right) E(s) \tag{4.1}$$

where, $E(s)$ and $U(s)$ are the error signal and output of the controller and k_{p} and k_{i} are the proportional and integral gains of the controller.

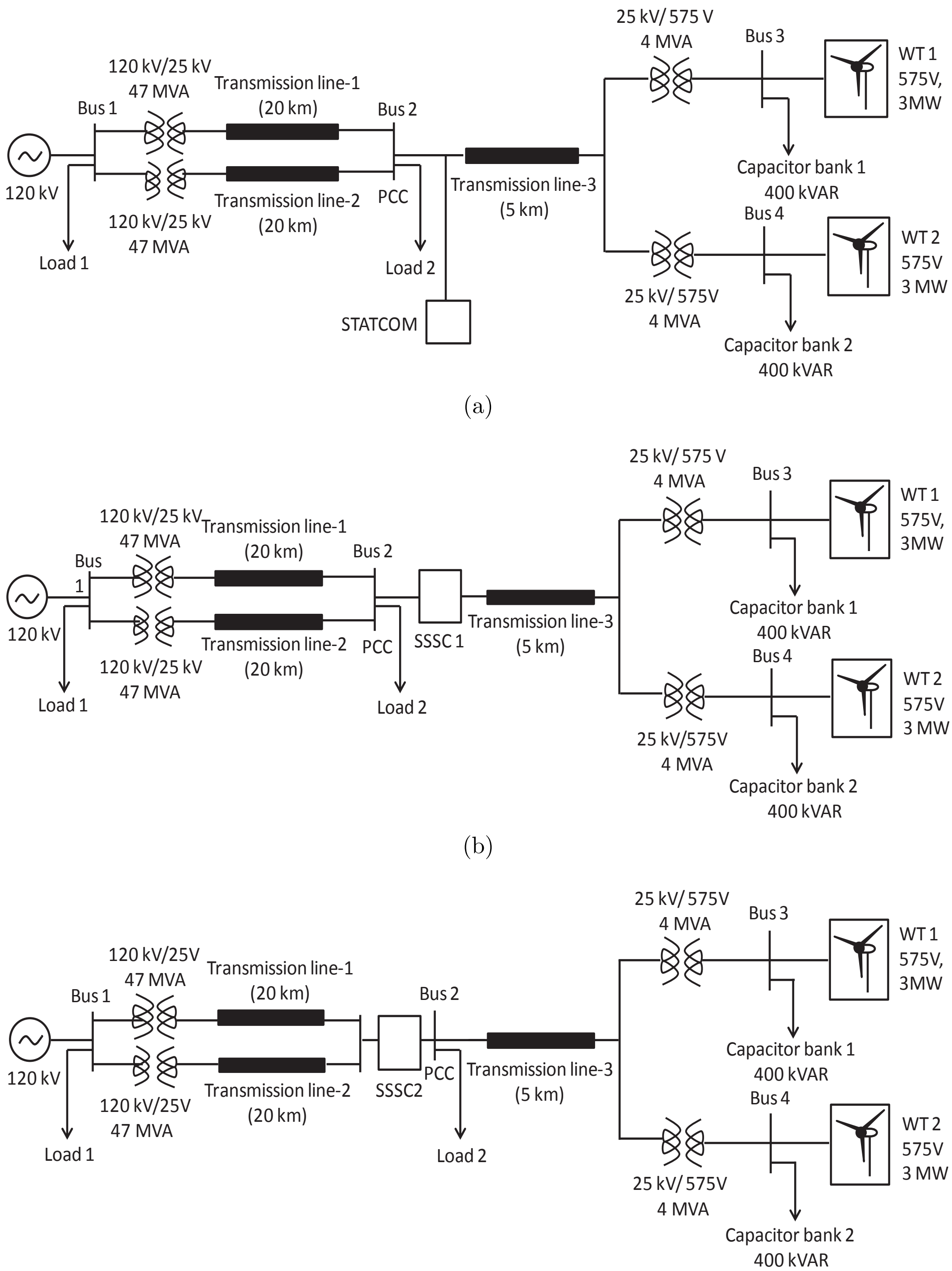

(c)

Figure 4.1. FSWT equipped with (a) STATCOM and (b) SSSC1 (b) SSSC2

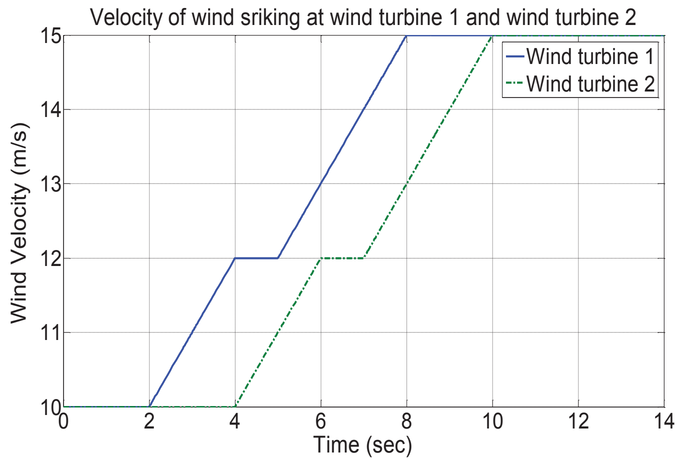

Figure 4.2. Wind speed variations

To choose the best proportional and integral gains, the trial and error method is applied for AC voltage, DC voltage and current regulators which compute the required magnitude and phase of the converter voltage and desired DC voltage and their different set points are listed in Table 4.1 and Table 4.2 for the STATCOM and SSSC, respectively. For the STATCOM, the gains, k_p and k_i, are 6 and 1010, 0.001 and 0.029 and 0.3 and 10, respectively, for PI_1, PI_2 and PI_3 blocks, as shown in Fig. 4.3(a). The SSSC can be represented by a series voltage source [99] and the control scheme of SSSC are shown in Fig. 4.3(b). The proportional and integral gains are chosen by the trial and error method for AC and DC voltage regulators which compute the converter voltage required to obtain the desired DC voltage and the injected voltage and the gains are 0.003 and 0.15, and 0.0001 and 0.02, respectively, for PI_1 and PI_2, as shown in Fig. 4.3(b). The PI_3 block in Fig. 4.3(a) and PI_1 block in Fig. 4.3(b) contain some other calculations apart from those for the PI controller. The details of these control schemes can be found in [190].

An increase in proportional gain decreases the rise time but increases the overshoot while a decrease in integral gain eliminates the overshoot problem but increases the steady-state error and the combined effect is shown in Fig. 4.4. Using the PI data set 1, shown in Table 4.1 and Table 4.2, more stable points are found in the simulation results.

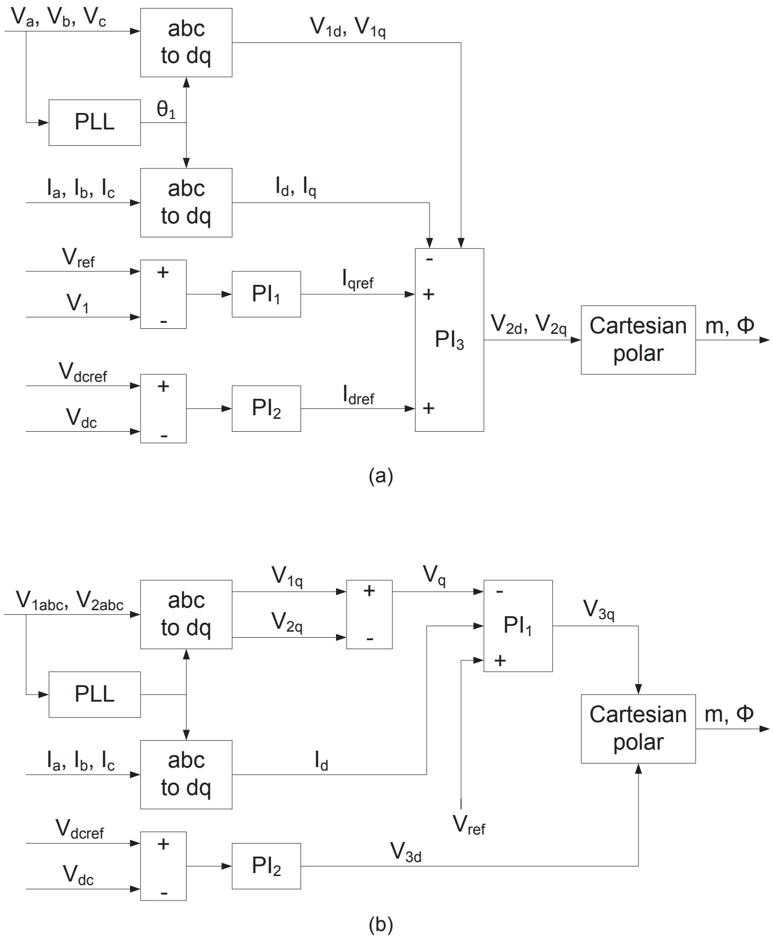

Figure 4.3. Control schemes of (a) STATCOM and (b) SSSC

Table 4.1. PI parameter tuning for STATCOM

PI data	k_{p1}	k_{i1}	k_{p2}	k_{i2}	k_{p3}	k_{i3}
1	6	1010	0.0001	0.029	0.30	10.0
2	8	1000	0.0004	0.020	0.70	5.0
3	12	1020	0.0010	0.029	1.20	10.0
4	1	1015	0.0008	0.015	0.10	10.0
5	1	950	0.0001	0.001	0.20	0.01

Table 4.2. PI parameter tuning for SSSC

PI data	k_{p1}	k_{i1}	k_{p2}	k_{i2}
1	0.003	0.15	0.0001	0.02
2	0.04	0.15	0.0018	0.020
3	0.01	0.1	0.0009	1.00
4	0.5	3	1	0.025
5	1.5	1.5	2	0.005

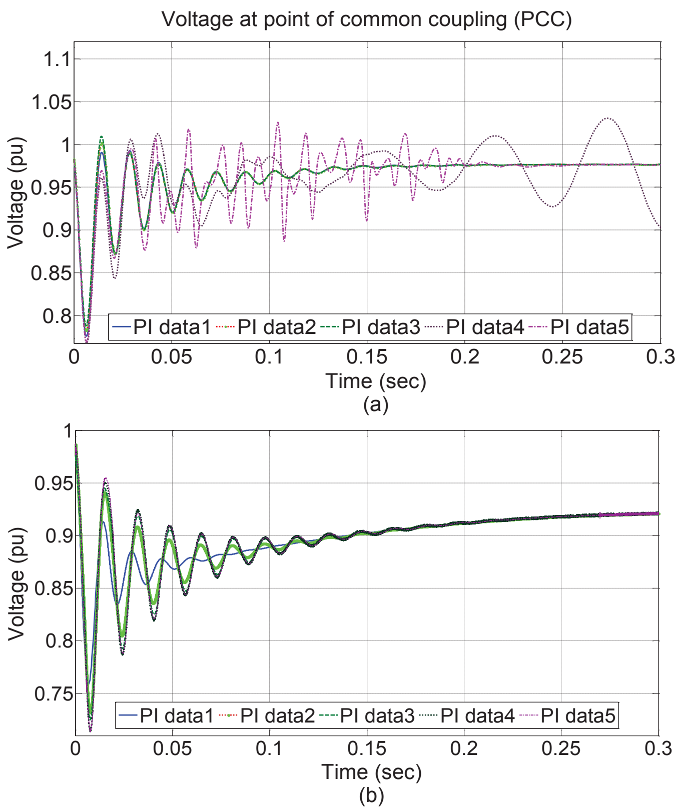

Figure 4.4. Responses of different PI parameters for (a) STATCOM and (b) SSSC

Table 4.3. Voltage variations

Voltage at PCC (pu)	Without FACTS	With STATCOM	With SSSC1	With SSSC2
Maximum	0.965	0.992	0.978	1.015
Minimum	0.955	0.990	0.973	1.014

4.2.1 Post-fault voltage recovery

To maintain acceptable voltage levels is an important objective of steady-state and dynamic stability analyses of a power system as a stable system contributes to its reliability [83]. As voltage instability may lead to voltage collapse, outage and system loss, the objective of this section is to analyse the steady-state and dynamic voltage stability at the point of interconnection of a wind farm and grid using the STATCOM and SSSC.

Firstly, the test system is simulated without any FACTS compensation device. A 400 kVAR capacitor bank is connected to bus 3 and bus 4, the WT is operated with a pitch controller to maintain the power within 3 MW. The active power and reactive power variations at bus 3 and bus 4 due to the changing wind speed are shown in Fig. 4.5(a) and Fig. 4.5(b), respectively. As the pitch angle changes with the wind speed, as shown in Fig. 4.6(a), this helps to maintain the active power level within the limit. However, without any compensating devices, the voltage at the PCC is slightly higher than 0.95 pu. A better voltage profile can be achieved using a 8 MVA STATCOM and 8 MVA SSSC, as shown in Fig. 4.6(b). A varying wind speed also results in a voltage fluctuation at the PCC. The maximum and minimum voltage levels obtained from the simulation are listed in Table 4.3. SSSC2 gives a better voltage level of about 1 pu than the STATCOM and SSSC1 which give voltages of about 0.99 pu and 0.97 pu, respectively. The network parameters are given in Appendix III.

A three-phase to ground-fault is applied at 11 s and cleared at 11.2 s at the terminal of WT2 at bus 4 and the power and voltage at the PCC afterwards are shown in Fig. 4.7. The STATCOM performs well at restoring the the voltage to the pre-fault operating point afterwards while SSSC1 takes longer. Although SSSC2 maintains a higher voltage level with the same MVA rating as the STATCOM and SSSC1, it takes longer to reach the pre-fault value and the intensity of the voltage dip is also higher.

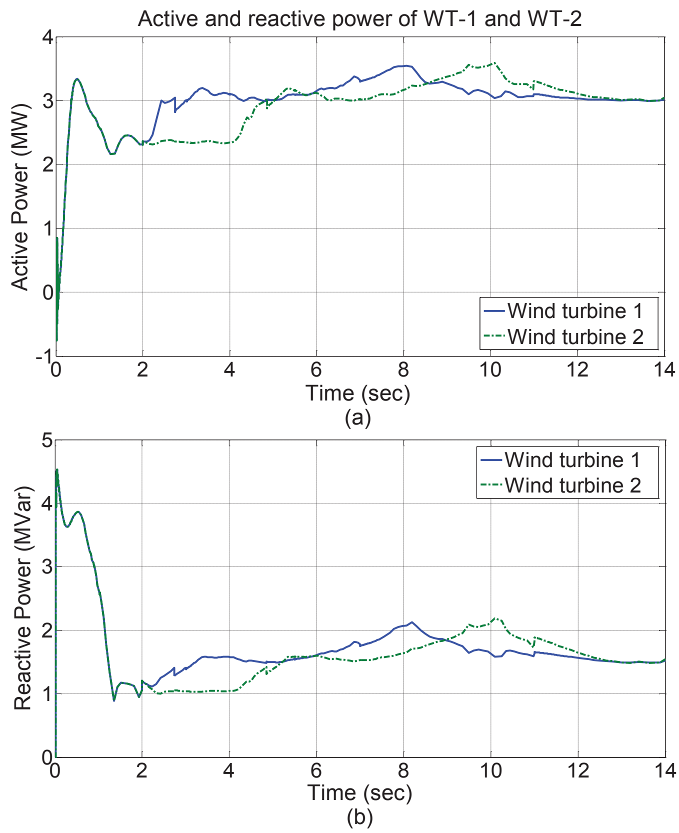

Figure 4.5. (a) Active power (b) reactive power variations for WT1 and WT2

4.2.2 Load variation and duration

Matching generation with demand is another important consideration in a power system. As the size of wind farm is increasing and an asynchronous generator is the most common type of wind power generating technology, establishing the dynamic reactive compensation of wind farms is necessary [104].

In this case, the effect of load changes on the dynamic performance of a wind farm is studied. The load connected at bus 2 is varied, as listed in Table 4.4, and the responses of the voltage and power at the PCC are shown in Fig. 4.8. The simulation is conducted with the changing wind speed for 4 s which causes fluctuations in voltage and power at the PCC even when the load is constant for a defined time period. For each load, the voltage listed in Table 4.4 is measured at the middle of the specified time duration. Due to the transients between 0 s to 1 s, the voltages given in Table 4.4 are below than the acceptable limit for SSSC1 and without FACTS. For the same load conditions, from 3 s to 4 s, voltages are in an

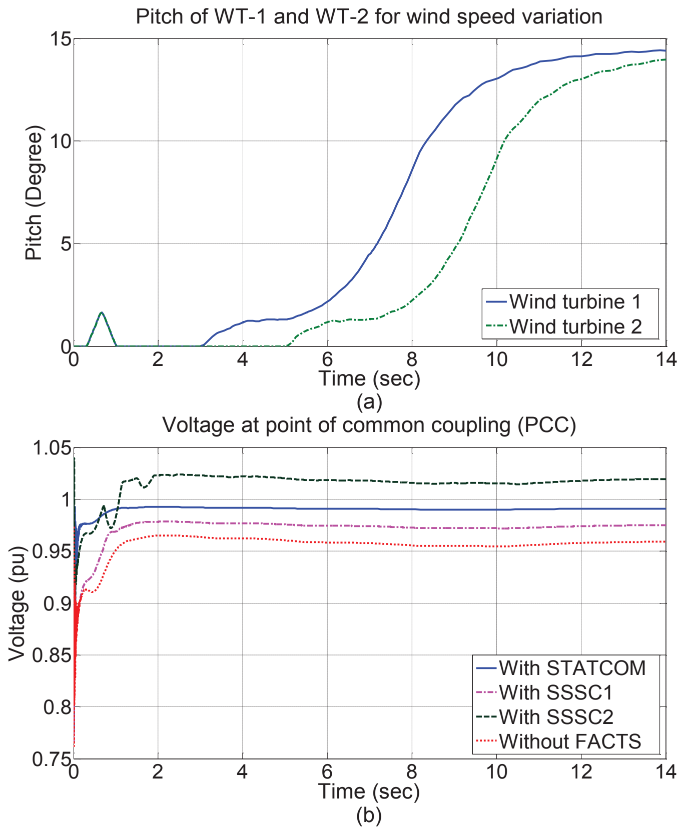

Figure 4.6. (a) Pitch angles of the WTs and (b) voltage at the PCC under normal operating conditions

Table 4.4. Voltage variations under variant load conditions

Time (sec)	0-1	1-2	2-3	3-4
P (MW)	4	3	5	4
Q (MVAR)	3	2	4	3
V_{PCC}[a] with STATCOM (pu)	0.971	0.990	0.985	0.987
V_{PCC} with SSSC1 (pu)	0.930	0.978	0.961	0.968
V_{PCC} with SSSC2 (pu)	0.962	1.020	1.000	1.012
V_{PCC} without FACTS (pu)	0.903	0.961	0.948	0.953

[a] Voltage at the PCC

acceptable range. For SSSC1 voltage level falls to 0.96 pu when a 5 MW, 4 MVAR load is connected. The SSSC takes a longer time than the STATCOM to settle and obtain a stable point from the transients caused by the changing load.

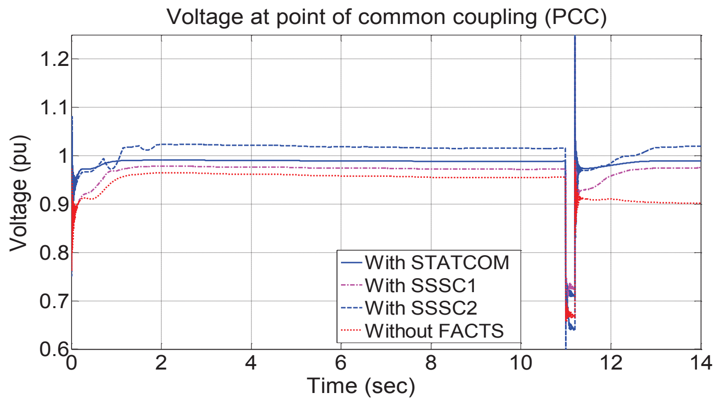

(a)

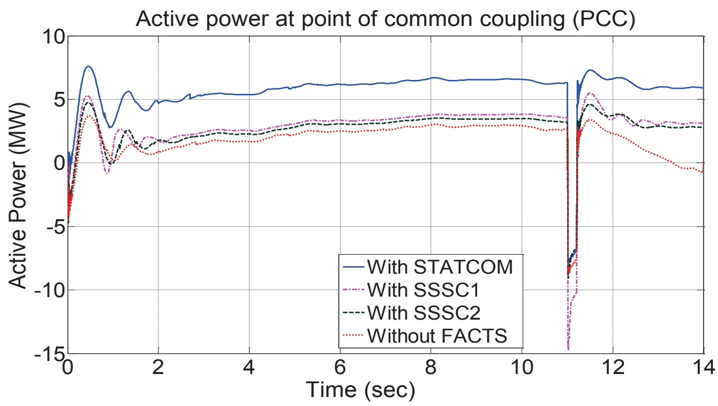

(b)

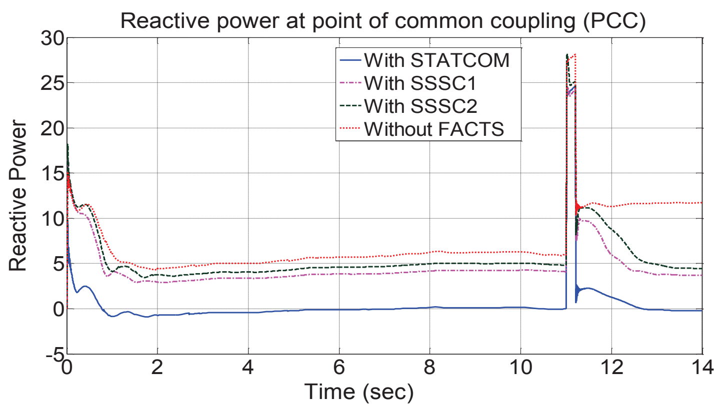

(c)

Figure 4.7. (a) Voltage (b) active power (c) reactive power at the PCC for investigation of the effect of three-phase-to-ground fault

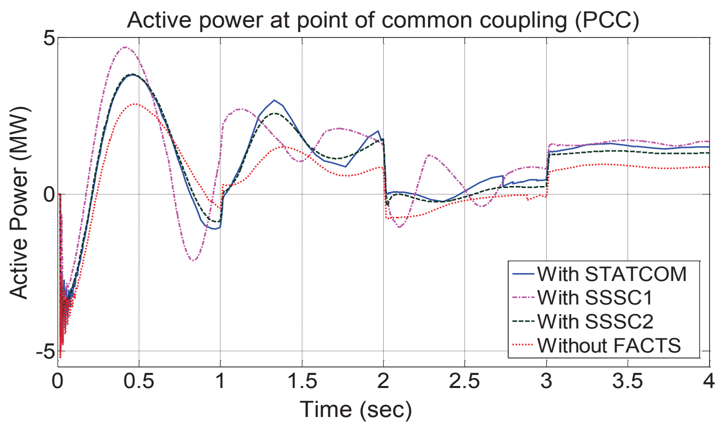

(a)

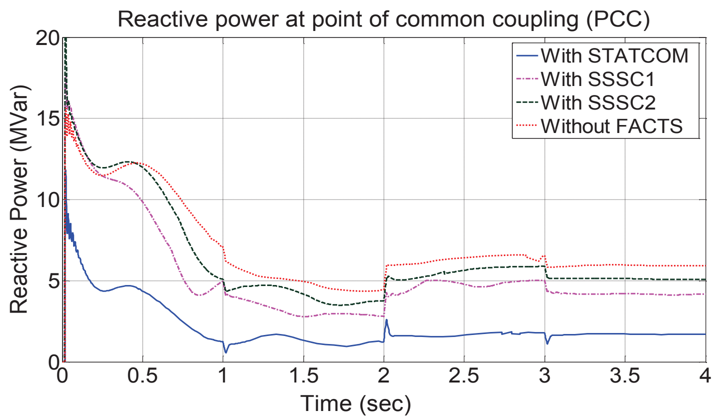

(b)

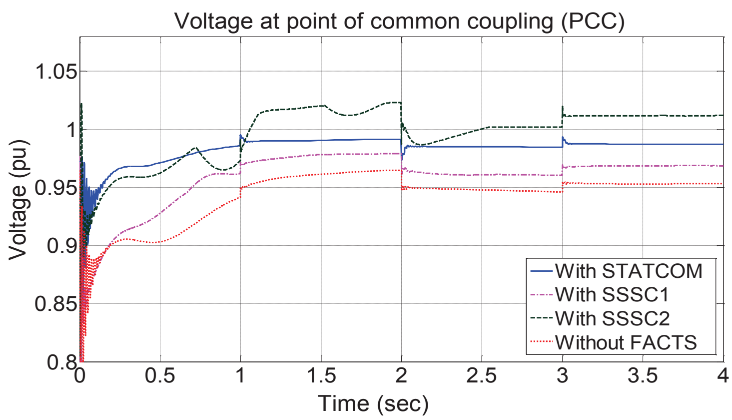

(c)

Figure 4.8. (a) Active power (b) reactive power (c) voltage at the PCC under various load conditions

Table 4.5. Voltage variations with different MVA ratings of FACTS devices

Rating	10 MVA	8 MVA	5 MVA	3 MVA
V_{PCC} with STATCOM (pu)	0.991	0.990	0.985	0.978
V_{PCC} with SSSC1 (pu)	0.975	0.974	0.973	0.971
V_{PCC} with SSSC2 (pu)	1.0151	1.0150	1.0148	1.0147

4.2.3 Positions of FACTS devices

The efficiency of a FACTS device depends on its position and its performance can vary depending on the network configuration. The SSSCs and STATCOM are placed at two different positions in the network, the load bus and generator bus, and their performances compared.

A 6 MVA STATCOM is connected to the load bus at bus 2 and generator bus at bus 3 and bus 4, with the combined effect shown in Fig. 4.9. For the STATCOM, two cases provide an almost mirror image with voltages of 0.987 pu and 0.985 pu while for the SSSCs, the picture is slightly different. A 6 MVA SSSC is placed between bus 2 and the double circuit transmission line which gives a voltage of about 1.0 pu and then the SSSC is placed between the generator bus of the WT and the 5 km transmission line which gives a voltage of about 0.972 pu. A SSSC injects a voltage in a series with the line at which it is connected and if this is connected between the PCC and WT, its terminal is affected by fluctuating wind characteristics. The situation is improved if it is connected in the same way as in the first case.

4.2.4 Comparison of ratings of STATCOM and SSSC

The cost of equipment depends on its rating or size. To investigate the effect of the rating of the FACTS device, the test system is simulated with 5 MVA, 8 MVA and 10 MVA STATCOM and SSSC. The higher the MVA rating, the better the performance, as shown in Fig. 4.10. Table 4.5 shows the voltage variation for a 15 m/s wind speed. Both the STATCOM and SSSC provide acceptable voltage limit, but the SSSC have a voltage rise problem just after the fault is cleared. From Table 4.5, it is clear that to maintain a nominal voltage level a lesser size SSSC2 is required than the STATCOM. Again, in the case of the SSSC1, a higher MVA rating is required to achieve the same voltage profile.

The effect of increasing the rating of the FACTS on its response is also investigated. For the STATCOM, when the MVA rating is increased from 3 MVA to 5 MVA, there is a 0.72 percent increase in its response at the PCC voltage and when

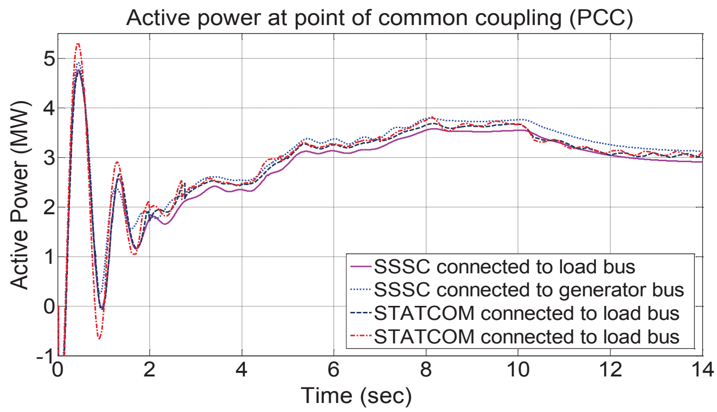

(a)

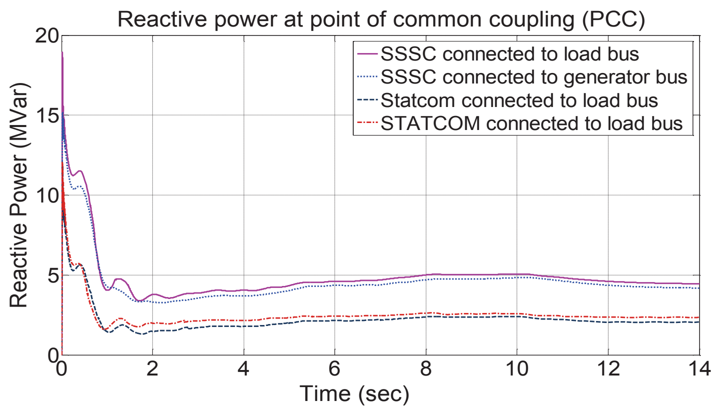

(b)

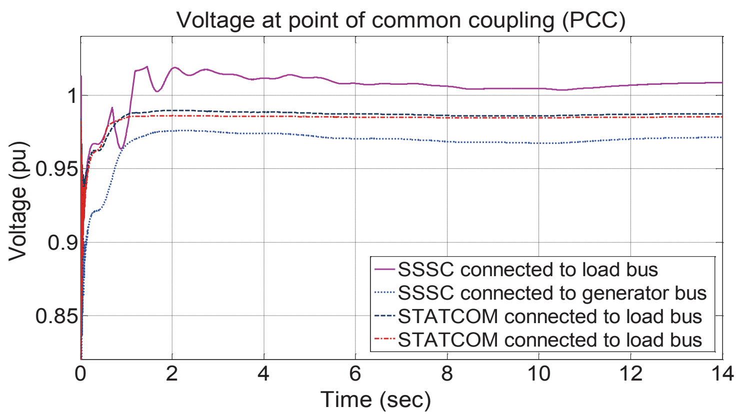

(c)

Figure 4.9. Responses of (a) active power (b) reactive power (c) voltage at the PCC for different positions of STATCOM and SSSC

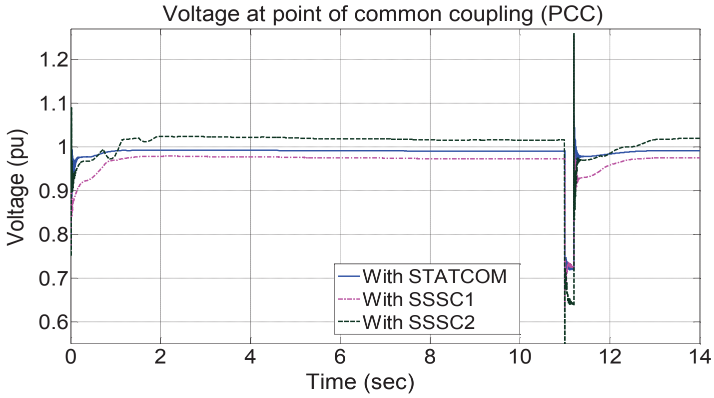

(a)

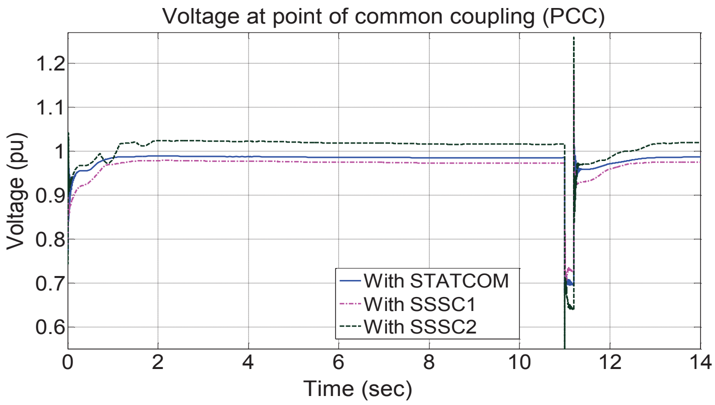

(b)

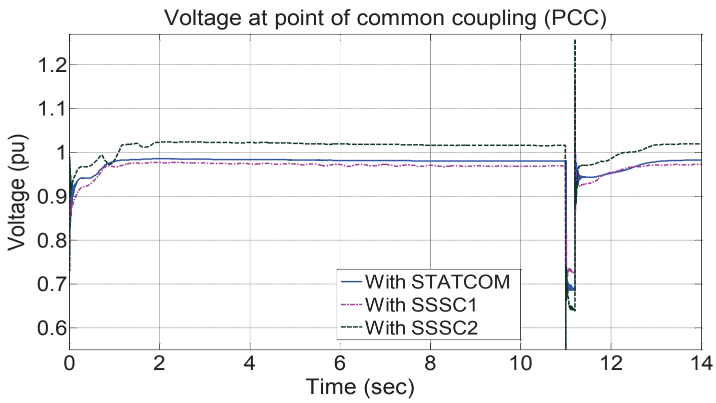

(c)

Figure 4.10. Voltages at the PCC for (a) 10 MVA STATCOM and 10 MVA SSSC, (b) 5 MVA STATCOM and 5 MVA SSSC and (c) 3 MVA STATCOM and 3 MVA SSSC

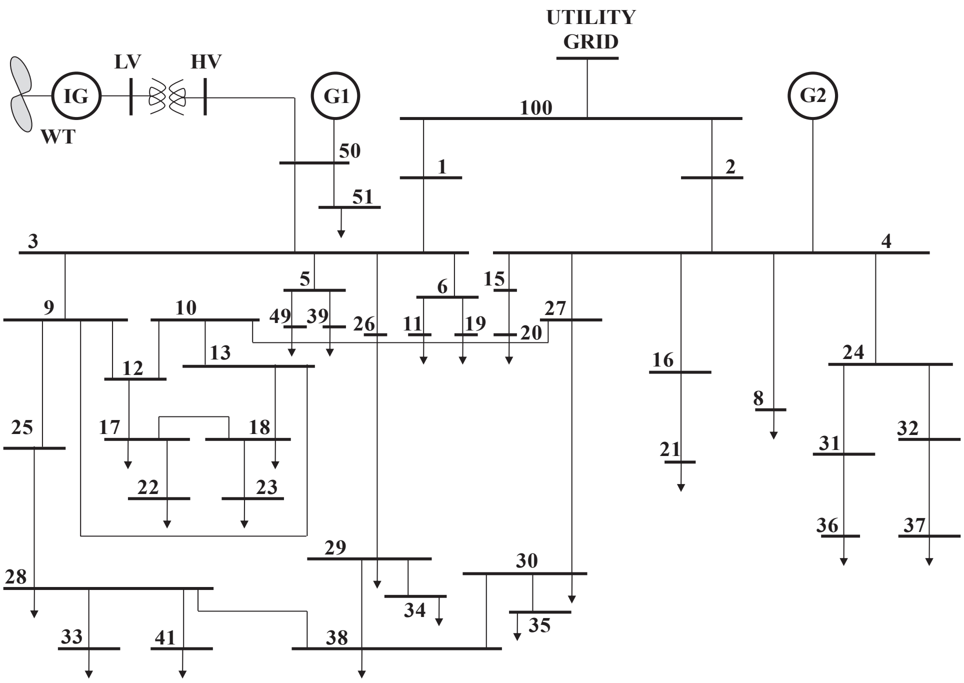

Figure 4.11. Single-line diagram of IEEE 43-bus distribution test system with wind DG connected at bus 50

it is increased from 8 MVA to 10 MVA, a 0.10 increase in voltage is found. The same case occurs for SSSC2, with 0.02% and a 0.01% increases, respectively.

4.3 Wind Farm Connected to Distribution Network using SC and TCSC

The steady-state stability of a power system may be defined as its capability to maintain synchronism and equilibrium between machines for a relatively slow change in load while transient stability is its capability to remain in synchronism and equilibrium under a sudden disturbance, i.e., fault, switching operation, etc. In an industrial power system, stability may involve the interactions among the utility and asynchronous or synchronous motor loads. Contingencies such as load rejection or connection, sudden loss of a generator or DG unit, outage of a tie-line, starting of large motors, and faults and their durations have a direct impact on system stability.

To test the effectiveness of series compensation on a distribution network with wind DG an IEEE 43-bus mesh distribution system [191] with slight modification is used for this study by connecting wind DG and transmission line and shown in Fig. 4.11. This complex industrial and commercial power system comprises 21.7 MW and 9 MVAR of dynamic and static loads, and has five different voltage levels: 69 kV, 13.8 kV, 4.16 kV, 2.4 kV and 0.48 kV. The generator unit, $G1$, connected at bus 50 is replaced by a DFIG-based wind DG unit with an equivalent power rating. Five 2.7 MW wind DG units are connected at bus 50 via a step-up transformer of 13.8 kV/0.69 kV, and a 15 km transmission line with a X/R ratio of 7. A SC is placed at the middle of the transmission line and later replaced by a TCSC to compensate the reactive power loss in the line and, thus, increase voltage stability. All the results presented in this section are simulated in the DIgSILENT PowerFactory 14.1 [138] environment. The details of the network parameters can be found in [191] and WT parameters are given in Appendix IV.

4.3.1 Motor start-up with wind DG

As the sizes of motors in modern industrial systems are becoming increasingly larger, the effect of their starting is prolonged throughout an industrial area. A starting motor is analogous to a small-impedance that draws a huge current from the system which could be 4 to 8 times of its rated current [192]. Several hundred or several thousand amps of starting current cause large voltage drops in a system [193]. Since the accelerating torque is determined by the motor terminal voltage, a large voltage drop appreciably reduces the accelerating torque which adversely affects the starting process by increasing its starting interval [168]. The sharp voltage drop disturbs the operation of the motor and other local loads connected in a distribution network and the voltage dip can be experienced by buses which are electrically remote from the point of the motor starting [191].

Generally, a motor starting study is undertaken before the motor is connected to investigate whether it can be successfully started under normal conditions or whether the voltage regulation of the network caused by a starting motor should be extracted to identify whether it impedes the normal operation of other equipment connected in the network. If DG units are connected in an industrial area, it is beneficial to study the motor starting process of the pre-existing loads to gain a deep insight into the system's voltage stability. The National Electrical Manufacturers Association (NEMA) has a standard that specifies the critical voltage level, which depends on load torque characteristics, that should be maintained during motor start-up and, for motor terminal, that voltage should be higher than or equal to 0.8 pu [191]. Different utilities have different grid codes and large motor start-up can violate the grid code requirements, specified for the PCC, by increasing the reactive power

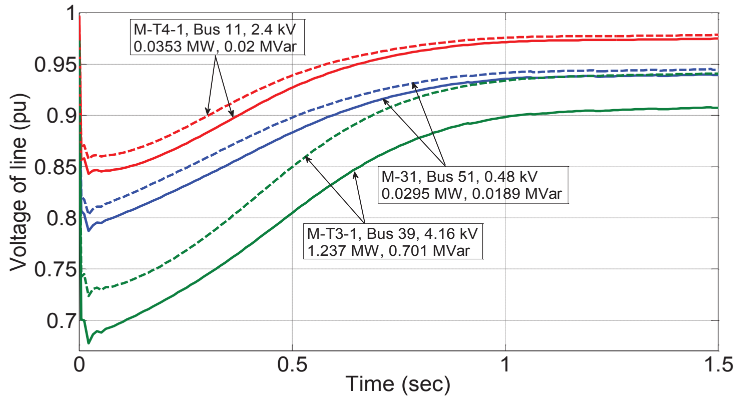

Figure 4.12. Voltage drops due to the starting of groups of motor at several buses

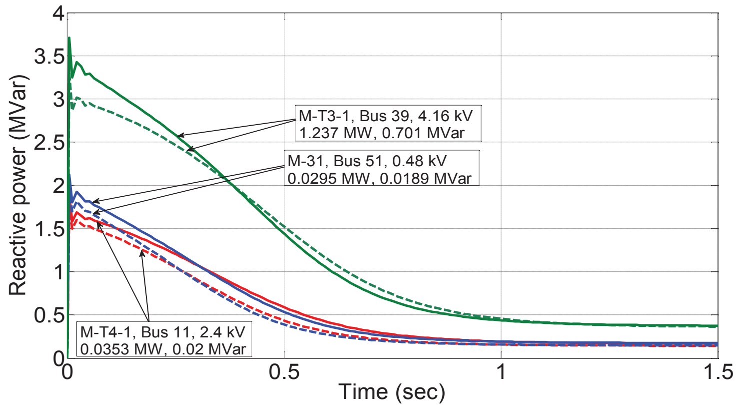

Figure 4.13. Reactive power demand due to starting of groups of motors at several buses

intake. Motor start-up can significantly affect the point of interconnection and a series of starting of motors in an industrial area can significantly increase voltage fluctuations. Again, a severe voltage depression may cause the break-down torque to be exceeded and, in such a stall mode, the motor draws a great deal of current from the connecting grid which can be alarming for a WT.

For this study, the weak connection of a network is considered. The impacts of motor starting are shown in Fig. 4.12 and Fig. 4.13. The terminal voltage and reactive power demand during a motor's starting period are investigated and, again, the reactive power drawn from the network is high with wind DG. Induction motors $M-31$, $M-T4-1$ and $M-T3-1$, connected at bus 51 (0.48 kV), 11 (2.4 kV) and 39 (4.16 kV), respectively, are used in the motor-starting analysis. $M-T4-1$ and $M-31$ are groups of 10 or 12 machines operating in parallel. As the rating of $M-T3-1$ is higher than the other two, it draws maximum reactive power which

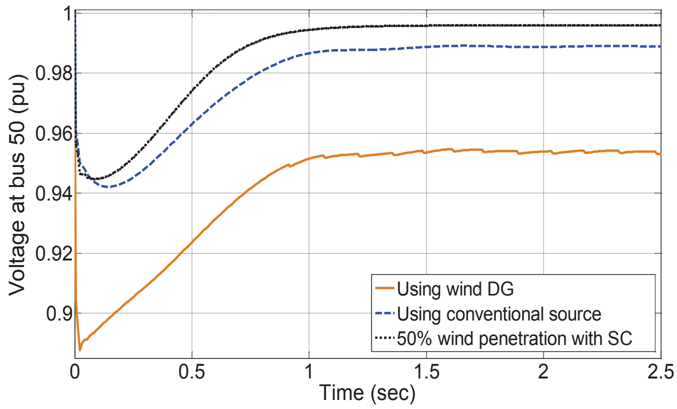

Figure 4.14. Impact of motors starting at the point of interconnection (bus 50)

causes a maximum voltage drop and, during starting, the terminal voltage is less than 0.8 pu. There are different methods for the soft starting of motors that can be implemented to resolve this problem as some utilities have enforced the consumer to take necessary steps if the starting process significantly reduces the voltage. For loads operated at nearly the critical voltage, the integration of WTs can adversely affect the situation. For $M - 31$, with conventional generation, the voltage level is slightly above 0.8 pu, but, with a WT the voltage level is below 0.8 pu. The impact of the motor starting is shown in Fig. 4.12, where using wind energy instead of a conventional source increases the voltage dip at the PCC. The wind penetration level and impact of series compensation are also shown in Fig. 4.12, Fig. 4.13 and Fig. 4.14 by the dotted lines. An increasing penetration of wind can lead the system to an unstable situation while 50 percent of wind penetration and 50 of conventional generation at bus 50 with series compensation increases stability and lowers the dip intensity.

4.3.2 Dynamic stability improvement

A powerful capability of series compensation is the ability to transfer more power by maintaining transmission line voltage even during an accelerating swing of a disturbing machine. The dynamic stability of a system can be increased by utilizing this advantageous characteristics of series compensation. Transient stability margin increases with the increase of series compensation. In practice, a maximum limit of 75 percent series compensation is used due to some factors, such as load balancing,

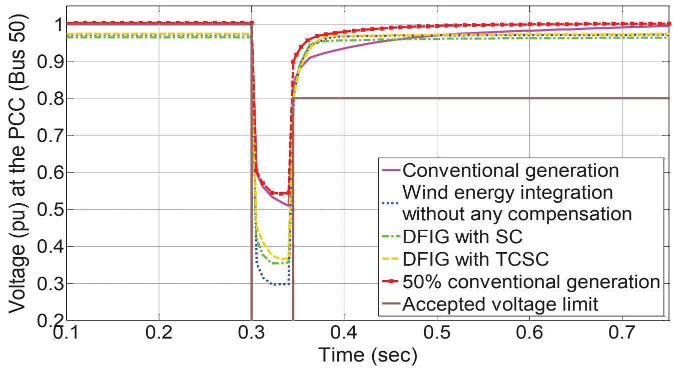

Figure 4.15. LVRT capability of different cases for three-phase short-circuit at middle of the line

exceeding the limit of the fault current, sub-synchronous resonance and power flow control problem [4].

In practice, fault scenarios, the pre-fault and post-fault conditions are often different. Power systems are designed to stay transiently stable under pre-fault conditions. According to grid codes, at the point of interconnection of a WT and utility, post-fault stability is an important consideration as stability degrades after a contingency due to the asynchronous generator and nature of wind. Most of the time, wind farms are not closely located to their load centre which necessitates a long transmission line that also increases voltage drop. Series compensation can handle dynamic disturbances and increase a system's stability and security.

A 5-cycle three-phase symmetrical short-circuit fault is applied in the middle of the line at 0.3 s, as shown in Fig. 4.15, to investigate the stability of the system with wind DG and series compensation. The accepted voltage limit according to the grid code imposed by Western Australian transmission system is also shown in Fig. 4.15. According to the LVRT capability requirement of Western Power grid code wind farms need to withstand any type of fault with a voltage drop to zero for 0.425 s and followed by a voltage restoration of 0.85 pu in next 10 s [106]. Implementing wind DG instead of a conventional synchronous generator degrades the voltage level to 0.95 pu from 1 pu while using a SC and TCSC raises the voltage level to 0.968 pu and 1 pu with a lower intensity voltage dip.

4.3.3 Impact of series compensation on load variation

Two types of load variations are considered: a static load connected at bus 49 and a synchronous motor as a dynamic load connected at bus 8 and the effects are

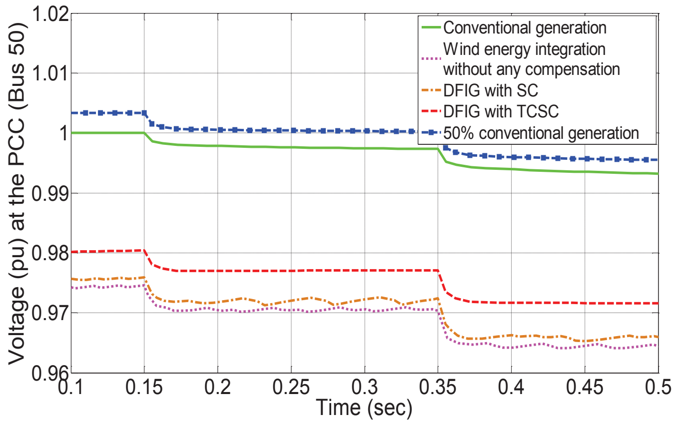

Figure 4.16. Voltage variations at PCC due to step changes in static load

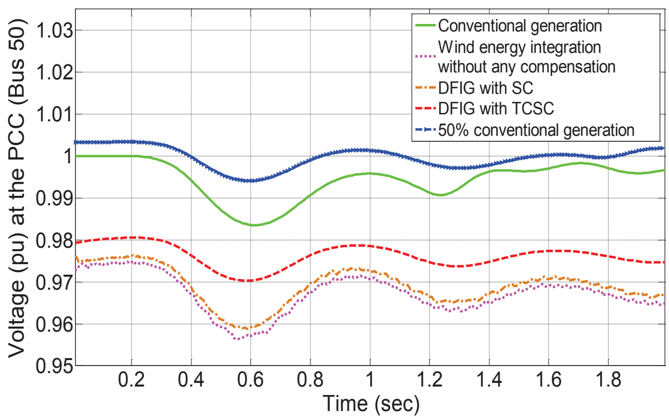

Figure 4.17. Voltage variations at PCC due to change in synchronous motor torque

shown in Fig. 4.16 and Fig. 4.17, respectively. The torque of synchronous machine is changed at 0.2 s and additional torque is removed at 0.6 s. Additional torque makes the system unstable and, even after its removal, the WT using SC and no compensation take longer time to stabilise the system. The conventional source, TCSC compensated system and hybrid system (50 percent wind and 50 percent conventional source) gradually reach the equilibrium point. A step change in static load is considered at 0.15 s and 0.35 s, and the total active power of the system is 1.613 MW and 0.819 MVAR. Induction generator's reactive power demand depends on its load, a variation in the reactive power of which causes fluctuating voltage which results in poor power quality and stability. In the first step, the total active power is changed by 47.76 percent and total reactive power by 50.79 percent and in the second step, by 71.64 percent and 76.19 percent, respectively. Series compensation increases the static voltage stability margin and lessens the possibility of the increasing load demand violating the voltage limit.

4.4 Short-Circuit Current Analysis of Wind Farm

A short-circuit analysis of an electrical system will quantify the maximum current that will flow for different types of faults which highly depends on the system's supply configurations. The contribution of a WT to a fault-level depends on the network parameters, the WT itself and additional arrangements for connecting the grid and WT. The network configuration, the proximity of a conventional generator, load portfolio, type of WT technology used to generate power, WT impedance, frequency converter system, connecting cable, step-up transformer, connection strength, wind integration level, etc., can directly or indirectly affect a system's short-circuit behaviour. In [20], the different approaches for fault-level analysis of a WT adopted by different utilities are presented. One approach is to use different wind energy penetrations and then analyse the general impact on the fault-level, a type of steady-state analysis conducted in a Transpower report [20], in which a WT is connected to a load centre. It is found that, with a sparsity of local generation, the WT increases the short-circuit level while it is possible to significantly decrease the fault-level if a WT is connected to conventional generation. A high short-circuit level affects the voltage stability of a system as it is difficult to maintain the voltage level appropriately. Similar studies of Irish, German and Iberian systems have been undertaken. Another approach is to perform a time domain simulation to ensure the correct operation of the system.

In one study, the Irish All Island Facilitation of Renewables [39], it is reported that the buses closer to the WT face increased fault levels with increases in wind penetration. Again, integrating of wind farms into an area where the fault-level is considerably high can further deteriorate the system. In New Zealand, national grid planning specifies different voltage levels for the short-circuited currents and powers [194] and the connection of an additional source cannot exceed those allowable limits. It is also highly recommended by NEM that a short-circuit current must be analysed with a WT, especially if it is connected in a HV network or weak grid.

The Integration of wind energy can change both the maximum and minimum levels of the fault current. In the Victorian transmission network, an increase in the

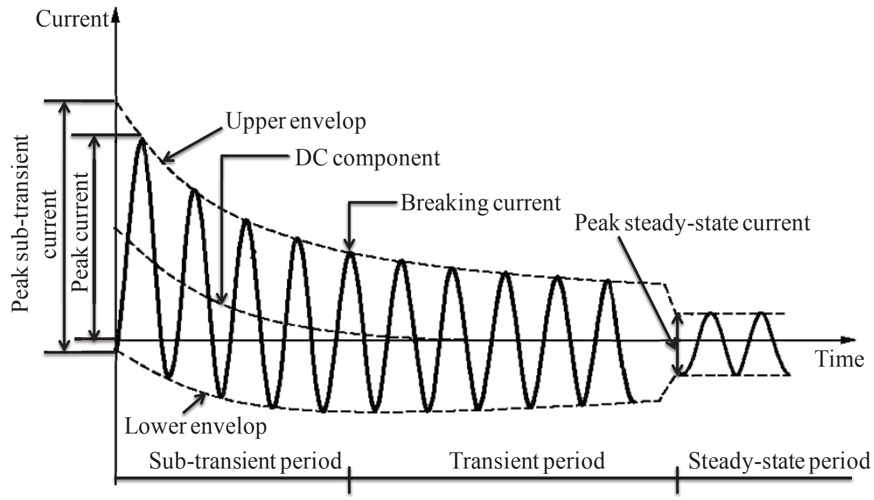

Figure 4.18. Different components of short-circuit current

fault current level due to the integration of wind energy has been reported whereas, in Tasmania, it is recommended the minimum fault current level be maintained above a certain level [20]. Minimum fault current maintenance is closely related to the protection of a system. However as, in this thesis, the stability of a network is the prime focus, only maximum fault current level is analysed.

In this section, a short-circuit current at the WT terminal and at the PCC is investigated considering three penetration levels of wind energy with and without compensation. Finally, the starting of a WT with a series compensated transmission line is examined.

4.4.1 Fault-level analysis of all busbars with increasing penetration level

Some parameters that are helpful in short-circuit analysis are the steady-state short-circuit current, I_{k}, initial AC short-circuit current, I''_{k}, and apparent power, S''_{k}, initial peak short-circuit current, i_{p}, AC-break short-circuit current, I_{b}, and power, S_{b}, and equivalent thermal short-circuit current, I_{th}. Fig. 4.18 sufficiently illustrates these parameters which are well defined in [195].

Fig. 4.19 shows the IEC-60 909-4, 8-bus HV test network (380 kV/ 110 kV/30 kV /10 kV) [196]. A DFIG-based wind farm is connected at bus LV and step-up transformers are used to connect it to a 100 km transmission line connected between bus 5 and bus HV, where bus 5 is considered the PCC. To investigate the wind penetration level, 5, 10 and 15 parallel WTs each rated at 1.5 MW, 690 V are considered

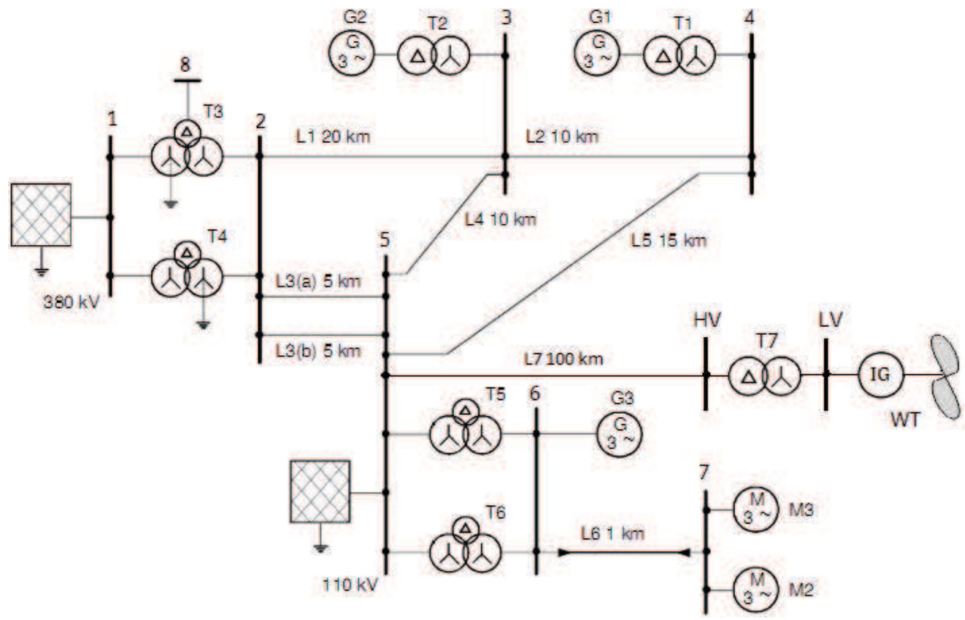

Figure 4.19. Single-line diagram of IEC HV test system for short-circuit analysis where WT is connected at bus 5 through long-distance transmission line

and series compensation is inserted in the transmission line connected between bus 5 and bus HV. The details of the network parameters can be found in [196] and WT parameters are given in Appendix V.

To analyse the impacts of a three-phase short-circuit fault, short-circuit of all bus-bars is considered and Table 4.6, Table 4.7 and Table 4.8 summarise the results. With an increasing penetration of wind power, the short-circuit sub-transient current also increases. At bus 5 and 4, the increases are considerably low, less than 0.5 percent whereas, at bus HV, the percent of increase is high and averages about 8.8 percent. It is very obvious that an increase in the short-circuit current will increase the short-circuit apparent power. With a compensated line, the percentage increases in the sub-transient current are about 0.06 percent for bus 4 and 5 and average 0.90 percent for bus HV which means that the rate of increase of sub-transient current is less if compensation is used. For bus LV, although the percentage increase is high with a compensated line, the numerical values are much lower than those for the wind farm without using series compensation. Series compensation does not have any impact on the steady-state short-circuit current but it reduces the peak current. The braking current is related to the switchgear equipment and for proper operation during contact separation, the current should be higher than the braking current.

Table 4.6. Fault-level analysis of symmetrical faults at all busbars with 5 WTs

Bus number		S''_{k} [MVA]	I''_{k} [kA]	i_{p} [kA]	I_{b} [kA]	S_{b} [MVA]	I_{k} [kA]	I_{th} [kA]
WC[a]	4	3101.83	16.28	36.95	16.07	3061.69	16.20	16.44
	5	6340.51	33.28	83.60	32.87	6263.33	33	33.93
	LV	87.52	73.23	153.83	49.54	59.21	23.04	47.93
	HV	321.32	1.69	3.42	1.67	317.95	1.57	1.70
WOC[b]	4	3113.74	16.34	37.05	16.10	3066.70	16.20	16.50
	5	6360.41	33.38	83.77	32.93	6273.71	33	34.03
	LV	200.87	168.08	370.33	144.22	172.36	118.06	150.31
	HV	352.89	1.85	3.7	1.73	329.71	1.57	1.86

[a] With compensation
[b] Without compensation

Table 4.7. Fault-level analysis of symmetrical faults at all busbars with 10 WTs

Bus number		S''_{k} [MVA]	I''_{k} [kA]	i_{p} [kA]	I_{b} [kA]	S_{b} [MVA]	I_{k} [kA]	I_{th} [kA]
WC[a]	4	3103.65	16.29	36.98	16.08	3063.51	16.20	16.45
	5	6343.65	33.30	83.65	32.90	6268.84	33	33.95
	LV	148.52	124.27	247.01	76.08	90.93	23.04	62.44
	HV	325.24	1.71	3.49	1.71	325.24	1.57	1.72
WOC[b]	4	3125.98	16.41	37.18	16.15	3077.80	16.20	16.57
	5	6381.11	33.49	83.99	33.03	6292.51	33	34.14
	LV	261.31	218.65	463.96	170.49	203.76	118.06	178.88
	TR	389.99	2.05	4.12	1.87	356.42	1.57	1.87

[a] With compensation
[b] Without compensation

Both a WT and series compensation can affect the braking current of the network as can an increasing penetration of wind energy. These issues need to be properly addressed for the protection of WTs.

The current levels listed in Table 4.6, Table 4.7 and Table 4.8 are above the current ratings specified by grid codes, because, short-circuit faults are analysed for all busbars which raises the current level beyond these limits. The intension of this study is to investigate the impact of wind energy penetration and series compensation on fault-levels.

Table 4.8. Fault-level analysis of symmetrical faults at all busbars with 15 WTs

Bus number		S''_{k} [MVA]	I''_{k} [kA]	i_{p} [kA]	I_{b} [kA]	S_{b} [MVA]	I_{k} [kA]	I_{th} [kA]
WC[a]	4	3104.39	16.29	37.0	16.08	3064.26	16.20	16.46
	5	6344.94	33.30	83.67	32.91	6270.15	33	33.95
	LV	209.65	175.42	340.35	102.64	122.66	23.04	73.57
	HV	326.85	1.72	3.53	1.72	326.85	1.57	1.73
WOC[b]	4	3133.70	16.45	37.26	16.20	3085.86	16.20	16.61
	5	6394.21	33.56	84.14	33.10	6306.26	33	34.21
	LV	322.04	269.47	557.53	196.84	235.25	118.06	203.34
	TR	417.07	2.19	4.45	1.99	379.60	1.57	1.97

[a]With compensation
[b]Without compensation

Table 4.9. Three-phase short-circuit fault at bus 4 with 10 WTs

Bus number		S''_{k} [MVA]	I''_{k} [kA]	i_{p} [kA]	I_{b} [kA]	S_{b} [MVA]	I_{k} [kA]	I_{th} [kA]
WC[a]	4	3101.83	16.28	36.95	16.07	3061.69	15.96	16.44
WOC[b]	4	3113.74	16.34	37.05	16.10	3066.70	16.20	16.50

[a]With compensation
[b]Without compensation

4.4.2 Fault-level analysis of single busbar with symmetrical and asymmetrical fault

In this case, a three-phase short-circuit fault at bus 4 and a two-phase short-circuit fault at bus HV are considered and summaries of the results are provided in Table 4.9 and Table 4.10, respectively. All the current and apparent power are in the specified range fixed by the utility. In bus HV, the use of a series compensating device reduces the short-circuit apparent power and braking apparent power of the two affected phases by approximately 8.94 percent and i_{p} and I_{b} by 8.75 and 7.18 percent, respectively. In both cases, using series compensation reduces the sub-transient current, sub-transient apparent power, peak current and braking current and braking apparent power.

4.4.3 Switching of wind farm

To generate a magnetising current, an induction machine requires reactive power. As a consequence, an inrush current generates during grid interconnection of an

Table 4.10. Two-phase short-circuit fault at bus HV for with 10 WTs

Line 1		Rated Voltage [kV]	Voltage [kV]	S''_{k} [MVA]	I''_{k} [kA]	i_{p} [kA]	I_{b} [kA]	S_{b} [MVA]
WC[a]	A	110	69.86	0	0	0	0	0
	B	110	34.93	92.76	1.46	2.97	1.46	92.76
	C	110	34.93	92.76	1.46	2.97	1.46	92.76
WOC[b]	A	110	69.86	0	0	0	0	0
	B	110	34.93	101.87	1.6	3.2	1.6	101.87
	C	110	34.93	101.87	1.6	3.2	1.6	101.87

[a] With compensation
[b] Without compensation

asynchronous machine based wind farms [197]. Normally, a pitch-regulated WT has smoother switching than a stall-regulated one. For a FSWT, this inrush current is 7 to 8 times greater than the rated current [11] which causes voltage disturbances in the grid and is also harmful for other equipment connected to the grid. Most VSWTs can efficiently control torque although switching may be required due to a low wind speed, higher shaft speed or due to inappropriate sensor responses [198]. Zou et al. [198] discussed the start-up procedure for a DFIG.

The wind farm connected at bus LV is disconnected at 0.1 s and re-connected at 0.2 s. The responses of the current and reactive power in the transmission line due to the switching operation of a wind farm with and without series compensation are given in Fig. 4.20 and Fig. 4.21, respectively. The connection of a wind farm to the grid produces an inrush current in the transmission line and without compensation, the peak current is almost double what it is with compensation. Due to the start-up, the reactive power demand is also very high. Using compensation reduces the sharp rises of inrush current and reactive power caused by the start-up procedure.

4.5 Summary and Conclusions

The impacts of series compensation using three different type of network configuration are analysed with FSWT and DFIG wind farms. A voltage source converter (VSC)-based series compensator, thyristor controlled series compensator and SC are used to evaluate their performances in different scenarios.

- The performances of series and shunt compensation in dynamically controlling and enhancing the stability of wind farms, where a FSWT is connected to an

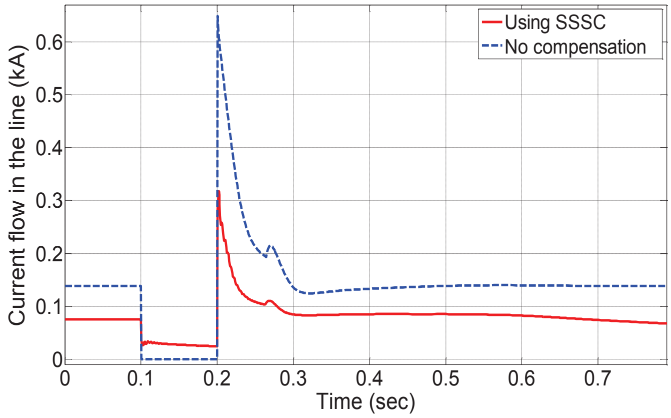

Figure 4.20. Generation of current transients in the long-distance transmission line due to switching of wind farm

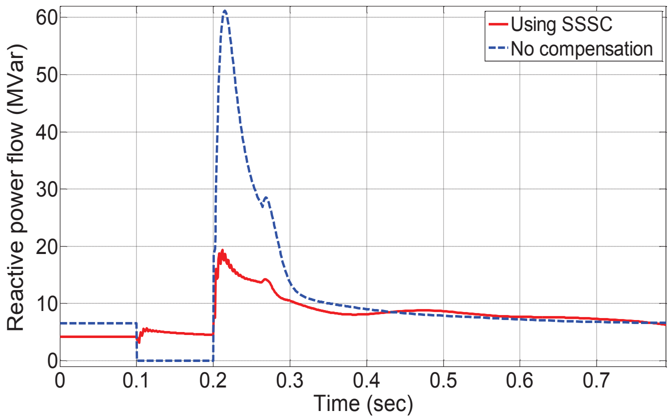

Figure 4.21. Peak reactive power demand in the long-distance transmission line due to switching of wind farm

infinite bus, are investigated. Both the STATCOM and SSSC can maintain a stable operation under normal conditions. Although a higher voltage level can be found from SSSC2, the reactive power consumption from the grid is lower with the STATCOM. Both the STATCOM and SSSC can restore the pre-fault value but the latter SSSC takes longer and has a voltage rise problem just after clearing the fault. The STATCOM is sufficiently quick to restore the fault and has a lower intensity voltage dip. The 8 MVA STATCOM and SSSC can maintain the voltage within permissible limits for a 6 MW wind farm but their performance deteriorate with a lower MVA rating which justifies simulating the system with 5 MVA and 3 MVA STATCOM and SSSC. The investigation results shows that, if a series compensating device is placed at a suitable position, a better voltage level can be obtained with smaller size. Changing the load conditions has a significant impact on the voltage dynamics of a power system with wind energy penetration. The rate of decrease in the voltage with increases in the load is more severe using the SSSC than STATCOM.

- A TCSC and SC are used in the IEEE 43-bus distribution system, where a DFIG is considered an embedded generator and different types of load variation are the main focus. An industrial distribution test system is chosen as load variations in such areas are intense. Motor start-up, varying torques of a synchronous machine and step changes in composite load are analysed in terms of voltage stability using series compensation which, it is found, is helpful for increasing stability, especially in a weak grid.
- Series compensation is an effective way of limiting fault current. A SSSC is implemented in a HV network where a DFIG-based wind farm supplies power through a long-distance transmission line. Fault-level is calculated for symmetrical and asymmetrical faults with increasing levels of wind energy penetration and it is found that series compensation can limit the sub-transient current and peak current and thereby minimise the short-circuit apparent power. In a series-compensated line, the reactive power loss and peak sub-transient current are considerably low.

The impacts of series compensation with wind energy on voltage stability, the reactive power flow control capability and fault current limiter are addressed in this chapter. The next chapter discusses the power quality issues of a wind farm with series compensation.

Chapter 5

Power Quality Enhancement of Wind Farms

5.1 Introduction

Reducing the distortions in voltage and current waveforms to permissible levels has been a problem in power systems, especially those with high penetration of wind energy. In this chapter, power quality problems due to the integration of wind power plant is investigated for transmission and distribution network using series compensation. Harmonic current distortion, flicker emissions, voltage sag analysis, relative voltage variations, voltage stability margin and sensitivity analysis are performed for fixed-speed wind turbine (FSWT) and doubly-fed induction generator (DFIG)-based wind farms using a series capacitor (SC) and controlled capacitor.

Embedded generation or decentralised generation can be defined as resources connected in a distribution network or on a consumer site, irrespective of the voltage rating required to meet the energy and reliability needs of consumers, through a distribution system which, essentially, supplies active power rather than reactive power [199]. A distribution system's distributed generator (DG) rating depends on its capacity which is related to its voltage level as the distribution system is not designed for power-generating devices. Although, the usage of DG units offers a number of technical, environmental and economical benefits, its special characteristics, such as low inertia and variable output power, can present many challenges regarding the stability of a power system. As connecting a wind turbine (WT) on the distribution side is responsible for large voltage variations in the feeder and changing fault-current levels, there are restrictions on integrating wind farms in a distribution network in terms of their rating and number of WTs, especially if the network is weak [32], [199].

Although, the increasing penetration of wind energy and the number of WTs can increase a system's local voltage level, it decreases its stability margin compared with that of a system without wind energy. An analysis shows that static

VAR compensator (SVC) and static synchronous compensator (STATCOM) types of shunt devices increases both the stability limit and voltage level [32]. Series compensation is used extensively in transmission networks [59], [61], [200] in order to improve transmission efficiency. Distributed shunt [32], [172] and series compensation [36], [52], [54] have also been connected to a distribution network to achieve better voltage regulation by improving the voltage drop in the feeder. The advantage of a SC over a shunt capacitor is its capability to naturally regulate voltage with the changes in the line current [201]. To date, the impact of wind DG and the dependency of series capacitive reactance on the stability margin, line reactance to resistance ratio (XRR), sensitivity and harmonic currents has not been discussed in detail.

Ferro-resonance, sub-synchronous resonance (SSR) and its inability to withstand fault levels are major disadvantages that limit the widespread use of series compensation in distribution network. Spark gaps, by-pass circuit breakers, choke and damping resistors are some techniques for overcoming these application problems [201]. Some practical examples of using SC are described in [52], [54] which shows that it is possible to overcome the ferro-resonance problem by choosing a proper location for the SC and improve the fault tolerance capability by implementing proper protection because wind-based DG units can have a considerable impact on the power flow and voltage profile of a distribution system as most WTs consists of induction generators which can significantly reduce a system's stability margin [202]. With the increasing number of wind generators, it is necessary to analyse the power quality characteristics of a distribution network using series compensation. In this chapter, wind DG integration into a grid using series compensation is analysed to investigate its impact on power quality.

Wind generators tend to influence the voltage at the point of common coupling (PCC) and, simultaneously, are responsible for the propagation of voltage fluctuations and harmonic distortions in the connected grid [35], [203]. For a transmission line, XRR ratio is generally high with a low resistance to minimise transmission loss. In a distribution network, resistance and inductance are both likely to cause substantial voltage drops in distribution lines. For a transmission network, interactions of the harmonics of the load and grid connected renewable energy sources are considerably lower than those in a distribution network. With the increasing use of nonlinear loads and power electronic devices, such as computers, fluorescent and mercury lamps, arc furnaces, arc welders, rectifiers, VSCs, pulse width modulation (PWM) inverters, feeder lines and cable capacitances, which are harmonic-generating sources [11], [115], [204] it is necessary to analyse the harmonic distortion levels using wind generators.

In this chapter, the following cases are considered for different scenarios.

- A conventional generating unit is displaced by a large wind farm at the transmission side and the impacts on voltage level and slow voltage variation rates are investigated for FSWT and DFIG-based wind farms using a SC and STATCOM.
- A harmonic current distortion analysis, in which the converter of the STATCOM and DFIG, is modelled as an unbalanced harmonic generating source and with class A type loads, is performed using series compensation.
- Sensitivity and static voltage stability analysis is performed with wind farms connected to a distribution network using series compensation.
- A DFIG-based wind farm is connected to a 43-bus distribution network and the performances of a thyristor controlled series compensator (TCSC) and SC is investigated for voltage sag and flicker emissions of wind farms in which increasing penetration of wind power is also addressed.

5.2 Power Quality Issues for Transmission System

To analyse different power quality issues on the transmission side, series compensation is introduced at the PCC to determine its impact on the voltage stability and low-voltage ride-through (LVRT) capability of both a FSWT and DFIG wind farm. One conventional generating unit of a 9-bus test system [205] is removed and replaced by a wind farm to investigate the impacts of high wind energy integration in the grid, on both at the voltage of the PCC and the network's other bus voltages.

In this section, simulation results for different cases are presented. Firstly, the impact on bus voltages of wind energy and a SC is investigated; then, the effects of a SC on voltage sag and LVRT are analysed; with the test results for harmonic currents and flicker emissions at the PCC are presented. In this study, the traditional multi-machine power generation system is replaced by a large wind power plant which can have adverse effects on the stability and dynamic nature of a power system.

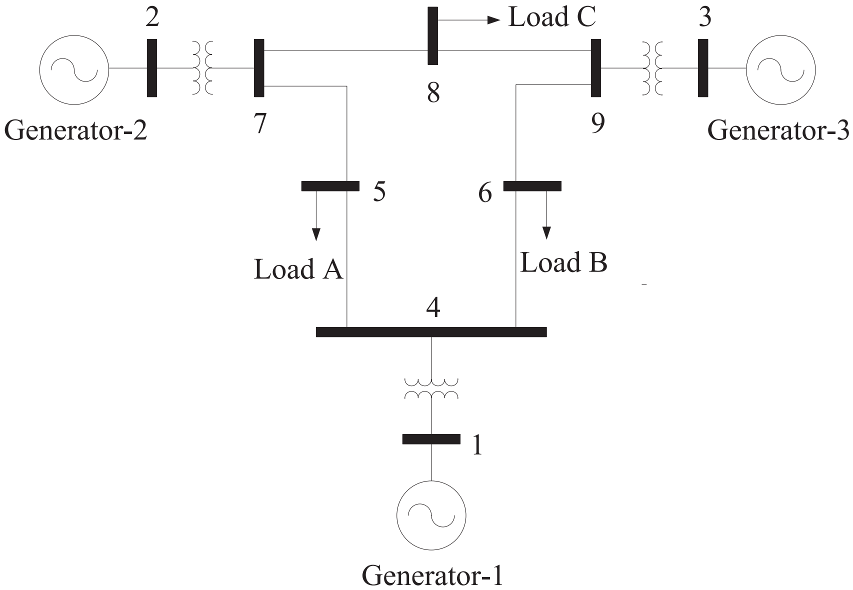

Figure 5.1. Single-line diagram of 3-machine 9-bus system

5.2.1 Case study

The well-known 9-bus test system [205] shown in Fig. 5.1 is modeled in DIgSILENT in order to analyse voltage stability and harmonic issues. It has three synchronous generators equipped with the automatic voltage regulators (AVRs) and a total rated power of 567.5 MVA, and its total load of 315 MW, 115 MVAR is modelled as a constant power load. The conventional generation at bus 2 is removed and replaced by a 192.5 MW wind farm through a step up transformer to compare the impacts of wind and conventional generation. The wind farm consists of 55 FSWTs, each rated at 3.5 MW, and a STATCOM is connected at the PCC, busbar 2, for dynamic voltage support. The FSWT is equipped with a 400 kVAR capacitor bank. Later, the same number of DFIGs with the same ratings is connected at the PCC with a SC inserted between bus 2 and bus 7. For harmonic analysis, the load connected at bus 5 is considered as a constant current load. As the installed wind farm provides 33 percent of the total power, the obtained system can be considered to have large wind energy penetration. The network parameters are given in [205] and WT parameters are given in Appendix VI.

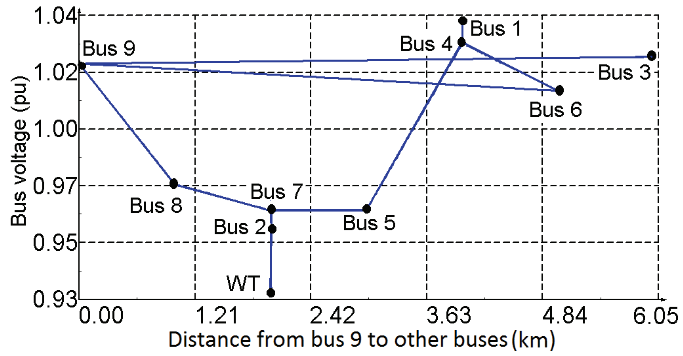

Figure 5.2. Voltage profile of 9-bus test system with FSWT and STATCOM

5.2.2 Voltage quality

This test case is simulated with conventional generating units and a wind energy source connected at bus 2. The most sensitive bus is bus 5 which has conventional generation with a voltage of 0.996 pu. After the integration of the FSWT-based wind farm, incorporated with a STATCOM at the PCC for reactive power control, the bus 5 voltage decreases to 0.963 pu and that at the PCC drops from 1.025 pu to 0.955 pu, as shown in Fig. 5.2. For wind energy penetration without any compensation, these voltages fall below 0.90 pu but, by inserting a SC between bus 2 and bus 7, not only does the voltage at bus 5 to to increase (0.980 pu.) but so do those of the other buses, as shown in Fig. 5.3. The DFIG improves the voltage at the PCC to 1.025 pu. compared with that of the FSWT equipped with a STATCOM while the voltage at the terminal at which the WT is connected increases to 1.0 pu. The DFIG with a SC enhances the voltage at the PCC at both the bus at which the WT is connected and bus 5 as shown in Fig. 5.4. In the test system, the WT is placed close to two conventional units that strengthen the grid. In the case of a weak grid, voltage stability is a major problem which can be overcome by a SC.

Using a voltage sag tool, short-circuits at selected load points within the system are calculated using the failure data of the system components to extract the voltage sag probability, with the exposed area limit considered 90 percent. Asymmetrical faults, i.e., phase-to-phase faults, occur more frequently than short-circuit faults and can have a more devastating impact on a wind farm [189]. During analyses, a 50% fault is considered a single phase-to-ground fault, a 6% fault a two-phase short-circuit, a 3% fault a two phase-to-ground fault and the remaining percentages three-phase short-circuit faults. Stochastic failure data is defined for all the terminals

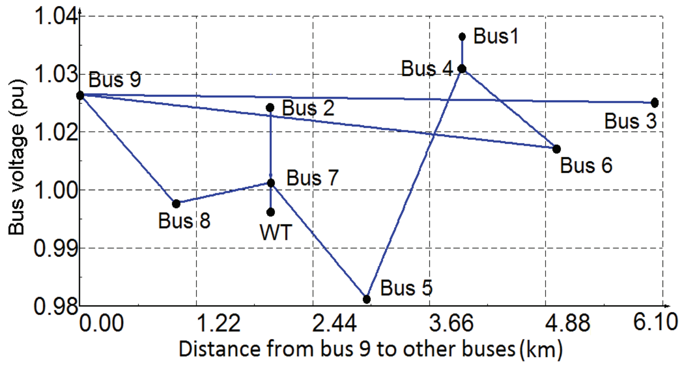

Figure 5.3. Voltage profile of 9-bus test system with FSWT, STATCOM and SC

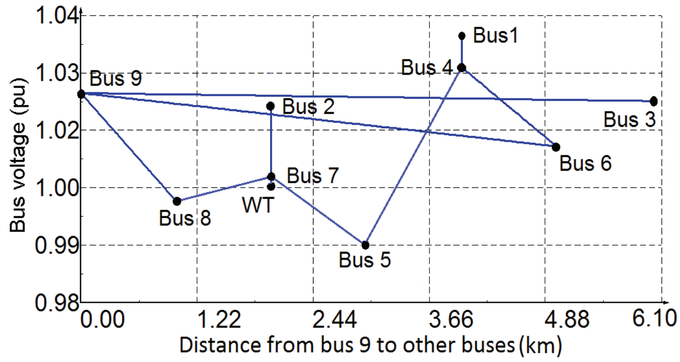

Figure 5.4. Voltage profile of 9-bus test system with DFIG and SC

in the system which are divided into four groups: the HV (busbar voltage rating of 230 kV); MV (busbar voltage rating between 13.8 kV and 18 kV); WT (the bus at which the WT is connected); and DC busbar. Each group is modelled using identical failure frequencies and repair durations, with the DC busbar of the STATCOM modelled using these groups' minimum probability failure data.

The voltage sag characteristics of this 9-bus test system with wind energy penetration, which are found to be significantly affected by the SC, are discussed in this section. In spite of the generator bus, other buses are seen to suffer from deep voltage sag (the remaining voltage is less than 0.4 pu.) while all incur shallow sag. The voltage sag characteristics of the conventional source, and FSWT and DFIG with FACTS devices are summarised in Table 5.1, which focuses on bus 2 and bus WT because this study is concerned mainly with large wind power penetration and its impact on the PCC. The voltage sag characteristics of the FSWT with a STATCOM show that bus 2 suffers deep sag due to wind energy penetration, with the three-phase short-circuit fault being mainly responsible, whereas wind energy penetration

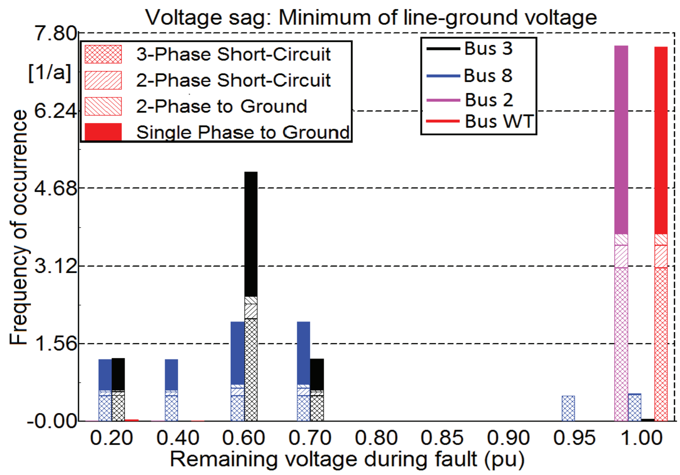

Figure 5.5. Voltage sag plots for selected buses using DFIG with SC (C= 0.003F)

has less effect on the moderate and shallow sags at the PCC. Series compensation is analysed using three different values of the SC. Although, with SC1 (0.009 F), deep sag increases more than with the other capacitor values, shallow sag has a lesser impact, especially when the remaining voltage is high. With SC2 (0.006 F), there is either no or less deep sag at the remaining voltages of 0.2 pu for the FSWT and DFIG, respectively, although moderate voltage sag is noticed for both. With SC3 (0.003 F), voltage sag is observed at two extreme points, i.e., the remaining voltages of 0.2 pu and 1.0 pu, where the frequencies of occurrence are low and high, respectively.

In Fig. 5.5, the voltage sag characteristics of the DFIG with a SC, where the X axis represents the remaining voltage of the bus bar during a fault and the Y axis represents the frequency of occurrence throughout the year in which the bar of the voltage sag plot is sub-divided into short-circuit types, are shown. If the capacitor value is decreased, the frequency of occurrence of shallow sag increases at the PCC and that of moderate sag tends to decrease. A SC causes more significant reductions in the annual frequency of occurrence of moderate voltage sag of other buses in the network. By choosing a proper value for a SC, voltage sag at the PCC and load points can be minimised.

Table 5.1. Voltage sags

FOC [a] \ Fault voltage		0.2	0.4	0.6	0.7	0.8	0.85	0.9	0.95	1.0
Conventional source	Bus 2	0.005	0	0.513	1.25	1.025	1.25	1.988	0.738	0.738
	WT	-	-	-	-	-	-	-	-	-
FSWT with STATCOM	Bus 2	0.017	0.512	0.512	0	2.275	0.737	1.988	0.738	0.738
	WT	0.093	0.512	0	1.25	0	3.013	1.475	0.513	0.738
FSWT with STATCOM and SC1	Bus 2	0.512	0.038	3.012	0.738	1.988	0.007	0.738	0	0.513
	WT	0.738	0.512	1.25	1.763	1.475	0.513	0.738	0	0.513
FSWT with STATCOM and SC2	Bus 2	0	2.275	2.213	0.513	0.738	0	0	0	1.763
	WT	0.093	1.25	3.238	0.738	0.513	0.738	0	0	1.025
FSWT with STATCOM and SC3	Bus 2	0.017	0	0	0	0	0	0	0	7.5
	WT	0.093	0	0	0	0	0	0	0	7.5
DFIG	Bus 2	0.006	0.513	1.25	0	3.750	0.738	0.513	0.736	0.019
	WT	0.033	0.012	0.513	1.25	1.76	3.013	1.475	0.513	0.738
DFIG with SC1	Bus 2	1.25	0.013	3.013	1.475	0.512	0.737	0	0	0.512
	WT	0.033	1.250	0.738	2.275	1.475	0.512	0.738	0	0.512
DFIG with SC2	Bus 2	0.012	3.012	1.987	0	0.737	0	0	0.737	1.025
	WT	0.033	1.760	2.725	0.512	1.25	0.737	0	0	0.513
DFIG with SC3	Bus 2	0	0	0	0	0	0	0	0	7.5
	WT	0.033	0	0	0	0	0	0	0	7.5

[a] Frequency of Occurrence

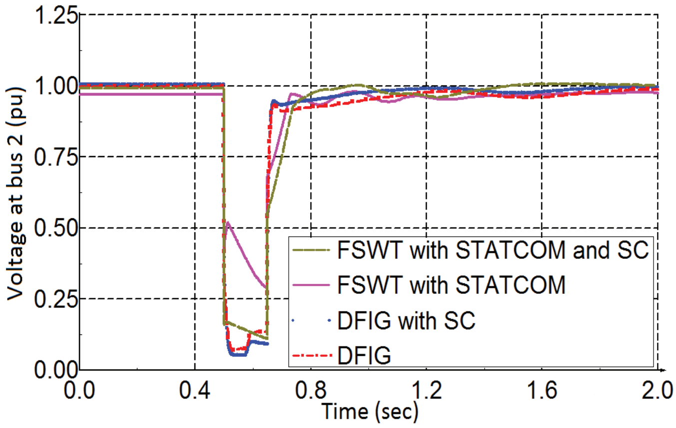

Figure 5.6. LVRT capabilities of wind farms for different cases

A three-phase short-circuit 9-cycle fault is applied at the middle of transmission line 3 at 0.50 s with the pre-fault voltage more rapidly recovered by the FSWT with a STATCOM and SC than the FSWT with a STATCOM. The DFIG shows better performances in terms of recovering voltages after the fault while the SC increases the CCT which, for the FSWT and DFIG wind farms with both shunt and series compensation, are 0.481 s, 0.502 s, 0.460 s and 0.465 s, respectively. It also enhances their LVRT capabilities, as shown in Fig. 5.6.

5.2.3 Harmonic current

To investigate the impact of the harmonic generating source at the PCC, the positive and negative sequence harmonic currents up to the 29th order for the FSWT and DFIG wind farms are shown in Fig. 5.7 which indicates that the harmonic current injection level is reduced at the PCC with a SC. As the harmonic current depends on the nature of the harmonics source, inserting a capacitor in a series or shunt may adversely impact its interaction with the existing harmonics source present in the network. Therefore, before connecting a series-compensating device, it is necessary to know the nature of the harmonics present in the system and the effect of their interactions.

5.2.4 Flicker

The short-term flicker severities, P_{st}, for the FSWT and DFIG wind farms with and without a SC are calculated using a flickermeter, with the flicker coefficient, flicker step factor and voltage change factor calculated for network impedance angles of $30\,^{\circ}$, $50\,^{\circ}$, $70\,^{\circ}$ and $85\,^{\circ}$, and the wind speed implicitly considered in the coefficients.

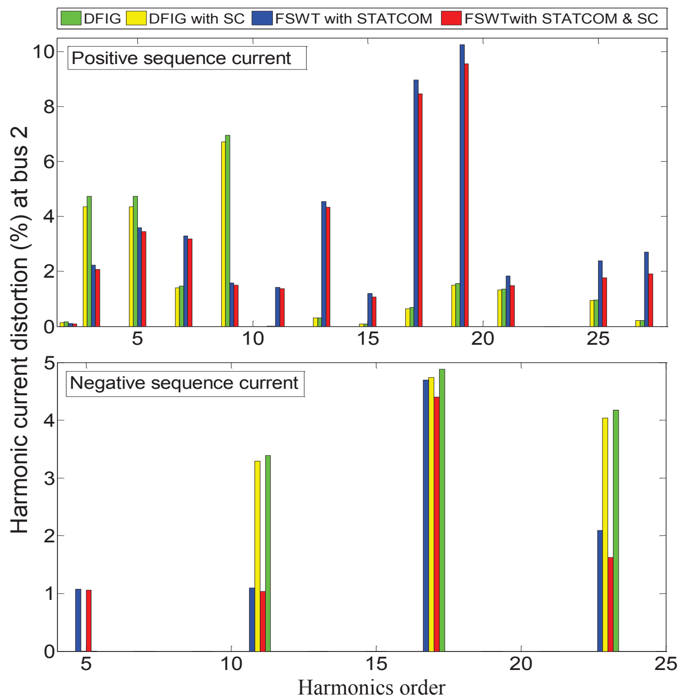

Figure 5.7. Positive and negative sequence harmonic currents at the PCC

Table 5.2. Contributions to flicker of wind farms

	$P_{\text{st-cont}}$	$P_{\text{lt-cont}}$	$P_{\text{st-sw}}$	$P_{\text{lt-sw}}$	d_{sw}
DFIG	0.0184	0.0184	0.0060	0.0048	0.0251
DFIG with SC	0.0164	0.0164	0.0052	0.0042	0.0222
FSWT	0.0232	0.0232	0.0077	0.0061	0.0266
FSWT with SC	0.0201	0.0201	0.0066	0.0053	0.0231

Table 5.2 shows the short-term flickers, P_{st}, and long-term flickers, P_{lt}, and percentages of relative voltage change, d_{sw}, for switching and continuous operations of the wind farms. The VSWT emits fewer flickers than the FSWT but both reduce the relative voltage change at the PCC when a SC is connected. The P_{st} and P_{lt} disturbance factors for continuous operation are observed to reduce by 10.87% and 13.36% for the DFIG and FSWT farms, respectively and, for switching operation, by 13.33% and 14.29%, and 14.29% and 13.10% for the DFIG and FSWT wind farms, respectively, due to the insertion of a SC. As, according to [103], flicker emissions from a wind farm need to be regulated based on the load's nature and total flicker severity at the PCC, they can be mitigated by connecting a SC, especially at the distribution side.

5.3 Power Quality Issues for Distribution System

The voltage profile and power quality issues of a distribution network with DFIG-based wind DG and series compensation, a SC and TCSC, are investigated. Series compensation is implemented to reduce voltage drops in the line and feeder, and to minimise the reactive power mismatch caused by integrating DFIG units. The converter of the DFIG is modelled as an unbalanced harmonic-generating source and the load according to IEC standard 61000. The impacts of DG and series compensation on the voltage profile, stability margin, dynamic stability and harmonic distortion of a distribution network are investigated in detail. The simulation results demonstrate that series compensation can enhance the collapse margin, reduce bus voltage sensitivity to reactive power and also improve both dynamic and transient voltage stabilities.

In the first case, Section 5.3.1, the DFIG is characterised as a Norton equivalent source and the load as a constant current source to investigate the impact of series compensation on the harmonic current due to interactions between wind DG and the utility. Voltage stability is analysed by applying different tools, such as the PV curve, sensitivity analysis and time-domain transient simulations, where variations in network parameters, XRR ratio and series reactance, are considered. In the second case, Section 5.3.6, a commercial, industrial distribution system is considered for assessing the flicker contribution of the wind farm which is followed by a voltage sag analysis using reliability data.

5.3.1 Case study 1

Case studies are conducted on a widely used 15-bus distribution network in the DIgSILENT PowerFactory environment to analyse the impact of series compensation. The performance of a system depends greatly on the locations and sizes of its compensating devices while the size of a SC depends on the inductive reactance present in the network. In [52], $5.3\,\Omega$ and $4.2\,\Omega$ series reactances are used for a distribution site whereas, in [54], $35\,\Omega$ is used. In this study, series compensation is limited to $4.2\ \Omega$ as, if it is higher than required, it may result in an over-compensation problem. In [206], the optimal DG locations are calculated for the test case described below, using an optimisation technique which shows that the possible DG allocation buses are buses 5, 11 and 13. In this case, DG is connected at bus 11.

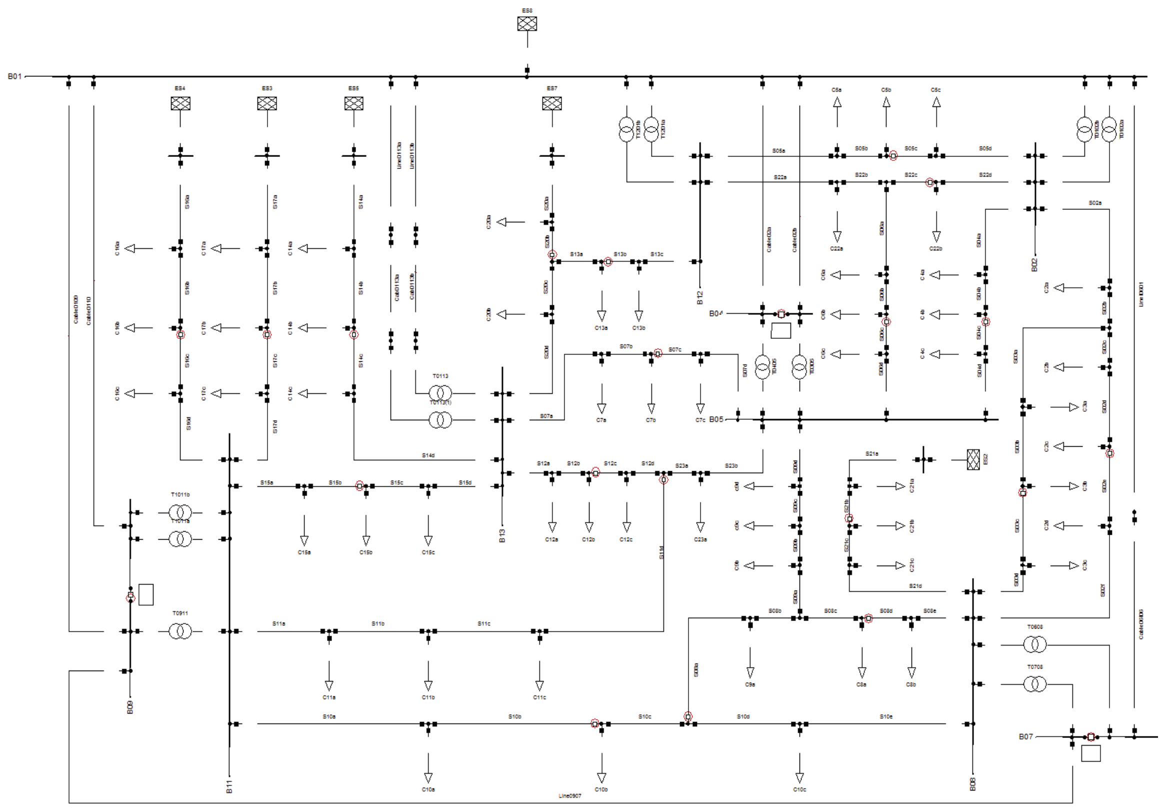

Figure 5.8. Single-line diagram of 33 kV/11 kV distribution test system

A 5 MW DFIG-based wind DG unit is connected to the 33 kV/11 kV distribution reliability test system (Distribution RTS) [138] and the single-line diagram of the 15-bus distribution test system is shown in Fig. 5.8. The DG is connected at the PCC, bus 11 (11 kV), through a step-up transformer followed by a 10 km transmission line as shown in Fig. 5.9. In the remainder of this chapter, the bus at which the wind DG unit is connected is denoted as the LV bus and the total load of the system is 52 MW, 9.71 MVAR. A SC with an impedance of 4.2 Ω is connected between the transmission line and bus 11 and, for harmonic analysis, the load, connected at bus 13, $C15c$, is considered a constant current load. Later, in order to investigate the performance of a TCSC in a distribution system, it is connected to the wind DG unit instead of the SC. The network parameters are given in [138] and WT parameters are given in Appendix VII.

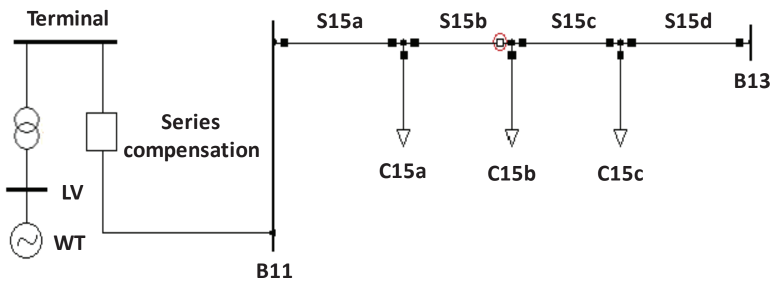

Figure 5.9. A part of distribution network where wind DG is connected at bus 11 and series compensation is used in the 10 km line

5.3.2 Voltage stability margin and bus sensitivity

Voltage instability, which is caused by the transmitted active power, injected reactive power and receiving end voltage, can affect all other parts of a network [147]. Voltage stability can be investigated from different aspects such as short term, long term, disturbance level, etc. The relationship between the transmitted active power and receiving end voltage is well described by a PV-curve analysis as a PV-curve describes a network's critical voltage and collapse margin which change with the insertion of a series compensating device and wind DG unit.

Wind power causes significant reductions in the stability margin [34] which depends on its penetration level, the number of operating turbines and location of the wind DG unit. For SC, four different series reactances, $4.2\,\Omega$, $2.0\,\Omega$, $0.637\,\Omega$, $0.064\,\Omega$, are used to investigate its impact on the collapse margin. By increasing the capacitive reactance of the line, the voltage stability margin of the network also increases, as shown in Fig. 5.10. Due to the integration of wind power in the distribution network, the collapse margin decreases by approximately 30 percent with increments in load, as shown in Fig. 5.10, which can be improved by using distributed series compensation in the line. Implementing the TCSC increases the system's load margin by 18.75 percent and its critical voltage by 2.9 percent. The load margins for all cases are listed in Table 5.3.

The bus sensitivities, $\frac{dv}{dQ}$, of buses 11, 8 and LV are analysed and shown in Fig. 5.11. Implementing a SC reduces bus sensitivity, i.e., the dependency of the voltage variations on changes in the reactive power. Using series compensation has the most significant impact on reducing the sensitivity of the bus where wind DG is connected. For a SC the sensitivity reduces to 0.0538 and for a TCSC to 0.0258. In these analyses, the XRR ratio is considered 7.

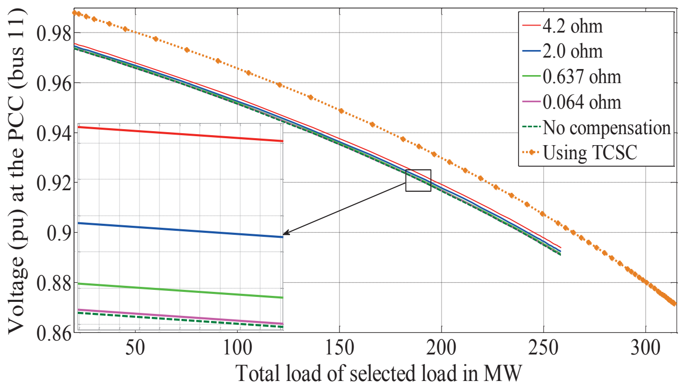

Figure 5.10. PV curves for different X_c and TCSC

Table 5.3. Load margin

Cases	Load margin in MW
No compensation	258.440
4.2 Ω	258.458
2 Ω	258.442
0.637 Ω	258.440
0.064 Ω	258.440
TCSC	313.661

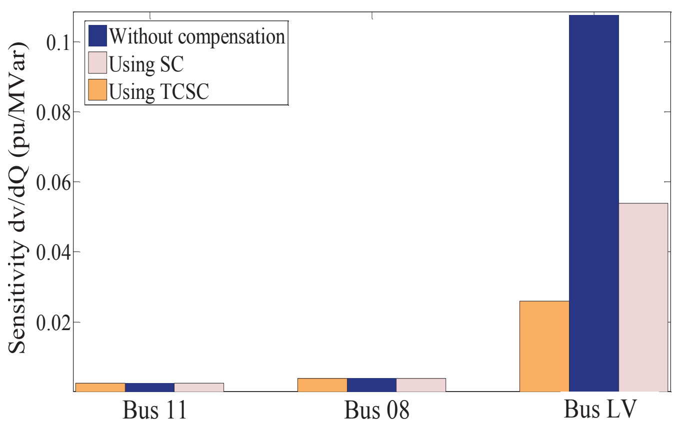

Figure 5.11. Impact of series compensation on bus sensitivity

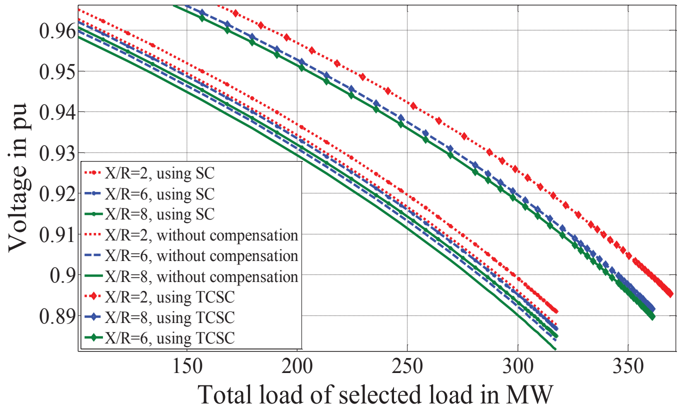

Figure 5.12. PV-curves for different XRR ratios

5.3.3 Line reactance to resistance ratio

The dependency of voltage stability and load stability is analysed in terms of the wind speed variations, short-circuit capacity ratio (SCC) at the PCC and XRR ratio of transmission line impedance in [42] which identifies whether the maximum penetration level of a wind farm is higher than a specific level, as determined by the SCC, and, if so, the system becomes unstable. The XRR ratio contributes significantly to enhancing the stability of a network and, generally, a distribution network has larger resistance, similar to its inductive reactance [199], than a transmission network as increases in its XRR ratio increase the voltage drop in its connecting line. For a wind DG unit, the XRR ratio of its connecting transmission line usually varies between 2 and 10 [42].

For different XRRs ratios, the impacts of wind DG with and without series compensation are investigated. In each case, the stability margin and critical voltage reduce with increases in the XRR ratio. In Fig. 5.12, only magnified portions of the results are shown for bus 11 for XRR=2, 6 and 10. For XRR=2, the collapse margin increases by 10 percent using a SC and the rate of decrease in the stability margin is less when a SC is used with the DFIG-based wind DG unit. By using a TCSC, there is a significant improvement in the voltage collapse margin. For XRR=2, the voltage collapse margin enhances by 20.31 percent, which is almost double than that of using a SC. Similar results are obtained for other XRR ratios.

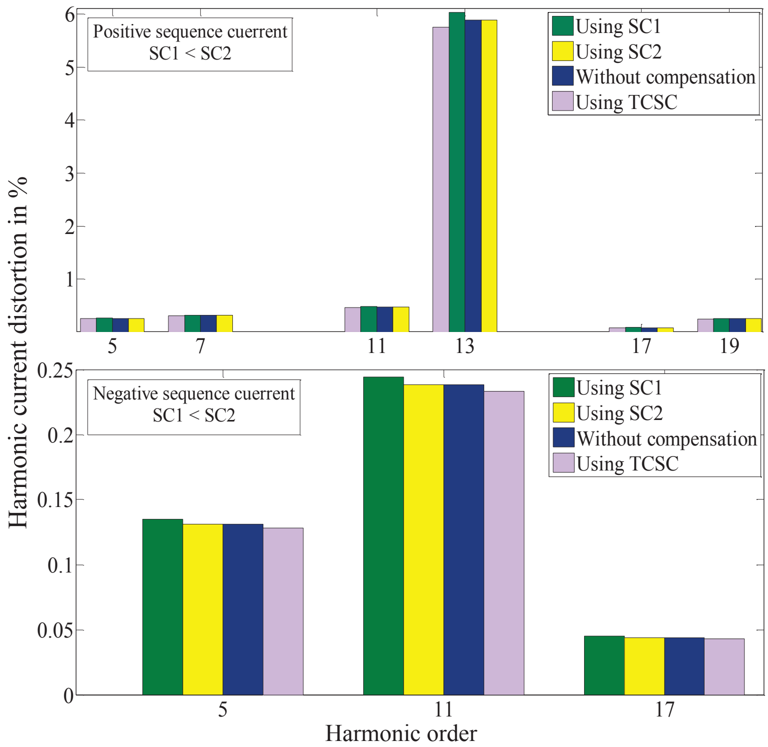

Figure 5.13. Positive and negative sequence harmonic currents at the PCC

5.3.4 Harmonic currents

To investigate the impact of the harmonic current at the PCC, the converter of the DFIG and a load, $C15c$, connected at bus 11 are modelled with an harmonic-generating source and the DFIG with an unbalanced harmonic-generating source according to IEC 61 000-3-6. The positive and negative sequence harmonic currents up to the 19th order of bus 11 of the distribution network with the DFIG-based wind DG are shown in Fig. 5.13. Harmonic distortions are analysed for two different values of a SC, i.e., $SC1$ and $SC2$ where $SC1 < SC2$, which shows that, for the larger SC, the harmonic currents tend to decrease. Harmonic analysis is also investigated for a TCSC and wind DG unit without compensation. It is found that, the 13th and 11th orders for the positive sequence and negative sequence, respectively, show more severe harmonic distortions than any other order as the TCSC reduces them. As the harmonic current depends on the nature of the harmonic source, inserting a capacitor in a series or shunt may adversely affect the existing harmonic sources present in the network. To comply with the relevant grid code, selecting a proper level of series compensation significantly reduce harmonic distortions.

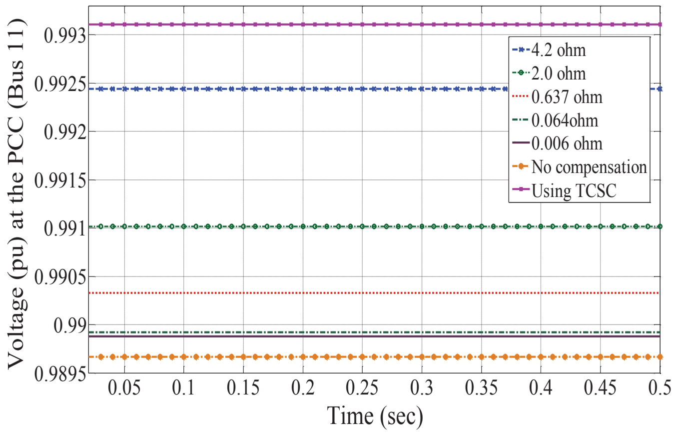

Figure 5.14. Voltage at the PCC with different X_c, TCSC and wind DG without series compensation

5.3.5 Steady-state and transient voltage stability

Voltage variation is seen to reduce with the integration of a series-compensating device, with the voltage at the PCC increasing with increase in series reactance, as shown in Fig. 5.14. As the TCSC can increase the effective impedance of the series-compensating capacitor, it provides better voltage stability than a SC. The problems of voltage dips, sudden load variations and interruptions in the power supply, which create disturbances to sensitive loads, can be overcome using series compensation.

In [32], the author paid attention to the long term short disturbances of wind farms. However, the paper did not consider an electromagnetic transient (EMT) simulation and detailed dynamic models were not used to represent WTs. In this thesis, a 9-cycle three-phase short-circuit fault is applied at 0.50 s in the middle of line $S15c$, close to the PCC. In Fig. 5.15, the fault impact is shown for a WT terminal and, in Fig. 5.16, at the PCC for two different compensation levels, where $SC1 > SC2$. From the EMT simulation, it is found that inserting $SC1$ at buses 11 and LV can more quickly stabilise the system than a wind DG without a SC. In both cases, SSRs are observed and inserting $SC2$ increases their impact. Also, a simulation carried out to determine the impact of a SC on the load voltage which shows that the SSR reduces with increasing distances from the PCC. Using the TCSC, with a NGH damper in the line mitigates the SSR phenomenon caused by the SC and also quickly stabilises the system voltage by reducing steady-state oscillations. During simulation, the XRR ratio is considered to be 7.

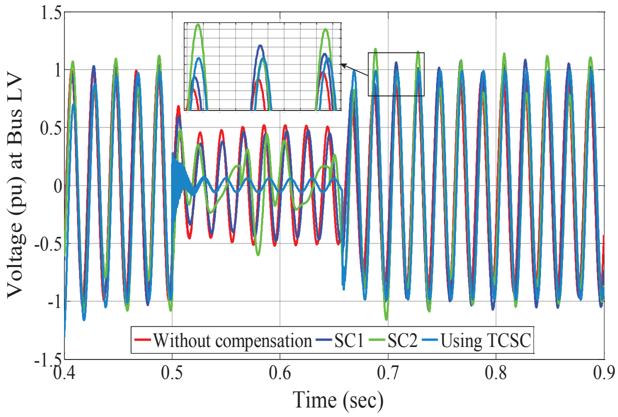

Figure 5.15. Voltage at the bus LV for three-phase short-circuit fault

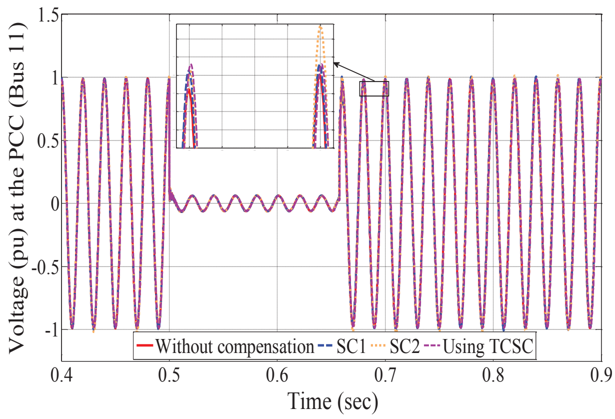

Figure 5.16. Voltage at the PCC for three-phase short-circuit fault

5.3.6 Case study 2

To test the effectiveness of series compensation for flicker in a distribution network with wind DG the IEEE 43-bus industrial and commercial distribution system [191] is used for this study with a little modification by connecting a wind farm to the PCC using transmission line and compensating devices and shown in Fig. 4.11 and described in Section 4.3 (Chapter 4). The network parameters are given in Appendix IV.

5.3.7 Flicker and voltage Sag

The flicker contributions of a wind farm with a DFIG and series-compensated line are summarised in Table 5.4. For continuous operation of the wind farm, approximately 6 percent decreases in flicker emissions are observed at the PCC and bus LV while during short-term and long-term switching operations, flicker emissions seem to be

Table 5.4. Flicker emission with DFIG and series compensated line

Bus		$P_{\text{st-cont}}$	$P_{\text{lt-cont}}$	$P_{\text{st-sw}}$	$P_{\text{lt-sw}}$	d_{sw} (%)
DFIG	LV	0.23	0.23	0.06	0.04	18.29
	PCC	0.0145	0.0145	0.0035	0.0022	1.1507
SC	LV	0.2162	0.2162	0.0126	0.0082	8.3357
	PCC	0.0137	0.0137	0.0008	0.0005	0.5273

Table 5.5. Flicker emissions using TCSC with increasing penetration of wind energy at bus 50

Bus		$P_{\text{st-cont}}$	$P_{\text{lt-cont}}$	$P_{\text{st-sw}}$	$P_{\text{lt-sw}}$	d_{sw} (%)
100%	LV	0.64	0.64	0.15	0.11	21.33
	PCC	0.02	0.02	0.0043	0.0028	0.6
50%	LV	0.6	0.6	0.13	0.10	18.04
	PCC	0.01	0.01	0.0040	0.0027	0.01

greatly affected by series compensation and an average decrease of 76 percent is found.

Although, wind energy penetration is increased by increasing the number of turbines, flicker emission rates also increases as observed at the PCC and LV bus with a TCSC-compensated network. Two cases are considered: 100 percent and 50 percent wind energy penetrations at the PCC using 5 and 2 WTs, respectively, with the flicker emission rates shown in Table 5.5. In both cases, the TCSC emission rates, especially at the PCC, are significantly low with slow voltage variations.

The results from the voltage sag analyses of wind energy penetration without any compensation and using a SC and TCSC are shown in Fig. 5.17, Fig. 5.18 and Fig. 5.19, respectively, in which the voltage sag characteristics of some selected buses, i.e., the WT terminal, LV, PCC, bus-50, and a load bus in the vicinity of the PCC with a dynamic load, bus 51, can be observed. For deep sag at the remaining voltages of 0.2 pu and 0.4 pu, frequencies of occurrence are comparatively low with moderate sag. In the bar graph, each bar is sub-divided into voltages at the short-circuited bus-bar which identifies the different voltage levels responsible for certain percentages of annual frequencies of occurrence. At 0.2 pu, the sag frequency is the same for the three cases but as, at 0.4 pu, sag frequency is observed for the DFIG and SC but not for the TCSC. The TCSC can reduce the dip in sag intensity at the WT terminal. The annual frequency of occurrence is also reduced with series compensation. With the SC, deep sag at the PCC is responsible for the HV, MV

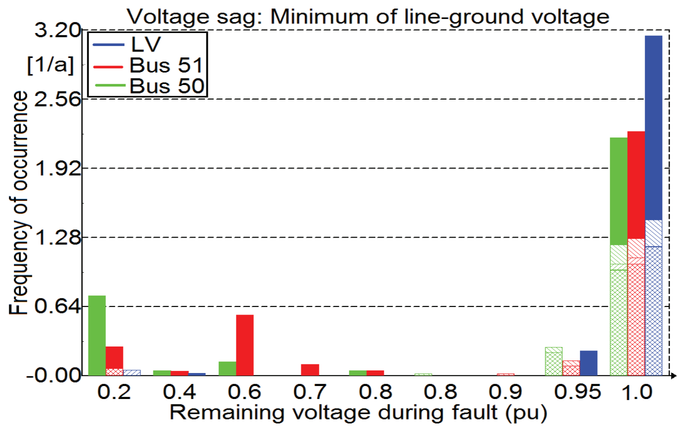

Figure 5.17. Voltage sag analysis with DFIG (solid portion of the bar: HV level, others portions: different LV levels)

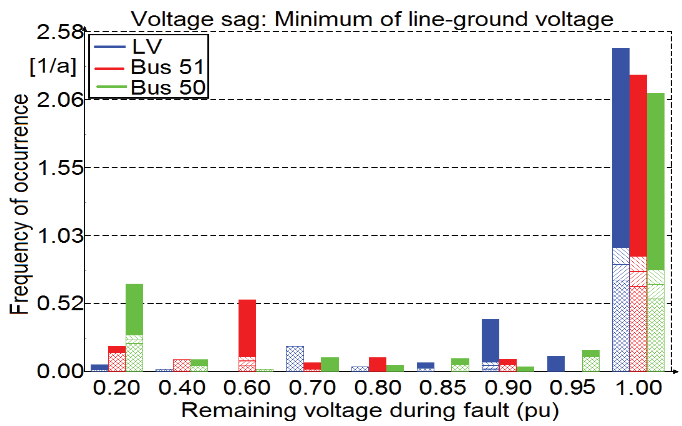

Figure 5.18. Voltage sag analysis with DFIG and SC (solid portion of the bar: HV level, others portions: different LV levels)

and LV network whereas, with the TCSC, deep sag at the PCC is responsible mainly for the HV network. The TCSC can reduce the impact of the fault for both the MV and LV networks. At 0.85 pu and 0.70 pu, the sag frequency is lower using a TCSC than a SC and for load bus, the sag frequency is also low with the TCSC at 0.60 pu the impact for the LV and MV networks are mitigated while the voltage sag is affected by the HV network; this is also true for the other cases.

5.4 Summary and Conclusions

The first part of this chapter focuses on the steady state and transient voltage stabilities, harmonic current, flicker and voltage sag severity of a transmission network

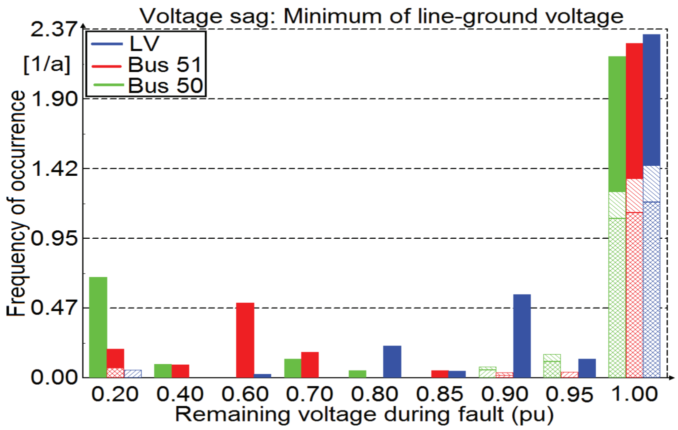

Figure 5.19. Voltage sag analysis with DFIG and TCSC (solid portion of the bar: HV level, others portions: different LV levels)

using FSWT and DFIG wind farms with series compensation from which the following conclusions can be drawn.

- For both types of wind farms, a SC can improve the voltage profile at the PCC, with 3.7% and 1.6% increases in the PCC voltage observed for the FSWT snd DFIG, respectively. A SC also enhances the LVRT capability of a wind farm, with 4.37% and 1.0% increases in the CCT observed for the FSWT and DFIG wind farms, respectively.
- A SC significantly influences voltage sag characteristics. If the series capacitance value is high, the frequency of occurrence of voltage sag is low at a low remaining fault voltage although frequency of occurrence of voltage sag is higher at the WT terminal when the remaining voltage is 1 pu. Therefore, while choosing an optimum value for a SC, these criteria need to be considered.
- It is shown in this study that, although a SC reduces harmonic current injection at the PCC, network impedance has a significant impact on harmonics. Inserting a SC can change the harmonic condition by its interaction with pre-existing harmonics. While a SC can increase dynamic voltage stability, it can also increase harmonic currents. Flicker is an essential power quality problem and as shown in this analysis, the emission rate is reduced using a SC.

From the study of the steady-state and transient voltage stabilities and power quality of DFIG-based wind DG using series compensation, the following conclusions can be drawn.

- The dependency of voltage on the transmitted active power and voltage variations with changes in the reactive power are analysed through PV curves and voltage sensitivity tools, respectively. In both cases, inserting a series-compensating device is advantageous as it increases the stability region in the PV curve and reduces bus sensitivity to the injected reactive power. The load margin increases more with increases in series reactance than with a wind DG unit without compensation and is further increased using a TCSC.
- As a network's voltage strength is weakened by increasing its XRR ratio, which means that it consumes a greater amount of reactive power, its voltage stability is reduced and, for a weak grid, its XRR ratio can impose a limit on the penetration level of wind energy. A SC can compensate a portion of the voltage drop in line and increase voltage stability. Also, to improve the stability margin of a line, especially if it has a high XRR ratio, a TCSC can be used as it has a better capability to increase the compensating voltage at a specific line current than a SC bank alone.
- In this study, it is shown that a series compensating device can reduce the harmonic current injection at the PCC and that network impedance significantly affects harmonic components. Inserting a SC or TCSC can change the harmonic conditions by interacting with the pre-existing harmonics of the network and increase dynamic voltage stability while generating harmonic currents. Again, as this can reduce some harmonic currents and increase others, before inserting any series compensation device into a network, it is necessary to determine the harmonics present and their interactions.
- As series compensation has the capability to cancel out a portion of a line's series inductance, it can reduce voltage regulation and enhance power transmission efficiency. Both steady-state and transient voltage stabilities increase with the aid of a SC which ensures faster voltage recovery than the DFIG without any compensation. As series reactance can increase SSR, a TCSC with a NGH damper can be used to damp oscillations.
- As series compensation improves flicker and voltage sag capabilities with increasing wind penetration, flicker can be mitigated. Capacitive compensation also reduces the frequency of occurrence of shallow sag and deep sag, which are mostly responsible for low-voltages during faults.

As series compensation offers reduced voltage variations and enhanced power transfer capabilities for the lines in both transmission and distribution networks, it is a potential solution to the need to improve the voltage stability of a weak distribution network in which voltage regulation is high.

Chapter 6

Conclusions and Suggestions for Future Work

6.1 Conclusion

The general conclusions drawn from this thesis and scope for future work are presented in this chapter. In addition, the benefits and shortcomings of using series compensation to mitigate voltage and power quality issues caused by the integration of an asynchronous machine-based wind farm in a grid are discussed.

From this work, the following conclusions can be drawn.

- Series compensation, both static and dynamic, can increase the voltage level, low-voltage ride-through (LVRT) capability and critical clearing time (CCT) of a power system and, thus, enhances the steady-state and transient voltage stabilities of wind farms for different network conditions, such as, static and composite load variations, motor start-ups, different line parameters, and symmetrical and asymmetrical faults. It can also reduce bus voltage sensitivity to the reactive power variations and, thus, make the voltage at the point of common coupling (PCC) less susceptible to the reactive power demand of the network. Again, series compensation is much more effective for increasing the voltage stability limit than shunt compensation with the same MVA rating.
- Short-circuit analyses of wind farms are conducted using a series compensated (SSSC) transmission line which can effectively reduce the sub-transient, peak and braking currents and short-circuit apparent power. However, the protection device setup needs to be reconfigured if series compensation is used because the maximum and minimum fault levels will change with the integration of these types of compensating devices in wind farms. The SSSC can also reduce the high inrush current and peak reactive power demand during the start-up of a wind farm.
- Flicker, which is an important and impulsive power quality issue for wind farms, can be mitigated using series compensation. Fixed-speed wind turbine

(FSWT) and doubly-fed induction generator (DFIG)-based wind farms are modelled with flicker coefficients when the rated apparent power of a WT and short-circuit apparent power of the grid at different network impedances are known. Short-term flicker, long-term flicker and slow-voltage variations are found to be reduced when a series capacitor (SC) or thyristor controlled series compensator (TCSC) is used.

- Voltage sag analyses of FSWT and DFIG wind farms using series compensation are an effective probabilistic approach for postulating the voltage sag severity of buses for different types of faults throughout the year. A SC can reduce a sag intensity, i.e., the fault voltage remaining during the contingency period and the frequencies of occurrence of a fault in a year, especially, at a WT terminal, PCC and other buses close to the compensation. Again, a controlled capacitor can reduce the sag frequency more than a simple capacitor.
- Harmonic emissions depend on a network's impedance. Series compensation can reduce them, especially with the aid of a harmonic filter, in both transmission and distribution networks. A SC and TCSC are simulated for both cases with unbalanced harmonic-generating sources and loads for FSWT and DFIG types of wind farms, and it is found that, with compensation, the positive and negative sequence harmonic current emissions are low.
- To remedy sub-synchronous resonance (SSR), a TCSC, which is a conventional thyristor-based variable impedance type of compensator, can be implemented in a similar way to the NGH damper principle. This scheme is simulated with a wind DG connected to a distribution network, and it is found that it can remove the SSR. In voltage source converter (VSC)-based series compensation, such as SSSC, the instantaneous output voltage of the converter can be kept in quadrature with the instantaneous line current which makes it immune to SSR.

6.2 Future Work

This work can be extended in different directions and it is suggested that the following areas are worth pursuing.

- To choose the proper size and location of a series compensation network, different optimisation methods for extracting favourable output could be considered. As series compensation can be operated in different modes, such as for the control of the line power-flow, bus voltage, line reactance, series voltage regulation and fault-current, the effectiveness of these modes could be investigated while, depending on requirements, arrangements for coping with ancillary issues, such as SSR and harmonic mitigation, could be integrated.

- The progressive development of full-scale WTs and permanent magnet generators motivate an investigation into their characteristics for power system stability and power quality using series compensation. Hybrid wind power systems combine wind power with other generation sources, such as solar, hydro-power and/or energy storage (e.g., fuel-cells). The advantage of a hybrid system is that a limitation of one particular source can be overcome by another. As interactions among different sources require accurate knowledge of their operations, extensive research needs to be conducted to identify and resolve their limiting factors to secure their reliable incorporation in a grid.
- For fault-level analysis, a detailed topology of wind farms and the operation of their associated protection systems should be tested at realistic power levels using series compensation. For simplicity, in this thesis, RMS simulations were used for fault-level calculations but, to gain a deeper insight, EMT simulations could be employed to explore the minimum and maximum fault-levels of wind farms. As a wind power plant generally contains two types of transformer, pad-mounted and substation transformer, the impact of series compensation on different types of transformer configurations could be investigated.
- The frequency polynomial characteristics of network elements, such as synchronous and asynchronous machines, transmission lines and transformers could be implemented in harmonic domain analysis by modelling a SC with frequency dependant characteristics to inherently include internal parameter variations and skin effect issues.

Chapter 7

Appendices

7.1 Appendix-I

SMIB system:

System parameters	
Synchronous machine	24 kV, 2200 MVA, 50 Hz x_d:1.81 pu, x_q:1.76 pu
Transformer	2220 MVA, 500 kV/24 kV
Transmission line	80 km, r1: 0.001 Ω/km, l1: 0.2 Ω/km

7.2 Appendix-II

Wind farm connected to infinite bus:

System parameters	
Utility	S''_{kmax}=6000 MVA, I''_{kmax}=31.491 83 kA
WT	No. of parallel machine: 30 Power: 2.0 MW, Voltage: 690 V Wind speed: 10 m/s R_s: 0.01pu, X_s: 0.1pu X_m: 3.5pu, $\frac{I_{\mathrm{lr}}}{I_{\mathrm{n}}}$: 7pu Inertia: 75 kgm^2, Shaft inertia: 4.02 D: 1.5, Pole pair: 2, f: 50 Hz
Transformer	T1: 30*2.5 MVA, 20 kV/0.69 kV T2: 80 MVA, 110 kV/20 kV

7.3 Appendix-III

WT connected to infinite bus using compensating devices:

System parameters	
Utility	Base voltage: 120 kV Frequency: 50 Hz Base MVA: 2500 MVA
STATCOM	Capacity: 8 MVA V_{DC}: 4 kV, C_{DC}: 375 µF $Z_{converter}$: 0.007+j 0.22pu
SSSC	Capacity: 8 MVA V_{DC}: 4 kV, C_{DC}: 375 µF $Z_{converter}$: 0.02+j 0.6pu Injected V_{max}: 0.6pu
WT1 and WT2	Power: 3 MW, Voltage: 575 V Wind speed: 10 m/s R_s: 0.0048pu, X_{ls}: 0.1248pu R_r: 0.0043pu, X_{lr}: 0.1791pu
Transformers	Transformer-1 47 MVA,120 kV/25 kV Transformer-2 4 MVA,25 kV/575 V
Transmission line	Line-1 and Line-2: 20 km, r1: 0.1153 Ω/km, r0: 0.413 Ω/km, l1: 1.05 mH/km, l0: 3.32 mH/km Line-3: 5 km, r1: 0.1153 Ω/km, r0: 0.413 Ω/km, l1: 1.05 mH/km, l0: 3.32 mH/km
Load	Load-1: 120 kV, 10 MW, 8 MVAR Load-2: 25 kV, 3 MW, 2 MVAR

7.4 Appendix-IV

WT connected to 43-bus distribution test network:

System parameters	
Utility	S''_{k}=300 MVA, I''_{k}=2.51 kA
WT	No. of parallel machines: 2 Power: 2.3 MW, Voltage: 690 V Wind speed: 12 m/s R_s: 0.01pu, X_s: 0.1pu X_m: 3.5pu, $\frac{I_{\mathrm{lr}}}{I_{\mathrm{n}}}$: 7pu Inertia: 75 kgm^2, Shaft inertia: 4.02 D: 1.5, Pole pair: 2, f: 60 Hz
Transformer	6 MVA, 13.8 kV/0.69 kV Copper loss: 2.5 kW
Transmission line	Line length: 15 km, r1: 0.13 Ω/km, r0: 0.413 Ω/km, l1: 0.78 Ω/km
SC	6.5 MVA, 13.8 kV, 530.5 µF
TCSC	6.5 MVA, 13.8 kV, X_{C}: 10 Ω, X_{L}: 30 Ω, R: 25 Ω

7.5 Appendix-V

WT connected to a HV network for short-circuit analysis:

System parameters	
WT	No. of parallel machine: 5, 10, 15 Power: 2.7 MW, Voltage: 690 V Wind speed: 15 m/s R_s: 0.01pu, X_s: 0.1pu X_m: 3.5pu, $\frac{I_{\mathrm{lr}}}{I_{\mathrm{n}}}$: 7pu Shaft inertia: 4.02 D: 1.5, Pole pair: 2, f: 60 Hz
Transformer	30 MVA, 110 kV/20 kV, 20 kV/0.69 kV Copper loss: 2.5 kW
Transmission Line	Line length: 100 km, r1: 0.12 Ω/km, l1: 0.386 Ω/km
SSSC	Capacity: 30 MVA, 110 kV V_{DC}: 15 kV, C_{DC}: 50 mF

7.6 Appendix-VI

System parameters	
WT	No. of parallel machine: 55 Power: 3.5 MW, Voltage: 960 V v_w: 12 m/s, R: 35 m R_s: 0.01pu, X_s: 0.1pu, X_m: 3.5pu ρ: 1.225 kgm^3, $\frac{I_{\mathrm{lr}}}{I_{\mathrm{n}}}$: 7pu, Shaft inertia: 4.02 Shaft torsional damping: 3 Nms/rad Pitch angle controller gain: 100 Pitch angle controller time constant: 1 s D: 1.5, Pole pair: 2, f: 50 Hz
DFIG converter and crowbar	Rated v_r: 1863 V, Rated P_r: 2222 kVA Maximum I_r for crowbar insertion: 1.5 pu
Transformer	200 MVA, 18 kV/0.960 kV Copper loss: 1 kW
SC	0.017 F, 200 MVA, 18 kV
STATCOM	Capacity: 200 MVA V_{AC}: 400 V, V_{DC}: 1.5 kV, C_{DC}: 250 mF

7.7 Appendix-VII

WT connected to 15-bus distribution network

System parameter	
WT	Power: 5 MW, Voltage: 690 V Wind speed: 10 m/s R_s: 0.01pu, X_s: 0.1pu X_m: 3.5pu, $\frac{I_{\mathrm{lr}}}{I_{\mathrm{n}}}$: 7pu Shaft inertia: 4.02 D: 1.5, Pole pair: 2, f: 50 Hz
Transformer	5.5 MVA, 11 kV/0.69 kV Copper loss: 5 kW
Transmission Line	Line length: 10 km, r1: 0.13 Ω/km, l1: 0.91 Ω/km, c1: 0.01 µF/km
SC	4.2 Ω, 11 kV, 5.5 MVA X_C: 7 Ω, R: 50 Ω, L: 50 mH

References

[1] R. Zheng and J. Zhong, "Generation adequacy assessment for power systems with wind turbine and energy storage," in *IEEE Innovative Smart Grid Technologies (ISGT)*, Jan. 2010, pp. 1 –6.

[2] Y. Chi, Y. Liu, W. Wang, and H. Dai, "Voltage stability analysis of wind farm integration into transmission network," in *International Conference on Power System Technology (POWERCON)*, Oct. 2006, pp. 1 –7.

[3] N. Capacitors, "Series capacitors case study," Nokian Capacitors Ltd., FI-33331 Tampere, Finland.

[4] L. G. Narain G. Hingorani, *Understanding FACTS: concepts and technology of flexible AC transmission systems.* New York, IEEE Press, 2010.

[5] Z. Chen, Y. Hu, and F. Blaabjerg, "Stability improvement of induction generator-based wind turbine systems," *IET Journal of Renewable Power Generation*, vol. 1, no. 1, pp. 81 –93, Mar. 2007.

[6] L.-R. Chang-Chien, C.-M. Hung, and Y.-C. Yin, "Dynamic reserve allocation for system contingency by DFIG wind farms," in *IEEE PES general meeting*, Jul. 2008, p. 1.

[7] M. J. Hossain, H. R. Pota, M. A. Mahmud, and R. A. Ramos, "Investigation of the impacts of large-scale wind power penetration on the angle and voltage stability of power systems," *IEEE Systems Journal*, vol. 6, no. 1, pp. 76–84, Mar. 2012.

[8] H. Polinder, "Overview of and trends in wind turbine generator systems," in *IEEE PES general meeting*, Jul. 2011, pp. 1 –8.

[9] R. Bansal, T. S. Bhatti, and D. Kothari, "Bibliography on the application of induction generators in nonconventional energy systems," *IEEE Trans. on Energy Conversion*, vol. 18, no. 3, pp. 433–439, 2003.

[10] M. Tazil, V. Kumar, R. Bansal, S. Kong, Z. Dong, W. Freitas, and H. Mathur, "Three-phase doubly fed induction generators: an overview," *IET Journal of Electric Power Applications*, vol. 4, no. 2, pp. 75 –89, Feb. 2010.

[11] T. Ackermann, *Wind power in power systems.* John Willey & Sons, Ltd, 2005.

[12] F. Wu, X.-P. Zhang, P. Ju, and M. Sterling, "Decentralized nonlinear control of wind turbine with doubly fed induction generator," *IEEE Trans. on Power Systems*, vol. 23, no. 2, pp. 613 –621, May 2008.

[13] M. Rahimi and M. Parniani, "Coordinated control approaches for low-voltage ride-through enhancement in wind turbines with doubly fed induction generators," *IEEE Trans. on Energy Conversion*, vol. 25, no. 3, pp. 873 –883, Sept. 2010.

[14] L. Yazhou, A. Mullane, G. Lightbody, and R. Yacamini, "Modeling of the wind turbine with a doubly fed induction generator for grid integration studies," *IEEE Trans. on Energy Conversion*, vol. 21, pp. 257–264, 2006.

[15] L. Zhang, C. Watthanasarn, and W. Shepherd, "Application of a matrix converter for the power control of a variable-speed wind-turbine driving a doubly-fed induction generator," in *23rd International Conference on Industrial Electronics, Control and Instrumentation (IECON)*, vol. 2, Nov 1997, pp. 906 –911.

[16] "Western wind and solar integration study: executive summary," The National Renewable Energy Laboratory (NREL), A national laboratory of the U.S. Department of Energy, GE Energy, May 2010.

[17] "China, US lead global wind energy installations in 2012: 44,711 MW was installed during the year," REVE, Wind Energy and Electric Vehicle Magazine, Feb. 2013.

[18] "Chapter-9: Wind energy, Australian energy resource assessment," Geoscience Australia and ABARE, External Publication-Report, Mar. 2010.

[19] "Wind integration: International experience WP2: Review of grid codes," Australian Energy market Operator (AEMO), Tech. Rep., 2 Oct. 2011.

[20] T. Ackermann and R. Kuwahata, "Lessons learned from international wind integration studies aemo wind integration wp4(a)," Energynautics GmbH, Germany, Commissioned by Australian Energy Market Operator, 16 Nov. 2011.

[21] J. Morren, S. de Haan, W. Kling, and J. Ferreira, "Wind turbines emulating inertia and supporting primary frequency control," *IEEE Trans. on Power Systems*, vol. 21, no. 1, pp. 433 – 434, Feb. 2006.

[22] "Wind power in the nordic region: conditions for the expansion of wind power in the nordic countries," Nordic Energy Research, NordVind, Oct. 2011.

[23] A. Kamga, S. Voller, and J. Verstege, "Congestion management in transmission systems with large scale integration of wind energy," in *IEEE PES Joint Symposium Integration of Wide-Scale Renewable Resources Into the Power Delivery System, CIGRE*, Jul. 2009.

[24] M. R. I. Sheikh and S. M. A. Razzak, "Stabilization of wind generator by using STATCOM/SMES," *Journal of Scientific Research*, vol. 1, no. 3, 2009.

[25] R. I. Sheikh, S. Muyeen, R. Takahashi, and J. Tamura, *Multi-area frequency and tie-line power flow control by fuzzy gain scheduled SMES, energy storage.* InTech Europe, 2010, ch. 5, pp. 87–102.

[26] A. Perdana, "Dynamic models of wind turbines," Ph.D. dissertation, Chalmers University of Technology, 2008.

[27] E. Muljadi, Z. Mills, R. Foster, J. Conto, and A. Ellis, "Fault analysis at a wind power plant for one year of observation," in *IEEE PES general meeting*, 2008, pp. 1–7.

[28] P. Barker and R. De Mello, "Determining the impact of distributed generation on power systems: Part 1 - radial distribution systems," in *IEEE PES Summer Meeting*, vol. 3, 2000, pp. 1645 –1656.

[29] K. Methaprayoon, W. Lee, C. Yingvivatanapong, and J. Liao, "An integration of ANN wind power estimation into UC considering the forecasting uncertainty," in *IEEE Industrial and Commercial Power Systems Technical Conference*, May 2005, pp. 116 –124.

[30] D. Shirmohammadi, H. Hong, A. Semlyen, and G. Luo, "A compensation-based power flow method for weakly meshed distribution and transmission networks," *IEEE Trans. on Power Systems*, vol. 3, no. 2, pp. 753 –762, May 1988.

[31] R. Grünbaum, "Voltage and power quality control in wind power applications by means of dynamic compensation," ABB Power Systems AB, AC Power Division, Vasteras, Sweeden, 1999.

[32] V. Salehi, S. Afsharnia, and S. Kahrobaee, "Improvement of voltage stability in wind farm connection to distribution network using FACTS devices," in *32nd Annual Conference on IEEE Industrial Electronics (IECON)*, 2006, pp. 4242–4247.

[33] N. K. Roy, H. R. Pota, and T. F. Orchi, "Small-signal stability assessment of active distribution networks with dynamic loads," in *22nd Australasian*

Universities Power Engineering Conference (AUPEC), Sep. 2012.

[34] T. Aziz, S. Dahal, N. Mithulananthan, and T. Saha, "Impact of widespread penetrations of renewable generation on distribution system stability," in *International Conference on Electrical and Computer Engineering (ICECE)*, 2010, pp. 338–341.

[35] J. Morren and S. de Haan, "Maximum penetration level of distributed generation without violating voltage limits," in *IET-CIRED Seminar on SmartGrids for Distribution*, Jun. 2008, pp. 1 –4.

[36] A. Pashaie, B. Zahawi, and D. Giaouris, "Distributed static series compensation for distribution network line voltage profile improvement," in *2nd IEEE PES International Conference and Exhibition on Innovative Smart Grid Technologies (ISGT Europe)*, Dec. 2011, pp. 1 –4.

[37] M. Molinas, J. Suul, and T. Undeland, "A simple method for analytical evaluation of LVRT in wind energy for induction generators with STATCOM or SVC," in *European Conference on Power Electronics and Applications*, Sept. 2007, pp. 1 –10.

[38] F. Iov, A. D. Hansen, P. Srensen, and N. A. Cutululis, "Mapping of grid faults and grid codes," Ris National Laboratory, Technical University of Denmark, Roskilde, Denmark, Jul. 2007.

[39] J. Bmer, K. Burges, C. Nabe, and M. Pller, "All island TSO facilitation of renewables studies, final report for work package 3," Ecofys and DIgSILENT, EIRGRID, Tech. Rep., 04 Jun. 2010.

[40] H. Bindner, "Power control for wind turbines in weak grids: concepts development," RISØ National Laboratory, Tech. Rep., 1999.

[41] M. Reza, P. Schavemaker, J. Slootweg, W. Kling, and L. Van Der Sluis, "Impacts of distributed generation penetration levels on power systems transient stability," in *IEEE PES general meeting*, 2004, pp. 2150–2155.

[42] F. Zhou, G. Joos, and C. Abbey, "Voltage stability in weak connection wind farms," in *IEEE PES General Meeting*, vol. 2, Jun. 2005, pp. 1483 – 1488.

[43] A. Oliva, S. Ang, J. Balda, and H. Chiacchiarini, "Harmonic distortion reduction in power inverters," in *IEEE 35th Annual Power Electronics Specialists Conference (PESC)*, vol. 2, Jun. 2004, pp. 1226 – 1231.

[44] A. Elmoudi, M. Lehtonen, and H. Nordman, "Effect of harmonics on transformers loss of life," in *IEEE International Symposium on Electrical Insulation*,

Jun. 2006, pp. 408 –411.

[45] T. Larsson and C. Poumarede, “STATCOM, an efficient means for flicker mitigation,” in *IEEE PES Winter Meeting,*, vol. 2, Feb. 1999, pp. 1208 – 1213.

[46] A. Feijoo and J. Cidras, “Analysis of mechanical power fluctuations in asynchronous WECs,” *IEEE Trans. on Energy Conversion*, vol. 14, no. 3, pp. 284 –291, Sep 1999.

[47] A. Larsson, “Flicker emission of wind turbines during continuous operation,” *IEEE Trans. on Energy Conversion*, vol. 17, no. 1, pp. 114 –118, Mar. 2002.

[48] E. Muljadi, N. Samaan, V. Gevorgian, J. Li, and S. Pasupulati, “Different factors affecting short circuit behavior of a wind power plant,” in *IEEE Industry Applications Society Annual Meeting (IAS)*, Oct. 2010, pp. 1 –9.

[49] T. Sulawa, Z. Zabar, D. Czarkowski, L. Birenbaum, S. Lee, and Y. Ten Ami, “Short circuit current of induction generators,” in *IEEE International Symposium on Circuits and Systems (ISCAS)*, 2007, pp. 2431–2434.

[50] V. Gevorgian and E. Muljadi, “Wind power plant short-circuit current contribution for different fault and wind turbine topologies,” in *9th Annual International Workshop on Large-Scale Integration of Wind Power into Power Systems as well as on Transmission Networks for Offshore Wind Power Plants*, Qubec, Canada, 18-19 Oct. 2010.

[51] “Effect of wind generation on reactive power contribution and dynamic voltage responses,” Wind Generation Investigation Project, Transpower New Zealand, Tech. Rep., Mar. 2008.

[52] L. Morgan, J. Barcus, and S. Ihara, “Distribution series capacitor with high-energy varistor protection,” *IEEE Trans. on Power Delivery*, vol. 8, no. 3, pp. 1413–1419, 1993.

[53] D. Divan and H. Johal, “Distributed FACTSa new concept for realizing grid power flow control,” *IEEE Trans. on Power Electronics*, vol. 22, no. 6, pp. 2253–2260, 2007.

[54] N. Jesus, H. Oliveira, and C. Figueiredo, “AES SULs experiences using series compensation on distribution system,” in *19th International Conference on Electricity Distribution (CIRED)*, 21-24 May 2007.

[55] N. Acharya and A. Sode-Yome, “Facts about flexible AC transmission systems (FACTS) controllers: practical installations and benefits,” in *Australian*

Universities Power Engineering Conference (AUPEC), vol. 2, Sept. 2005.

[56] J. Kumara, A. Bandara, A. Atputharajah, and J. Ekanayake, "Design and testing of an TCSC for distribution network applications," in *First International Conference on Industrial and Information Systems*, Aug. 2006, pp. 151 –155.

[57] N. Joshi and N. Mohan, "Application of TCSC in wind farm application," in *International Symposium on Power Electronics, Electrical Drives, Automation and Motion (SPEEDAM)*, May 2006, pp. 1196 –1200.

[58] E. Leonidaki, N. Hatziargyriou, B. Papadias, and G. Georgantzis, "Investigation of power system harmonics and SSR phenomena related to thyristor controlled series capacitors," in *8th International Conference On Harmonics and Quality of Power*, vol. 2, Oct. 1998, pp. 848 –852.

[59] L. Gyugyi, C. Schauder, and K. Sen, "Static synchronous series compensator: a solid-state approach to the series compensation of transmission lines," *IEEE Trans. on Power Delivery*, vol. 12, no. 1, pp. 406–417, 1997.

[60] T. Kumano and N. Hasegawa, "Fault ride-through enhancement of wind power plant using series variable impedance," in *18th International Federation of Automatic Control (IFAC) World Congress*, Aug. 28 - Sep. 2, 2011.

[61] A. Adamczyk, R. Teodorescu, R. N. Mukerjee, and P. Rodriguez, "Overview of FACTS devices for wind power plants directly connected to the transmission network," *IEEE International Symposium on Industrial Electronics (ISIE)*, pp. 3742–3748, 2010.

[62] M. R. Banaei, "Enhancement of power system stability by means of SSSC and STATCOM: A comparative study," in *7th International Conference on Electrical and Electronics Engineering (ELECO)*, 2011, pp. 348–352.

[63] M. H. Haque, "Damping improvement by FACTS devices: A comparison between STATCOM and SSSC," *Journal of Electric Power Systems Research*, vol. 76, pp. 865–872, 2006.

[64] D.-N. Truong and L. Wang, "Application of a static synchronous series compensator to improve stability of a SG-based power system with an offshore wind farm," in *IEEE PES general meeting*, 2012.

[65] L. Wang and D.-N. Truong, "Application of a SVeC and a SSSC on damping improvement of a SG-based power system with a PMSG-based offshore wind farm," in *IEEE PES general meeting*, 2012.

[66] Y. Zhang and Y. Zhang, "A novel power injection model of embedded SSSC with multi-control modes for power flow analysis inclusive of practical constraints," *Journal of Electric Power Systems Research*, vol. 76, pp. 374–381, 2006.

[67] C. Alvarez, H. Amarís, and O. Samuelsson, "Voltage dip mitigation at wind farms," in *EWEC*, 2007.

[68] C. Wessels and F. Fuchs, "Concept and performance of voltage swell mitigation in wind farms with FACTS," in *European Wind Energy Conference & Exhibition (EWEC)*, vol. 16, no. 19.03, 2009.

[69] M. Fang, A. Gardiner, A. MacDougall, and G. Mathieson, "A novel series dynamic voltage restorer for distribution systems," in *International Conference on Power System Technology*, vol. 1, Aug. 1998, pp. 38 –42.

[70] O. Abdel-Baqi and A. Nasiri, "Series voltage compensation for DFIG wind turbine low-voltage ride-through solution," *IEEE Trans. on Energy Conversion*, vol. 26, no. 1, pp. 272–280, 2011.

[71] F. Lingling, Y. Haiping, and M. Zhixin, "Modal analysis of a DFIG-based wind farm interfaced with a series compensated network," *IEEE Trans. on Energy Conversion*, vol. 26, pp. 1010–1020, 2011.

[72] B. Agrawal, "Reactors, capacitors, SVC, PSS: Long term transmission planning seminar," Arizona Public Service Co., Sept. 2009.

[73] R. K. Suman, C. Lal, M. Kumar, I. Alam, and A. Goswami, "Cost-benefit analysis of TCSC installation to power system operation," in *International Conference on Energy, Automation, and Signal (ICEAS)*, Dec., 2011, pp. 1–6.

[74] F. Al Jowder and B.-T. Ooi, "Series compensation of radial power system by a combination of SSSC and dielectric capacitors," *IEEE Trans. on Power Delivery*, vol. 20, no. 1, pp. 458–465, Jan. 2005.

[75] P.-A. Lof, T. Smed, G. Andersson, and D. Hill, "Fast calculation of a voltage stability index," *IEEE Trans. on Power Systems*, vol. 7, no. 1, pp. 54 –64, Feb. 1992.

[76] C. Kenneth, "Chubais post and career on line for moscow power failure," *The Russia Journal, e-archive of print editions of the newspaper*, 2005.

[77] A. Atputharajah and T. Saha, "Power system blackouts - literature review," in *International Conference on Industrial and Information Systems (ICIIS)*, Dec. 2009, pp. 460 –465.

[78] "Final report system disturbance on 4 nov. 2006," Union for the co-ordination of transmission of electricity (UCTE), Interim report, 2006.

[79] M. Begovic and A. Phadke, "Control of voltage stability using sensitivity analysis," *IEEE Trans. on Power Systems*, vol. 7, no. 1, pp. 114 –123, Feb 1992.

[80] M. Moghavvemi and M. Faruque, "Technique for assessment of voltage stability in ill-conditioned radial distribution network," *IEEE Power Engineering Review*, vol. 21, no. 1, pp. 58 –60, Jan. 2001.

[81] M. Chakravorty and D. Das, "Voltage stability analysis of radial distribution networks," *International Journal of Electrical Power & Energy Systems*, vol. 23, no. 2, pp. 129 – 135, 2001.

[82] T. Rahman and G. Jasmon, "A new technique for voltage stability analysis in a power system and improved loadflow algorithm for distribution network," in *International Conference on Energy Management and Power Delivery(EMPD)*, vol. 2, Nov. 1995, pp. 714 –719.

[83] M. Kashem, V. Ganapathy, and G. Jasmon, "Network reconfiguration for enhancement of voltage stability in distribution networks," *IEE Proceedings on Generation, Transmission and Distribution*, vol. 147, no. 3, pp. 171 –175, May 2000.

[84] G. Jasmon, L. Callistus, and C. Lee, "Maximizing voltage stability in distribution networks via loss minimization," *International Journal of Electrical Power & Energy Systems*, vol. 13, no. 3, pp. 148 – 152, 1991.

[85] M. Ntshangase, S. K. Kariuki, S. Chowdhury, and S. P. Chowdhury, "Voltage stability analysis of electricity networks with DFIG-based wind power plants," in *IEEE PES general meeting*, Jun. 2012.

[86] R. Yang and G. Hug-Glanzmann, "Optimal usage of transmission capacity with FACTS devices in the presence of wind generation: A two-stage approach," in *IEEE PES general meeting*, Jun. 2012.

[87] S. Salman and A. Teo, "Windmill modeling consideration and factors influencing the stability of a grid-connected wind power-based embedded generator," *IEEE Trans. on Power Systems*, vol. 18, no. 2, pp. 793 – 802, May 2003.

[88] L. Ha and T. Saha, "Investigation of power loss and voltage stability limits for large wind farm connections to a subtransmission network," in *IEEE PES general meeting*, vol. 2, Jun. 2004, pp. 2251 –2256.

[89] M. Palsson, T. Toftevaag, K. Uhlen, and J. Tande, "Large-scale wind power

integration and voltage stability limits in regional networks," in *IEEE PES Summer Meeting*, vol. 2, Jul. 2002, pp. 762 –769.

[90] H. Chen, J. Chen, D. Shi, and X. Duan, "Power flow study and voltage stability analysis for distribution systems with distributed generation," in *IEEE PES general meeting*, 2006.

[91] G. Jasmon and L. Lee, "Distribution network reduction for voltage stability analysis and loadflow calculations," *International Journal of Electrical Power & Energy Systems*, vol. 13, no. 1, pp. 9 – 13, 1991.

[92] G. Brownell and H. Clark, "Analysis and solutions for bulk system voltage instability," *IEEE Computer Applications in Power*, vol. 2, no. 3, pp. 31–35, 1989.

[93] T. F. Orchi, M. J. Hossain, H. R. Pota, and M. S. Rahman, "Impact of distributed generation and series compensation on distribution network," in *8th IEEE Conference on Industrial Electronics and Applications (ICIEA)*, 2013 [accepted].

[94] M. K. Dosoglu and A. Ozturk, "Investigation of different load changes in wind farm by using FACTS devices," *Journal of Advances in Engineering Software*, vol. 45, pp. 292–300, 2012.

[95] R. C. Bansal, "Automatic reactive-power control of isolated wind–diesel hybrid power systems," *IEEE Trans. on Industrial Electronics*, vol. 53, no. 4, pp. 1116–1126, 2006.

[96] R. Jayashri and R. P. K. Devi, "FACTS controllers for grid connected wind energy conversion systems," *Journal of Solar Energy Engineering*, vol. 131, pp. 11 008–7, 2009.

[97] Z. Linyuan, L. Jinjun, and L. Fangcheng, "Design and implementation of STATCOM combined with series dynamic breaking resistor for low voltage ride-through of wind farms," *IEEE Energy Conversion Congress and Exposition (ECCE)*, pp. 2501–2506, 2010.

[98] A. Causebrook, D. J. Atkinson, and A. G. Jack, "Fault ride-through of large wind farms using series dynamic braking resistors," *IEEE Trans. on Power Systems*, vol. 22, pp. 966–975, 2007.

[99] M. H. Haque, "Stability improvement by FACTS devices: a comparison between STATCOM and SSSC," *IEEE PES general meeting*, vol. 2, pp. 1708–1713, 2005.

[100] T. Sun, Z. Chen, and F. Blaabjerg, “Flicker study on variable speed wind turbines with doubly fed induction generators,” *IEEE Transactions on Energy Conversion*, vol. 20, no. 4, pp. 896 – 905, Dec. 2005.

[101] ——, “Flicker mitigation of grid connected wind turbines using STATCOM,” in *2nd International Conference on Power Electronics, Machines and Drives (PEMD)*, vol. 1, Mar.-2 Apr. 2004, pp. 175 – 180.

[102] H.-S. Ko, G.-G. Yoon, and W.-P. Hong, “Active use of DFIG-based variable-speed wind-turbine for voltage regulation at a remote location,” *IEEE Trans. on Power Systems*, vol. 22, no. 4, pp. 1916 –1925, Nov. 2007.

[103] M. Ammar, “Flicker emission of distributed wind power: A review of impacts, modeling, grid codes and mitigation techniques,” in *IEEE PES general meeting*, Jul. 2012, pp. 1 –7.

[104] V. Akhmatov, H. Knudsen, A. H. Nielsen, J. K. Pedersen, and N. K. Poulsen, “Modelling and transient stability of large wind farms,” *International Journal of Electrical Power & Energy Systems*, vol. 25, no. 2, pp. 123 – 144, 2003.

[105] M. Mohseni, M. A. Masoum, and S. Islam, “Emergency control of DFIG-based wind turbines to meet new european grid code requirements,” in *IEEE PES Innovative Smart Grid Technologies (ISGT)*, 2011, pp. 1–6.

[106] M. Mohseni, M. A. S. Masoum, and S. M. Islam, “Low voltage ride-through of DFIG wind turbines complying with western-power grid code in australia,” in *IEEE PES General Meeting*, Jul. 2011, pp. 1 –8.

[107] M. Tsili and S. Papathanassiou, “A review of grid code technical requirements for wind farms,” *IET Journal of Renewable Power Generation*, vol. 3, no. 3, pp. 308 –332, Sept. 2009.

[108] R. Mustapa, M. Serwan, N. Hamzah, and Z. Zakaria, “The propagation of voltage sag through transformer connections in a power system network,” in *4th International Power Engineering and Optimization Conference (PEOCO)*, Jun. 2010, pp. 1 –6.

[109] J. Enquist, “Ride-through of offshore wind parks,” Master’s thesis, Department of Electric Power Engineering, Division of Energy and Environment, Chalmers University of Technology, Gteborg, Sweden, 2007.

[110] DIgSILENT PowerFactory 14.1, “User’s manual, volume 2/2, edition 1,” May 2011.

[111] M. Mohseni, S. Islam, and M. Masoum, "Impacts of symmetrical and asymmetrical voltage sags on DFIG-based wind turbines considering phase-angle jump, voltage recovery, and sag parameters," *IEEE Trans. on Power Electronics*, vol. 26, no. 5, pp. 1587 –1598, may 2011.

[112] J. Arrillaga, B. C. Smith, N. R. Watson, and A. R. Wood, *Power system harmonic analysis*. New York, Wiley, 1997.

[113] J. Wasilewski, W. Wiechowski, and C. Bak, "Harmonic domain modeling of a distribution system using the DIgSILENT powerfactory software," in *International Conference on Future Power Systems*, Nov. 2005, pp. 1–7.

[114] A. Testa and R. Langella, "Power system subharmonics," in *IEEE PES General Meeting*, vol. 3, Jun. 2005, pp. 2237 – 2242.

[115] M. Bradt, B. Badrzadeh, E. Camm, D. Mueller, J. Schoene, T. Siebert, T. Smith, M. Starke, and R. Walling, "Harmonics and resonance issues in wind power plants," in *IEEE PES general meeting*, Jul. 2011, pp. 1 –8.

[116] A. Larsson, "The power quality of wind turbines," Ph.D. dissertation, Department of Electric Power Engineering, Chalmers University of Technology, 2000.

[117] J. Svensson, "Grid connected voltage source converter-control principle and wind energy application," Ph.D. dissertation, School of Electrical and Computer Engineering, Chalmeres University of Technology, 1998.

[118] T. Hoevenaars, K. LeDoux, and M. Colosino, "Interpreting IEEE STD 519 and meeting its harmonic limits in VFD applications," in *IEEE Industry Applications Society 50th Annual Petroleum and Chemical Industry Conference*, 2003, pp. 145–150.

[119] F. Azcondo, A. Ortiz, M. Maana, F. Diaz, C. Braas, C. Renedo, S. Perez, F. Delgado, and R. Casanueva, "Effects of flicker on different types of 150-W high-pressure sodium lamps and ballasts," in *IEEE 42nd Industry Applications Conference*, Sept. 2007, pp. 833 –838.

[120] A. Ekberg and J. Hasselstrom, "Design critera for electrical networks upon installation of wind power production," in *20th International Conference and Exhibition on Electricity Distribution (CIRED)-Part 1*. Prague: IET, 8-11 Jun. 2009, pp. 1–4.

[121] X. Yang and J. Gauthier, "How can flicker level be determined before a customer is connected to the electric grid," in *IEEE PES general meeting*, Jul.

2009, pp. 1 –6.

[122] A. De Vos and C. Rowbotham, “Knowledge representation for power system modelling,” in *22nd IEEE PES International Conference on Power Industry Computer Applications. Innovative Computing for Power - Electric Energy Meets the Market.*, 2001, pp. 50 –56.

[123] M. A. Mahmud, “Robust nonlinear feedback linearizing control for power systems to enhance transient stability,” Ph.D. dissertation, School of Engineering and Information Technology, The University of New South Wales, Canberra, Australia, Nov. 2012.

[124] G. Andersson, “Modelling and analysis of electric power systems power flow analysis fault analysis power systems dynamics and stability,” Lecture 227-0526-00, ITET ETH Zurich, Sep. 2008.

[125] M. Hossain, “Dynamic voltage stability augmentation in interconnected power systems with renewable energy,” Ph.D. dissertation, School of Engineering and Information Technology, Australian Defence Force Academy, University of New South Wales, 2010.

[126] M. Elizondo, S. Lu, N. Zhou, and N. Samaan, “Model reduction, validation, and calibration of wind power plants for dynamic studies,” in *IEEE PES general meeting*, Jul. 2011, pp. 1 –8.

[127] L. Fan, H. Yin, and Z. Miao, “On active/reactive power modulation of DFIG-based wind generation for interarea oscillation damping,” *IEEE Trans. on Energy Conversion*, vol. 26, no. 2, pp. 513 –521, Jun. 2011.

[128] F. Poitiers, T. Bouaouiche, and M. Machmoum, “Advanced control of a doubly-fed induction generator for wind energy conversion,” *Journal of Electric Power Systems Research*, vol. 79, no. 7, pp. 1085 – 1096, 2009.

[129] M. Hossain, H. Pota, V. Ugrinovskii, and R. Ramos, “Simultaneous STATCOM and pitch angle control for improved LVRT capability of fixed-speed wind turbines,” *IEEE Trans. on Sustainable Energy*, vol. 1, no. 3, pp. 142 –151, Oct. 2010.

[130] R. Pena, J. Clare, and G. Asher, “Doubly fed induction generator using back-to-back PWM converters and its application to variable-speed wind-energy generation,” *IEE Proceedings on Electric Power Applications*, vol. 143, no. 3, pp. 231 –241, May 1996.

[131] A. Petersson, T. Thiringer, L. Harnefors, and T. Petru, “Modeling and experimental verification of grid interaction of a DFIG wind turbine,” *IEEE Trans. on Energy Conversion*, vol. 20, no. 4, pp. 878 – 886, Dec. 2005.

[132] O. Wasynczuk, D. T. Man, and J. P. Sullivan, “Dynamic behavior of a class of wind turbine generators during random wind fluctuations,” *IEEE Power Engineering Review*, vol. PER-1, no. 6, pp. 47 –48, Jun. 1981.

[133] M. Aktarujjaman, M. Haque, K. Muttaqi, M. Negnevitsky, and G. Ledwich, “Control dynamics of a doubly fed induction generator under sub- and super-synchronous modes of operation,” in *IEEE PES general meeting*, Jul. 2008, pp. 1 –9.

[134] J. B. Ekanayake, L. Holdsworth, and N. Jenkins, “Comparison of 5th order and 3rd order machine models for doubly fed induction generator (DFIG) wind turbines,” *Journal of Electric Power Systems Research*, vol. 67, pp. 207–215, 2003.

[135] H. Xiaoqing, W. Pengmin, W. Peng, and Q. Wenping, “Transient stability studies of doubly-fed induction generator using different drive train models,” *IEEE PES general meeting*, pp. 1–6, 2011.

[136] H. Saadat, *Power system analysis*, 2nd ed. McGraw-Hill Book Co, 2002.

[137] M. Mahmud, M. Hossain, and H. Pota, “Investigation of critical parameters for power systems stability with dynamic loads,” in *IEEE PES general meeting*, Jul. 2010, pp. 1 –6.

[138] *Power System Calculation Package, DIgSILENT*, 2007. [Online]. Available: http://www.Digsilent.de/software

[139] P. Kundur, *Power system stability and control*. McGraw-Hill, Inc., 1994.

[140] N. K. Roy, M. J. Hossain, and H. R. Pota, “Effects of load modeling in power distribution system with distributed wind generation,” in *21st Australasian Universities Power Engineering Conference (AUPEC)*, 25-28 Sept. 2011.

[141] “Complex load model,” DIgSILENT Technical Documentation, Tech. Rep., 2008.

[142] “General load model,” DIgSILENT Technical Documentation, Tech. Rep., 2008.

[143] T. Frantz, T. Gentile, S. Ihara, N. Simons, and M. Waldron, “Load behavior observed in LILCO and RG&E systems,” *IEEE Trans. on Power Apparatus and Systems*, no. 4, pp. 819–831, 1984.

[144] "Determining load characteristics for transient performance," General Electric Company, EPRI Report of project RP849-7, 1981.

[145] D. Hill, "Nonlinear dynamic load models with recovery for voltage stability studies," *IEEE Trans. on Power Systems*, vol. 8, no. 1, pp. 166–176, 1993.

[146] R. F. Martin, "Harmonic currents," Compliance engineering magazine, 1999.

[147] N. Linh, "Voltage stability analysis of grids connected wind generators," in *4th IEEE Conference on Industrial Electronics and Applications (ICIEA)*, 2009, pp. 2657–2660.

[148] E. W. Golding and R. Harris, *The generation of electricity by wind power.* John Willey & Sons, Ltd, 1976.

[149] T. Kovarik, C. Pipher, and J. Hurst, *Wind energy.* Domus Book, Chicago, New York, 1979.

[150] M. R. I. Sheikh, S. M. Muyeen, R. Takahashi, and J. Tamura, "Smoothing control of wind generator output fluctuations by PWM voltage source converter and chopper controlled SMES," *European Trans. on Electrical Power*, vol. 21, no. 1, pp. 680–697, 2011.

[151] S. Heier, *Grid integration of wind energy conversion systems.* John Wiley and Sons, 1998.

[152] R. Bansal, T. Bhatti, and D. Kothari, "On some of the design aspects of wind energy conversion systems," *Energy Conversion and Management*, vol. 43, no. 16, pp. 2175 – 2187, 2002.

[153] S. O. Pepainas, "Adaptive control and parameter identification of a doubly-fed induction generator for wind power," Ph.D. dissertation, Naval Postgraduate School Monterey, California, Sep. 2011.

[154] J. Pedersen, K. Helgelsen-Pedersen, N. K. Poulsen, V. Akhmatov, and A. H. Nielsen, "Contribution to a dynamic wind turbine model validation from a wind farm islanding experiment," *Journal of Electric Power Systems Research*, vol. 64, no. 1, pp. 41 – 51, 2003.

[155] E. Hinrichsen and P. Nolan, "Dynamics and stability of wind turbine generators," *IEEE Trans. on Power Apparatus and Systems*, vol. PAS-101, no. 8, pp. 2640 –2648, Aug. 1982.

[156] D. Trudnowski, A. Gentile, J. Khan, and E. Petritz, "Fixed-speed wind-generator and wind-park modeling for transient stability studies," *IEEE Trans. on Power Systems*, vol. 19, no. 4, pp. 1911 – 1917, Nov. 2004.

[157] B. Boukhezzar, L. Lupu, H. Siguerdidjane, and M. Hand, "Multivariable control strategy for variable speed, variable pitch wind turbines," *Journal of Renewable Energy*, vol. 32, no. 8, pp. 1273 – 1287, 2007.

[158] D. Aguglia, P. Viarouge, R. Wamkeue, and J. Cros, *Optimal selection of drive components for doubly-fed induction generator based wind turbines.* InTech, Apr., 2011, ch. 25, pp. 571–592.

[159] B. Pokharel, "Modeling, control and analysis of a doubly fed induction generator based wind turbine system with voltage regulation," Master's thesis, The Faculty of the Graduate School, Tennessee Technological University, 2011.

[160] V. Akhmatov, "Analysis of dynamic behaviour of electric power systems with large amount of wind power," Ph.D. dissertation, Electric Power Engineering, Technical University of Denmark, 2003.

[161] A. G. G. Rodrguez, "Improvement of a fixed-speed wind turbine soft-starter based on a sliding-mode controller," Ph.D. dissertation, Department of Electrical Engineering, University of Seville, Mar. 2006.

[162] C. Wang, L. Shi, L. Wang, and Y. Ni, "Small signal stability analysis considering grid-connected wind farms of DFIG type," in *IEEE PES general meeting*, july 2008, pp. 1 –6.

[163] G. Richards, "Reduced order model for single and double cage induction motors during start-up," *IEEE Trans. on Energy Conversion*, vol. 3, no. 2, pp. 335–341, 1988.

[164] T. Thiringer and J. Luomi, "Comparison of reduced-order dynamic models of induction machines," *IEEE Trans. on Power Systems*, vol. 16, no. 1, pp. 119–126, 2001.

[165] T. Thiringer, "Measurements and modelling of low-frequency disturbances in induction machines," Ph.D. dissertation, Department of Electric Power Engineering, Chalmers University of Technology, 1996.

[166] S. M. Barakati, "Modeling and controller design of a wind energy conversion system including a matrix converter," Ph.D. dissertation, Department of Electrical and Computer Engineering, University of Waterloo, 2008.

[167] P. C. Krause, *Analysis of electrical machinery.* McGraw-Hill Book Co, 1987.

[168] J. Rosenblatt and M. H. Friedman, *Direct and alternating current machinery*, 2nd ed. Charles E. Merrill Publishing company and A. Bell & Howell company, 1988.

[169] N. Gunaratnam and D. Novotny, “The effects of neglecting stator transients in induction machine modeling,” *IEEE Trans. on Power Apparatus and Systems*, vol. PAS-99, no. 6, pp. 2050 –2059, Nov. 1980.

[170] M. J. Hossain, T. K. Saha, N. Mithulananthan, and H. R. Pota, “Control strategies for augmenting LVRT capability of DFIGs in interconnected power systems,” *IEEE Trans. on Industrial Electronics*, vol. 60, no. 6, pp. 2510 – 2522, Jun. 2013.

[171] W. Qiao, R. Harley, and G. Venayagamoorthy, “Effects of FACTS devices on a power system which includes a large wind farm,” in *IEEE PES Power Systems Conference and Exposition (PSCE)*, 2006, pp. 2070–2076.

[172] N. Roy, M. Hossain, and H. Pota, “Voltage profile improvement for distributed wind generation using D-STATCOM,” in *IEEE PES general meeting*, 2011, pp. 1–6.

[173] C. Rong, “Analysis of STATCOM for voltage dip mitigation,” Master’s thesis, Department of Electric Power Engineering, Chalmers University of technology, Dec. 2004.

[174] S. Panda and N. P. Padhy, “MATLAB/SIMULINK based model of single-machine infinite-bus with TCSC for stability studies and tuning employing GA,” *International Journal of Computer Science and Engineering*, vol. 1, no. 1, pp. 50–59, 2007.

[175] D. Divan, W. Brumsickle, R. Schneider, B. Kranz, R. Gascoigne, D. Bradshaw, M. Ingram, and I. Grant, “A distributed static series compensator system for realizing active power flow control on existing power lines,” in *IEEE PES Power Systems Conference and Exposition*, Oct. 2004, pp. 654 – 661 vol.2.

[176] C. Collins, G. Bathurst, N. Watson, and A. Wood, “Harmonic domain approach to STATCOM modelling,” *IEE Proceedings on Generation, Transmission and Distribution*, vol. 152, no. 2, pp. 194 – 200, Mar. 2005.

[177] C. D. Collins, “FACTS device modelling in the harmonic domain,” Ph.D. dissertation, University of Canterbury, Christchurch, New Zealand, Apr. 2006.

[178] G. Reed, R. Pape, and M. Takeda, “Advantages of voltage sourced converter (VSC) based design concepts for FACTS and HVDC-link applications,” in *IEEE PES general meeting*, vol. 3, Jul. 13-17 2003, pp. 1816–1821.

[179] O. Carlson, A. Grauers, J. Svensson, and A. Larsson, “A comparison of electrical system for variable speed operation of wind turbine,” in *European*

Wind Energy Association Conference and Exhibition (EWEC'94), Thessaloniki, Greece, 10-14 Oct. 1994, pp. 500–505.

[180] M. Lindgren, "Modeling and control of voltage source converters connected to the grid," Ph.D. dissertation, School of Electrical and Computer Engineering, Chalmers University of Technology, 1998.

[181] K. E. Okedu, S. M. Muyeen, R. Takahashi, and J. Tamura, "Comparative study of wind farm stabilization using variable speed generator and FACTS device," *IEEE GCC Conference and Exhibition (GCC)*, pp. 569–572, 2011.

[182] C. Han, A. Huang, M. Baran, S. Bhattacharya, W. Litzenberger, L. Anderson, A. Johnson, and A. Edris, "STATCOM impact study on the integration of a large wind farm into a weak loop power system," *IEEE Trans. on Energy conversion*, vol. 23, no. 1, pp. 226–233, 2008.

[183] M. Hossain, H. Pota, and C. Kumble, "Decentralized robust static synchronous compensator control for wind farms to augment dynamic transfer capability," *Journal of Renewable and Sustainable Energy*, vol. 2, p. 022701, 2010.

[184] N. I. Yousif, "Subsynchronous resonance risk assessment in interconnected power systems," Master's thesis, School of Electrical and Computer Engineering, RMIT University, Jan. 2011.

[185] K. R. Padiyar, *Analysis of subsynchronous resonance in power systems.* Springer, 1999.

[186] A. Von Jouanne and B. Banerjee, "Assessment of voltage unbalance," *IEEE Trans. on Power Delivery,*, vol. 16, no. 4, pp. 782–790, 2001.

[187] N. A. Lahaani, D. Aouzellag, and B. Mendil, "Static compensator for maintaining voltage stability of wind farm integration to a distribution network," *Journal of Renewable Energy*, vol. 35, no. 11, pp. 2476 – 2482, 2010.

[188] V. Van Thong, J. Driesen, and R. Belmans, "Power quality and voltage stability of distribution system with distributed energy resources," *International Journal of Distributed Energy Resources*, vol. 1, no. 3, pp. 227–240, 2005.

[189] M. M. Kyaw and V. K. Ramachandaramurthy, "Fault ride through and voltage regulation for grid connected wind turbine," *Journal of Renewable Energy*, vol. 36, pp. 206–215, 2011.

[190] *MATLAB R2010b, ed. Natick, Massachusetts: The MathWorks Inc., 2010.*

[191] *IEEE recommended practice for industrial and commercial power systems analysis*, IEEE 399-1997, 1998.

[192] Z. Fan, S. Shuqin, Z. Lei, L. Wenping, W. Jian, and H. Liang, "Study on large asynchronous motor starting check for auxiliary power system," in *Asia-Pacific Power and Energy Engineering Conference (APPEEC)*, Mar. 2010, pp. 1 –4.

[193] C. Tian, B. Chen, and S. Huan, "Research of high-voltage motor soft-starting based on self-excitation magnetic controlled reactor," in *IEEE Power Engineering and Automation Conference (PEAM)*, vol. 1, Sept. 2011, pp. 234 –237.

[194] P. Strange, "Incorporating the grid reliability report and the grid economic investment report," Annual Planning Report, Transpower New Zealand The National Grid, Mar. 2012.

[195] D. Sweeting, "Applying IEC 60909, short-circuit current calculations," in *58th Annual IEEE Petroleum and Chemical Industry Conference (PCIC)*, Sept. 2011, pp. 1 –6.

[196] *Short-circuit currents in three-phase AC systems Part 4: Examples for the calculation of short-circuit current*, IEC 60909-4, 2000.

[197] A. Larsson, "Flicker emission of wind turbines caused by switching operations," *IEEE Trans. on Energy Conversion*, vol. 17, no. 1, pp. 119 –123, Mar. 2002.

[198] J. Zou, G. Qin, G. Zheng, and H. Xu, "Stability analysis of the startup process of the VSCF wind turbine," *Journal of Computational Information Systems*, pp. 3575–3582, 2010.

[199] T. Ackermann, G. Andersson, and L. Sder, "Distributed generation: a definition," *Journal of Electric Power Systems Research*, vol. 57, no. 3, pp. 195 – 204, 2001.

[200] T. F. Orchi, H. R. Pota, and M. J. Hossain, "Stability improvement of wind farms using shunt and series compensation," in *22nd Australasian Universities Power Engineering Conference (AUPEC)*, Sep. 2012.

[201] R. A. Barr, "Series compensation of distribution and subtransmission lines," Ph.D. dissertation, Department of Electrical and Computer Engineering, Universisty of Wollonngong, 1997.

[202] W. Freitas, L. DaSilva, and A. Morelato, "Small-disturbance voltage stability of distribution systems with induction generators," *IEEE Trans. on Power Systems*, vol. 20, no. 3, pp. 1653 – 1654, Aug. 2005.

[203] Z. Chen and E. Spooner, "Grid power quality with variable speed wind turbines," *IEEE Trans. on Energy Conversion*, vol. 16, no. 2, pp. 148 –154, Jun. 2001.

[204] Y. Hsiao, "Design of filters for reducing harmonic distortion and correcting power factor in industrial distribution systems," *Tamkang Journal of Science and Engineering*, vol. 4, no. 3, pp. 193–200, 2001.

[205] P. M. Anderson and A. A. Foud, *Power system control and stability*, U. Ames, Iowa, Ed. The Iowa State University Press, 1977.

[206] M. Ahmadigorji, A. Abbaspour, A. Rajabi-Ghahnavieh, M. Fotuhi-Firuzabad *et al.*, "Optimal DG placement in distribution systems using cost/worth analysis," *World Academy of Science, Engineering and Technology*, 2009.